

GLYCOGEN SYNTHASE KINASE-3 α IN THE DEVELOPMENT OF
ATHEROSCLEROSIS

INVESTIGATING THE ROLE OF GLYCOGEN SYNTHASE KINASE-3 α IN THE
INITIATION AND PROGRESSION OF ATHEROSCLEROSIS

By: Nicole S. Banko, B.M.Sc. (Hons.)

A Thesis

Submitted to the School of Graduate Studies
in Partial Fulfillment of the Requirements
for the Degree Master of Science

McMaster University

© Copyright by Nicole S. Banko, September 2012

McMaster University Master of Science (2012) Hamilton, Ontario
(Biochemistry and Biomedical Sciences)

TITLE: Investigating the Role of Glycogen Synthase Kinase-3 α in the
Initiation and Progression of Atherosclerosis

AUTHOR: Nicole S. Banko, B.M.Sc. (University of Western Ontario)

SUPERVISOR: Dr. Geoff Werstuck

NUMBER OF PAGES: xiv, 85

ABSTRACT

Atherosclerosis is a chronic inflammatory disease of the arterial wall and is the primary cause of coronary artery disease, the most common cause of death in western societies. Risk factors for cardiovascular disease include dyslipidemia, diabetes, smoking, and obesity. These risk factors have also been shown to promote vascular endoplasmic reticulum (ER) stress; a cellular response characterized by the accumulation of misfolded proteins in the ER. Thickening and decreased stability of arterial plaque can lead to thrombosis and subsequent clinical complications of myocardial infarction and stroke. However, the exact mechanisms that lead to the development of atherosclerosis remain unclear. Here we show that inhibition, as well as a deficiency of glycogen synthase kinase (GSK)-3 α , can protect against accelerated atherosclerosis in a low-density lipoprotein receptor (LDLR) knockout mouse model. Compared to LDLR^{-/-} controls, mice deficient in GSK-3 α showed a decrease in lesion volume in the aortic root as well as protection against diet-induced hepatic steatosis. In addition, necrotic core volume was significantly reduced in LDLR^{-/-}GSK-3 α ^{-/-} mice compared to controls, a characteristic indicative of advanced plaque formation. Furthermore, hepatic and vascular ER stress levels were unaffected by the deletion of GSK-3 α , a result that is consistent with the hypothesis that GSK-3 α functions downstream of ER stress. Macrophages isolated from GSK-3 α deficient mice had a reduction in unesterified cholesterol accumulation as well as a significant increase in the expression of the anti-inflammatory cytokine IL-10. Finally, BMT experiments showed a significant decrease in plaque size in the aortic sinus of LDLR^{-/-}GSK-3 α ^{+/+} mice transplanted with GSK-3 α deficient bone marrow. These results

demonstrate a possible link between ER stress-induced activation of GSK-3 α and the downstream effects leading to atherogenic initiation and progression.

ACKNOWLEDGEMENTS

I would like to first and foremost thank my supervisor, Dr. Geoff Werstuck. I truly appreciate the confidence he showed in me by originally offering me this position and I am tremendously thankful that I was able to contribute to his research program. My achievements can be attributed to his wealth of knowledge and experience. It was incredibly rewarding to be a part of his lab and I am most thankful for his guidance and support throughout these past two years. Your assistance and advice were invaluable.

Over the course of my research, I was able to spend many hours with excellent lab technicians whose skills were a vital part for my experiments. I would like to sincerely thank Dr. Peter Shi and Dr. Mohammad Khan. Their contributions and assistance helped me to achieve success and attain my Master's degree. This project would not have been possible without you.

I would like to thank Dr. Brad Doble and Dr. Suleiman Igdoura for serving on my committee. Your thoughts, recommendations and advice were an inspiration to me during this process.

I would like to thank the friends and colleagues in my lab with whom I have worked so close with over the last two years - Melec Zeadin, Cameron McAlpine, Daniel Venegas, Dan Beriault, Kaley Veerman, Christina Petlura, and Lisa Walter. You were extremely welcoming and helpful and I truly enjoyed our time together. I would also like to thank Preeya Raja for her assistance with my project. I am a better person in having met you all and I wish you all much success in your future endeavors.

Finally, I would also like to thank my family and friends for their loving support and guidance. There were many times when things would get overwhelming and I truly appreciated them taking the time to be there and listen. Thank you for believing in me and for always being there. You are all my strength and motivation.

TABLE OF CONTENTS

Abstract.....	iii
Acknowledgements.....	v
Table of Contents.....	vii
List of Tables.....	ix
List of Figures.....	x
Abbreviations.....	xii

Chapter 1: Introduction

1.1	Atherosclerosis.....	1
	1.1.1 Epidemiology and Risk Factors.....	1
	1.1.2 Pathophysiology.....	2
1.2	Diabetes Mellitus.....	3
1.3	Dyslipidemia.....	5
1.4	ER Stress.....	7
	1.4.1 Diabetes Mellitus and ER stress.....	7
	1.4.2 Dyslipidemia and ER stress.....	8
1.5	The Unfolded Protein Response.....	9
1.6	Glycogen Synthase Kinase (GSK)-3.....	12
	1.6.1 Discovery.....	12
	1.6.2 Composition and Structure.....	13
	1.6.3 Properties and Function.....	14
1.7	Glycogen Synthase Kinase-3 and Atherosclerosis.....	17
	1.7.1 GSK-3 and Lipid Accumulation.....	17
	1.7.2 GSK-3 and the Inflammatory Response.....	18
	1.7.3 GSK-3 and Apoptosis.....	20

Chapter 2: Hypothesis and Objectives

2.1	Rationales and Hypothesis.....	23
2.2	Objectives.....	23

Chapter 3: Materials and Methods

3.1	Animal Model and Genotyping.....	26
3.2	Plasma and Tissue Analysis.....	27
3.3	Tissue Collection and Staining.....	27
3.4	Immunohistochemistry and Immunofluorescence.....	28
3.5	Immunobot Analysis.....	29
3.6	Lipid Staining.....	29
3.7	Liver Lipid Assay.....	30
3.8	Activity Assay.....	30
3.9	Cell Isolation and Culture.....	31
3.10	Free Cholesterol Staining of Peritoneal Macrophages.....	31
3.11	Quantitative RT-PCR.....	32

3.12	Bone Marrow Experiments.....	33
3.13	Statistical Analyses.....	36
Chapter 4: Results		
4.1	Valproate-supplemented high fat diet fed LDLR ^{-/-} mice have decreased atherosclerosis.....	37
4.2	Characterization of a novel LDLR ^{-/-} GSK-3 α ^{-/-} mouse model.....	39
4.2.1	Characterization of a novel mouse strain.....	39
4.2.2	Metabolic parameters.....	40
4.2.3	GSK-3 α deficiency does not significantly change plasma lipid profiles in LDLR ^{-/-} mice.....	42
4.3	GSK-3 α deficiency has no significant effect on ER stress levels in HFD-fed LDLR ^{-/-} mice.....	43
4.4	Effect of GSK-3 α deficiency on hepatic steatosis.....	45
4.4.1	GSK-3 α deficiency significantly reduces hepatic neutral lipid accumulation in LDLR ^{-/-} and LDLR ^{+/+} mice.....	45
4.4.2	Effect of GSK-3 α deficiency on total hepatic cholesterol and lipid biosynthesis protein levels.....	47
4.4.3	GSK-3 α deficiency does not detectably alter the aortic sinus in LDLR ^{+/+} mice.....	48
4.5	Effect of GSK-3 α deficiency on atherosclerosis.....	49
4.5.1	GSK-3 α deficiency significantly attenuates atherosclerosis in HFD-fed LDLR ^{-/-} mice.....	49
4.5.2	Effect of GSK-3 α deficiency on macrophages and smooth muscle cells.....	51
4.6	ER stress-induced free cholesterol accumulation was significantly reduced in GSK-3 α deficient peritoneal macrophages.....	52
4.7	Effect of ER stress-induced GSK-3 α deficient peritoneal macrophages on inflammatory cytokine production.....	55
4.8	Effect of GSK-3 α ^{+/+} and GSK-3 α ^{-/-} bone marrow derived macrophages on atherosclerosis in LDLR ^{-/-} mice.....	56
4.8.1	Genotyping of BMT mice.....	56
4.8.2	Metabolic parameters.....	58
4.8.3	Lesion analysis in BMT mice.....	59
Chapter 5: Discussion.....		61
Chapter 6: Conclusion and Future Directions.....		70
Chapter 7: References.....		72

LIST OF TABLES

Table 1	qRT-PCR primers and conditions.....	33
Table 2	Metabolic parameters in LDLR ^{-/-} mice supplemented with and without valproate.....	42
Table 3	Metabolic parameters in LDLR ^{-/-} GSK-3 α ^{+/+} , LDLR ^{-/-} GSK-3 α ^{+/-} , LDLR ^{-/-} GSK-3 α ^{-/-} mice.....	42
Table 4	Metabolic parameters in BMT mice.....	59

LIST OF FIGURES

Figure 1	The progression of atherosclerosis.....	3
Figure 2	Mechanisms by which diabetes and dyslipidemia cause ER stress.....	8
Figure 3	An overview of the unfolded protein response.....	10
Figure 4	Schematic representation of murine GSK-3 α and GSK-3 β	14
Figure 5	Regulation of GSK-3 α/β	15
Figure 6	Working model of the association between hyperglycemia and dyslipidemia in the induction of ER stress, unfolded protein response, and progression of atherosclerosis.....	25
Figure 7	Outline of BMT protocol.....	34
Figure 8	HFD-fed LDLR ^{-/-} mice supplemented with valproate have a significant decrease in aortic lesion and necrotic core volume.....	38
Figure 9	Characterization of a novel LDLR ^{-/-} GSK-3 α ^{-/-} mouse strain.....	40
Figure 10	Plasma Lipid Profiles.....	43
Figure 11	GSK-3 α deficiency has no significant effect on ER stress levels in HFD-fed LDLR ^{-/-} mice.....	44
Figure 12	GSK-3 α deficiency significantly reduces hepatic lipid accumulation in HFD-fed LDLR ^{-/-} and LDLR ^{+/+} mice.....	46
Figure 13	Effect of GSK-3 α deficiency on total hepatic cholesterol and lipid biosynthesis protein levels in LDLR ^{-/-} mice.....	48
Figure 14	GSK-3 α deficiency does not result in lesion development in the aortic root of HFD-fed LDLR ^{+/+} mice.....	49
Figure 15	GSK-3 α deficiency significantly attenuates atherosclerosis in HFD-fed LDLR ^{-/-} mice.....	50
Figure 16	Effect of GSK-3 α deficiency on macrophages and smooth muscle cells in HFD-fed LDLR ^{-/-} mice.....	52

Figure 17	ER stress-induced free cholesterol accumulation is significantly reduced in GSK-3 α deficient peritoneal macrophages.....	54
Figure 18	Effect of ER stress-induced GSK-3 α deficient peritoneal macrophages on inflammatory cytokine mRNA levels.....	56
Figure 19	Genotype analysis of BMT recipient mice.....	57
Figure 20	Effect of GSK-3 α deficient bone marrow derived macrophages on atherogenesis in HFD-fed LDLR ^{-/-} mice.....	60

ABBREVIATIONS

AGE	Advanced glycation end products
APC	Adenomatous polyposis coli
ATF6	Activating transcription factor 6
ApoB-100	Apolipoprotein B-100
ApoE	Apolipoprotein E
ASK1	Apoptosis-signaling kinase 1
BAX	Bcl-2 associated X protein
BCL2	B-cell lymphoma 2
BM	Bone marrow
BMT	Bone marrow transplantation
CE	Cholesterol esters
CEH	Cholesterol ester hydrolase
CHD	Coronary heart disease
CHOP	C/EBP homologous protein
CVD	Cardiovascular disease
DM	Diabetes Mellitus
EC	Endothelial cell
ECM	Extracellular matrix
ER	Endoplasmic reticulum
FFA	Free fatty acids
FAS	Fatty acid synthase
FC	Free cholesterol
FPLC	Fast performance liquid chromatography
GADD153	Growth arrest and DNA damage inducible gene 153
GRP78	Glucose regulatory protein 78

GSK-3	Glycogen synthase kinase 3
GlcN	Glucosamine
HDAC	Histone deacetylases
HDL	High density lipoprotein
HMG-CoA	3-hydroxy-3-methylglutaryl-coenzyme A
IFN	Interferon
IHC	Immunohistochemistry
IL	Interleukin
IRE1	Inositol-requiring enzyme-1
KDEL	Lysine, Glutamic acid, Aspartic acid, Leucine
LDL	Low density lipoprotein
LDLR	Low density lipoprotein receptor
MI	Myocardial infarction
NAFLD	Nonalcoholic fatty liver disease
NF- κ B	Nuclear factor kappa B
NO	Nitric oxide
NRF2	Nuclear factor erythroid 2-related factor 2
oxLDL	Oxidized low density lipoprotein
PDI	Protein disulfide isomerase
PERK	Protein kinase RNA-like endoplasmic reticulum kinase
PI3K	Phosphatidylinositol 3-kinases
PKB	Protein kinase B
PKC	Protein kinase C
PP1	Protein phosphatase 1
RAGE	Receptor for advanced glycation end products
RCT	Reverse cholesterol transport

ROS	Reactive oxygen species
qRT-PCR	Quantitative reverse transcriptase polymerase chain reaction
SEM	Standard error of the mean
SMC	Smooth muscle cells
SREBP	Sterol regulatory element binding protein
T1D	Type 1 diabetes
T2D	Type 2 diabetes
TM	Tunicamycin
TNF α	Tumor necrosis factor alpha
UPR	Unfolded protein response
VLDL	Very-low density lipoprotein
VPA	Valproic acid
XBP1	X-box binding protein 1

CHAPTER 1: INTRODUCTION

1.1 ATHEROSCLEROSIS

1.1.1 Epidemiology and Risk Factors

Cardiovascular disease (CVD) is the leading cause of death in Western societies with coronary heart disease (CHD) making up the majority of total CVD (Ross, 1999; Smith & Breslow, 1997). Although the age-specific death rate has declined since 1970, the risk of mortality due to CVD still remains high (Lloyd-Jones, Larson, Beiser, & Levy, 1999). In 2008, an estimated 17.3 million people died as a result of CVD, with approximately 7.3 million due to CHD (World Health Organization Fact Sheet No. 317). The World Health Organization (WHO) predicts that 23.6 million people will die from CVD by 2030. Atherosclerosis is the main determinant of CVD. It is a chronic inflammatory disease characterized by lipid accumulation and plaque formation in the inner lining of arteries. Multiple risk factors are known to accelerate the progression of atherosclerosis, including; dyslipidemia, diabetes, obesity, smoking, hypertension and physical inactivity (Yusuf et al., 2004). Over time, advanced plaques can become unstable and rupture, leading to thrombosis and subsequent clinical complications of myocardial infarction and stroke (Navab et al., 1996). The exact mechanisms that lead to the initiation and progression of atherosclerosis remain unclear. An understanding of the molecular pathways that lead to atherogenesis will provide new insights to aid the development of therapeutic strategies to treat and prevent cardiovascular disease.

1.1.2 Pathophysiology

Atherosclerosis is a progressive inflammatory disease that involves the development of plaque in the walls of arteries (Ross, 1999) (Fig. 1). In humans, plaque formation occurs in areas of turbulent blood flow, mainly at bifurcations in the coronary arteries and ascending aortic arch (Pasterkamp, de Kleijn, & Borst, 2000). Initiation of plaque formation begins with the accumulation of cholesterol in the artery wall. Low-density lipoprotein (LDL) particles enter the intima of the arteries and subsequently become oxidized (Navab, et al., 1996; Steinberg et al., 1989). Accumulation of oxidized LDL (oxLDL) causes endothelial cell stimulation, which results in surface expression of cell adhesion molecules and initiation of an inflammatory response (Ross, 1999). This response initiates the recruitment of monocytes to the site of injury, which differentiate into macrophages and engulf the oxLDL particles by means of scavenger receptors (Cybulsky & Gimbrone, 1991; Steinberg, et al., 1989). Lipid engorged macrophages, known as foam cells, and migration of vascular smooth muscle cells (SMC) from the medial layer to the intima contribute to the growing plaque. As lesion development progresses, apoptosis of macrophages and accumulation of cellular debris leads to the formation of a necrotic core. The growing necrotic core destabilizes the plaque, which becomes prone to rupture. The high clinical incidences of myocardial infarction and stroke due to atherosclerosis have prompted a growing interest into the study of molecular pathways that cause these events.

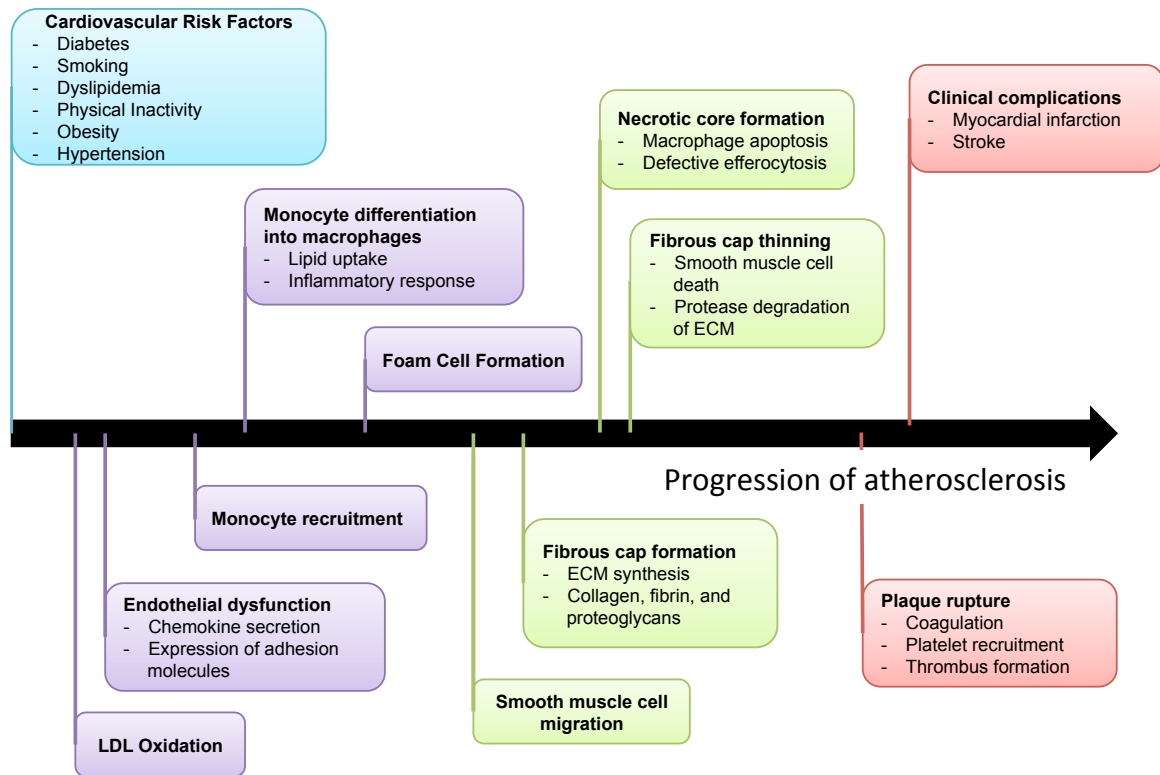


Figure 1 | **The progression of atherosclerosis.** An overview of the initiation and progression of atherosclerosis, with the various cardiovascular risk factors that are known to accelerate atherosclerosis outlined in blue. The early stages of plaque formation are present at a young age (purple), with progression to more advanced plaque occurring over decades (green) and eventually leading to the clinical consequences of atherosclerosis (red).

1.2 DIABETES MELLITUS

The risk of cardiovascular disease is increased 3-fold in individuals affected by diabetes (Barrett-Connor, Cohn, Wingard, & Edelstein, 1991; Haffner, 1998; W. L. Lee, Cheung, Cape, & Zinman, 2000). Diabetes Mellitus is a metabolic disorder that is characterized by a deficiency in insulin action resulting from elevated blood glucose levels (Mohler, He, Wu, Hwang, & Miller, 2009). It affects approximately 3-5% of individuals in western societies, with a global occurrence of more than 366 million as of

2011 (Guariguata, Whiting, Weil, & Unwin, 2011; Zimmet, Alberti, & Shaw, 2001). There are two common forms of diabetes, known as type 1 (T1D) and type 2 (T2D) diabetes. T1D results from a loss of beta cells in the pancreas. This occurs as a result of an autoimmune response against the beta cells, resulting in insulin deficiency (Faideau, Larger, Lepault, Carel, & Boitard, 2005). In contrast, T2D involves a combination of peripheral insulin resistance and subsequent beta cell loss. Both T1D and T2D are characterized by chronic hyperglycemia, which can lead to complications in the kidneys, nerves, eyes, heart, and blood vessels (Norris et al., 2002; Pyram, Kansara, Banerji, & Loney-Hutchinson, 2012). This increase in blood glucose is associated with an increased risk of both micro- and macro-vascular diseases (Brownlee, 2001).

Much of the research examining the link between diabetes and atherosclerosis has focused on hyperglycemia-associated increased glycolytic pathway activity and oxidative stress (Giacco & Brownlee, 2010; Lin et al., 2005). Increased glycolysis in arterial endothelial cells causes a change in voltage across the mitochondrial membrane leading to an increase in the production of reactive oxygen species (ROS) (Giacco & Brownlee, 2010; Korshunov, Skulachev, & Starkov, 1997). Overproduction of ROS molecules results in activation of pro-inflammatory cytokines that are associated with an increased risk of atherosclerosis (Y. W. Lee, Kim, Lee, & Hirani, 2010). However, virtually every well-controlled clinical trial examining anti-oxidant treatments has failed to show a cardiovascular benefit (Lonn et al., 2002; Yusuf, Dagenais, Pogue, Bosch, & Sleight, 2000). Therefore, examination of these pathways, as well as other metabolic factors, is required to further clarify the link between diabetes and cardiovascular disease.

1.3 DYSLIPIDEMIA

One of the most common risk factors in the development of atherosclerosis is an imbalance of cholesterol and triglycerides in the circulating plasma. Cholesterol cannot diffuse through the blood on its own, but must be carried by means of water-soluble lipoproteins. Five major groups of lipoproteins have been identified, which transport triglycerides and cholesterol between cells. The smallest lipoproteins, known as high-density lipoproteins (HDL), are involved in the clearance of cholesterol from peripheral tissues, a process known as reverse cholesterol transport (RCT) (Ross & Glomset, 1973). Conversely, low-density lipoproteins (LDL) move cholesterol and triglycerides from the liver to peripheral cells. The development of atherosclerosis has been associated with a higher LDL to HDL ratio (Nicholls et al., 2007; Tani, Matsumoto, Nakamura, Nagao, & Hirayama, 2012). All LDL particles contain a single apolipoprotein B-100 (ApoB-100) molecule that acts as a ligand for the low-density lipoprotein receptor (LDLR). This receptor removes LDL cholesterol from the plasma and therefore is responsible for the regulation of total plasma cholesterol levels (Brown & Goldstein, 1986). One commonly used mouse model to investigate atherosclerotic development is the LDLR knockout mouse model (Ishibashi et al, 1993). Genetic deletion of the LDLR gene results in a moderate increase in plasma cholesterol levels with regular chow-diet feeding. When fed a diet high in cholesterol, LDLR knockout mice exhibit a significant increase in plasma cholesterol levels and develop advanced atherosclerotic lesions in the aortic root (Ishibashi et al, 1994). Thus, the LDLR knockout mouse has become a commonly used model of diet-induced atherosclerosis.

The precise molecular mechanisms by which dyslipidemia, and other cardiovascular risk factors, promote atherosclerosis remain unclear. However, recent evidence has pointed to a role in ER stress and the activation of the unfolded protein response (Erbay et al., 2009; Khan, Pichna, Shi, Bowes, & Werstuck, 2009; Werstuck et al., 2006).

ER STRESS

The endoplasmic reticulum is a membranous organelle that surrounds the nucleus of every eukaryotic cell and is involved in various metabolic processes, including both lipid and protein synthesis. It is also the main organelle for calcium regulation in the cell (Rizzuto et al., 2003). The phospholipid membrane of the ER provides a barrier between the cytoplasm and the ER lumen to allow for suitable conditions for protein synthesis and processing to occur. During translation, many proteins are translocated into the ER where they are glycosylated, folded and further modified. Dysregulation in protein modification and folding leads to the accumulation of misfolded proteins within the ER – a condition known as ER stress. These misfolded proteins are known to form aggregates in both the ER as well as the cytoplasm, which is thought to be highly toxic to the cell (Bence, Sampat, & Kopito, 2001). ER stress has been associated with a variety of disease states, including liver and kidney disease, diabetes, inflammation, as well as neurodegenerative disorders such as Alzheimer's disease (AD), Parkinson's disease, and bipolar disorder (L. Ozcan & Tabas, 2012). Specifically, risk factors that promote the development of atherosclerosis, such as diabetes and dyslipidemia, are associated with elevated levels of ER stress.

1.4.1 *Diabetes Mellitus and ER stress*

In vitro and *in vivo* evidence have shown that hyperglycemia promotes an increase in glucose flux through the hexosamine biosynthetic pathway and the accumulation of intracellular glucosamine (U. Ozcan et al., 2004) (Fig. 2a). Studies have revealed glucosamine as a potent ER stress-inducing agent in vascular cells as well as in an ApoE-deficient mouse model (Beriault, Sharma, Shi, Khan, & Werstuck, 2011; A. J. Kim, Shi, Austin, & Werstuck, 2005). Although it is still not known how glucosamine induces ER stress, studies have shown that high levels of glucosamine can disrupt N-linked glycosylation of ApoB-100 in a human liver carcinoma (HepG2) cell line (Qiu, Avramoglu, Rutledge, Tsai, & Adeli, 2006). It is hypothesized that glucosamine-induced ER stress plays a role in the development of atherosclerosis through activation of both the nuclear factor-kappa B (NF- κ B) and the sterol regulatory element binding protein (SREBP) pathways (A. J. Kim, et al., 2005; Werstuck et al., 2001).

1.4.2 *Dyslipidemia and ER stress*

Another contributor to ER stress-induction is an imbalance of triglycerides and cholesterol. High levels of unesterified cholesterol are thought to be toxic within the ER. This is possibly due to a depletion of ER calcium stores as well as an increase in cholesterol in the ER membrane, which can lead to membrane dysfunction (Feng et al., 2003) (Fig. 2b). Chronic loading of unesterified cholesterol into macrophages leads to subsequent activation of C/EBP Homologous Protein (CHOP) and eventually activation of cell death pathways (Feng, et al., 2003). Although unesterified cholesterol can activate

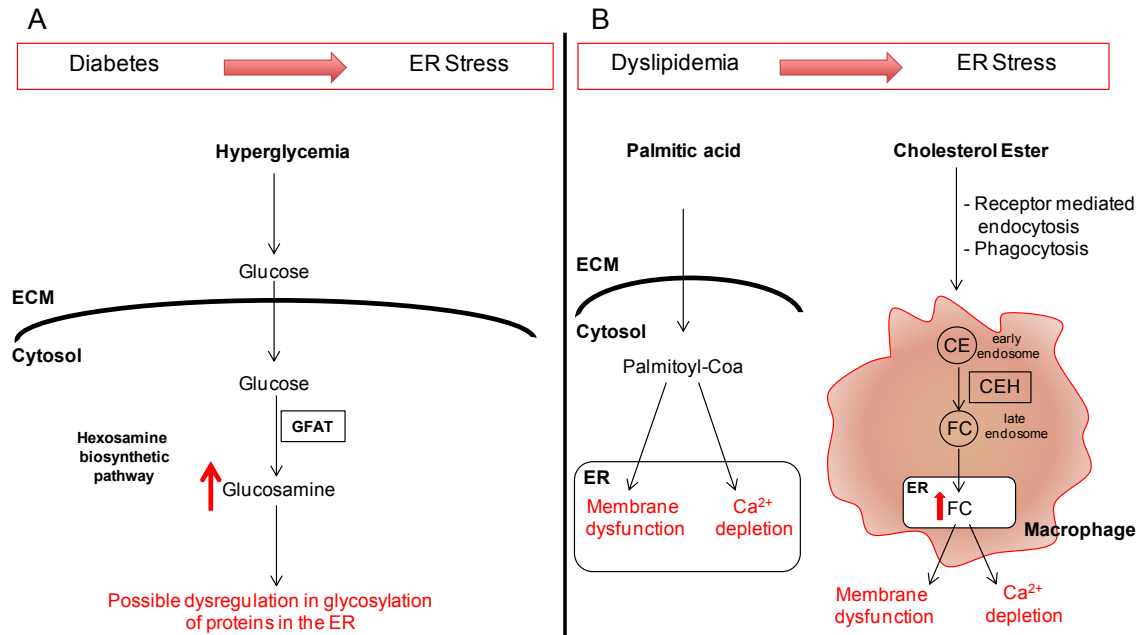


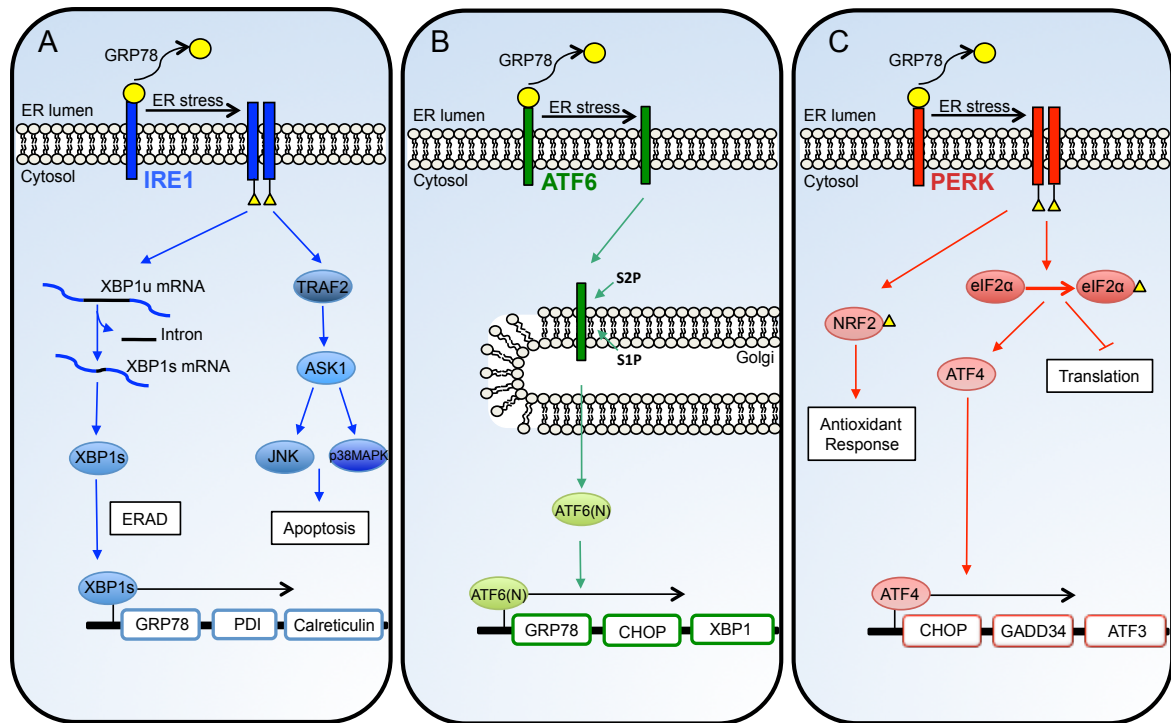
Figure 2 | **Mechanisms by which diabetes and dyslipidemia cause ER stress.** A | A consequence of diabetes is an increase in glucose levels within the cell. Under these conditions there is an increase in glucose flux through the hexosamine biosynthetic pathway leading to an increase in intracellular glucosamine. Disruption in this pathway and an increase in glucosamine have been shown to cause ER stress, possibly due to disruption of N-linked glycosylation. B | Both the saturated fatty acid palmitate and unesterified cholesterol have been shown to cause ER stress. Palmitate translocates to the cytosol where it is converted to palmitoyl-CoA. In the ER, palmitate can incorporate into the lipid components of the ER membrane, leading to membrane dysfunction and subsequent ER stress. Palmitate has also been shown to induce calcium release from the ER, which can also lead to ER stress. In addition, free cholesterol (FC) loading into macrophages and other cell types causes ER stress. Cholesterol esters (CE) are converted into free cholesterol by cholesterol ester hydrolase (CEH), where they are trafficked from late endosomes into the ER. Free cholesterol can incorporate into the ER membrane leading to membrane dysfunction, as well as depletion of calcium stores, both resulting in ER stress.

apoptotic signaling pathways, cholesterol esters that are seen in early foam cell formation do not induce apoptosis, possibly due to their compartmentalization in intracellular lipid vesicles. Unesterified cholesterol has also been found to induce expression of tumor necrosis factor alpha (TNF- α) and interleukin 6 (IL-6) cytokines in macrophages by activating the NF- κ B pathway and therefore has a role in activation of pro-inflammatory pathways in the developing plaque (Y. Li et al., 2005). In addition to unesterified

cholesterol, the saturated fatty acid palmitate has also been associated with ER stress (Gwiazda, Yang, Lin, & Johnson, 2009) (Fig. 2b). Laybutt and colleagues (2007) have shown that palmitate can trigger ER stress in a mouse pancreatic beta cell line (MIN6) contributing to pancreatic β cell apoptosis (Laybutt et al., 2007). In addition, palmitate was found to cause an imbalance in Ca^{2+} homeostasis in the ER, another factor contributing to the initiation of ER stress and UPR activation (Gwiazda, et al., 2009; Wei, Bai, Song, & Hao, 2009). Finally, a study done in Chinese hamster ovary (CHO) cells as well as rat H9c2 cardiomyocytes showed that palmitate-induced ER stress resulted in the incorporation of palmitate into the lipid component of the ER membrane, leading to ER membrane dysfunction (Borradaile et al., 2006). Therefore, both unesterified cholesterol as well as saturated fatty acids such as palmitic acid have been shown to induce ER stress within various cell types.

1.5 THE UNFOLDED PROTEIN RESPONSE

As a direct response to ER stress, cells activate the unfolded protein response (UPR), which works to increase the expression of molecular chaperones and foldases, as well as to enhance unfolded protein degradation (Travers et al., 2000). If the level of ER stress is too great, the cell responds by initiating apoptosis. There are three transmembrane proteins involved in the activation of the UPR; ATF6, PERK, and IRE1 (Fig. 3). In the absence of ER stress, glucose regulatory protein 78 (GRP78) is bound to each of these transmembrane stress sensors. GRP78 is retained within the ER through a specific KDEL anchor sequence (Suzuki, Lu, Zahed, Kita, & Suzuki, 2007). When unfolded proteins accumulate, GRP78 is released and binds to misfolded proteins to aid in



Adapted from Hetz (Nat Rev Mol Cell Biol 2012) (Hetz, 2012)

Figure 3 | Overview of the Unfolded Protein Response. It is well established that conditions of ER stress activate three distinct pathways (PERK, IRE1, and ATF6) that make up the UPR. Under normal conditions in the ER, the molecular chaperone GRP78 is bound to each of these transmembrane proteins. Upon ER stress, GRP78 is released from these proteins to bind to misfolded proteins and aid in their refolding. A | Activated IRE1 exhibits endoribonuclease activity leading to splicing of mRNA encoding the X-box-binding-protein (XBP1). XBP1 acts as a transcription factor to promote expression of several ER chaperones. In addition, activation of IRE1 can induce cell death by recruiting TRAF2 to the ER membrane. This results in activation of apoptosis-signaling kinase-1 (ASK1), which can activate both the JNK and p38MAPK pathways leading to apoptosis. B | Dissociation of GRP78 from ATF6 upon ER stress results in translocation from the ER membrane to the Golgi. Site-1 and site-2 proteases cleave ATF6, resulting in migration to the nucleus where it acts as a transcription factor to promote expression of various molecular chaperones. C | Activation of PERK results in phosphorylation of the α subunit of the eukaryotic translation initiation factor 2 (eIF2 α) protein, which attenuates further translation. PERK activation also results in ATF4 translation which controls transcription of molecular chaperones and genes involved in apoptosis. In addition, PERK activation can also phosphorylate nuclear factor erythroid 2-related factor 2 (NRF2), which regulates redox metabolism.

their refolding (Jousse et al., 1999). Binding of GRP78 to unfolded proteins allows for other factors, such as protein disulfide isomerase (PDI), to assist in proper protein folding.

PDI contributes to protein folding by aiding in disulfide bond rearrangement (J. Li &

Holbrook, 2004). Activation of activating transcription factor 6 (ATF6) and inositol-requiring enzyme-1 (IRE1) results in increased production of molecular chaperones and foldases through transcriptional regulation and also promotes degradation of unfolded proteins (Gotoh, Oyadomari, Mori, & Mori, 2002; Rutkowski et al., 2008) (Fig. 3a and 3b). Protein kinase RNA-like endoplasmic reticulum kinase (PERK) activation results in inhibition of proteins involved in general protein translation (Rutkowski, et al., 2008). (Fig. 3c). Failure of these pathways to aid in proper protein folding results in induction of apoptosis through the intrinsic (mitochondrial) pathway involving CHOP expression (Song, De Sarno, & Jope, 2002). CHOP, a protein encoded by GADD153 (growth arrest and DNA damage inducible gene 153), initiates apoptosis through regulation of the anti-apoptotic mitochondrial protein B-cell lymphoma 2 (Bcl-2) (J. Li & Holbrook, 2004). All three UPR pathways are thought to be required for maximal expression of CHOP (Oyadomari & Mori, 2004).

In addition to apoptosis, conditions of ER stress have been shown to trigger other pathways involved in the acceleration of atherosclerosis. This can be seen through activation of the transcription factor nuclear factor-kappa B (NF- κ B) and the sterol regulatory element binding proteins (SREBP), which promote inflammation and lipid accumulation, respectively (A. J. Kim, et al., 2005; Werstuck, et al., 2001). In mouse models of hyperglycemia, hyperhomocysteinemia and obesity, elevated levels of ER stress are associated with accelerated atherosclerosis (U. Ozcan, et al., 2004; Werstuck, et al., 2001; Zhou et al., 2004). While the molecular mechanisms that link chronic ER stress and the unfolded protein response to the acceleration of atherosclerosis remain unclear,

growing evidence has supported a role for ER stress-induced activation of the protein kinase glycogen synthase kinase (GSK)-3 in several of the hallmark features of atherosclerosis, including lipid accumulation, apoptosis, and inflammation.

1.6 GLYCOGEN SYNTHASE KINASE 3

1.6.1 Discovery

Glycogen synthase kinase-3 is a highly conserved serine/threonine kinase that was first classified as the rate-limiting enzyme in the final step of glycogen synthesis (Rylatt et al., 1980; Woodgett & Cohen, 1984). Growing interest in this protein began when it was identified as a key regulatory enzyme in both the insulin and WNT signaling pathways (Doble & Woodgett, 2003). To date, GSK-3 has been implicated in many physiological processes, including; cell cycle regulation, cell proliferation, and cell growth and development (Patel, Doble, & Woodgett, 2004; Rubinfeld et al., 1996; Xu, Kim, & Gumbiner, 2009). A multitude of GSK-3 substrates have been identified, including; transcription factors, structural proteins, and metabolic enzymes (Doble & Woodgett, 2003; Frame & Cohen, 2001). Many studies involving GSK-3 have specifically focused on its role in neurological disorders, such as Alzheimer's disease and bipolar disorder. This protein was first implicated in Alzheimer's disease because of its ability to phosphorylate and subsequently regulate Tau protein (Ishiguro et al., 1993). However, since this discovery, GSK-3 has been associated with many other disease states, including; cancer, T1D, T2D and more recently, cardiovascular disease (Eldar-Finkelman, Schreyer, Shinohara, LeBoeuf, & Krebs, 1999; Frame & Cohen, 2001; Laviola et al.,

2001; Phiel, Wilson, Lee, & Klein, 2003). Therefore, GSK-3 has become a lucrative target for therapeutic interventions in multiple disease states.

1.6.2 Composition and Structure

There are two forms of GSK-3 (α and β), encoded by distinct genes and sharing 98% sequence homology in their kinase domain (Woodgett, 1990) (Fig. 4). The gene encoding GSK-3 α is located on mouse chromosome 7/human chromosome 19, while the GSK-3 β gene is located on mouse chromosome 16/human chromosome 3 (Kaidanovich-Beilin & Woodgett, 2011; Shaw et al., 1998). These two forms also differ in molecular mass, with a molecular weight of 51kDa and 47kDa, for GSK-3 α and GSK-3 β , respectively. A difference in molecular weight between these two proteins is a result of an N-terminal glycine rich extension on GSK-3 α (Dajani et al., 2001). In addition, a minor splice variant of GSK-3 β , termed GSK-3 β 2, exists as a result of a 13-residue insert within the kinase domain (Mukai, Ishiguro, Sano, & Fujita, 2002).

GSK-3 α/β shares similar structural features with other protein kinases, including; a small N-terminal lobe, large C-terminal lobe, and an ATP-binding pocket located between the two regions (Dajani, et al., 2001). The N-terminal region consists mainly of β -sheets, while the majority of the C-terminal region contains α -helices. GSK-3 β substrates have been shown to incorporate themselves into a highly conserved binding pocket consisting of three essential amino acids; lysine 205, arginine 96 and arginine 108 (Bax et al., 2001; Dajani, et al., 2001). In addition, this kinase is unique in that it prefers

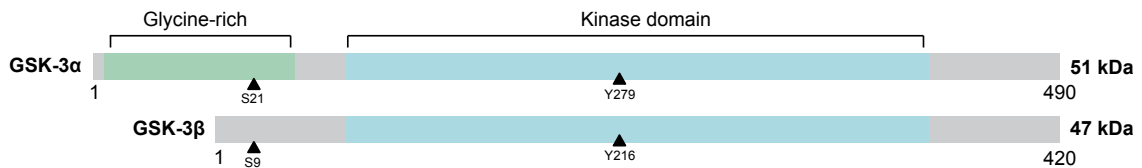
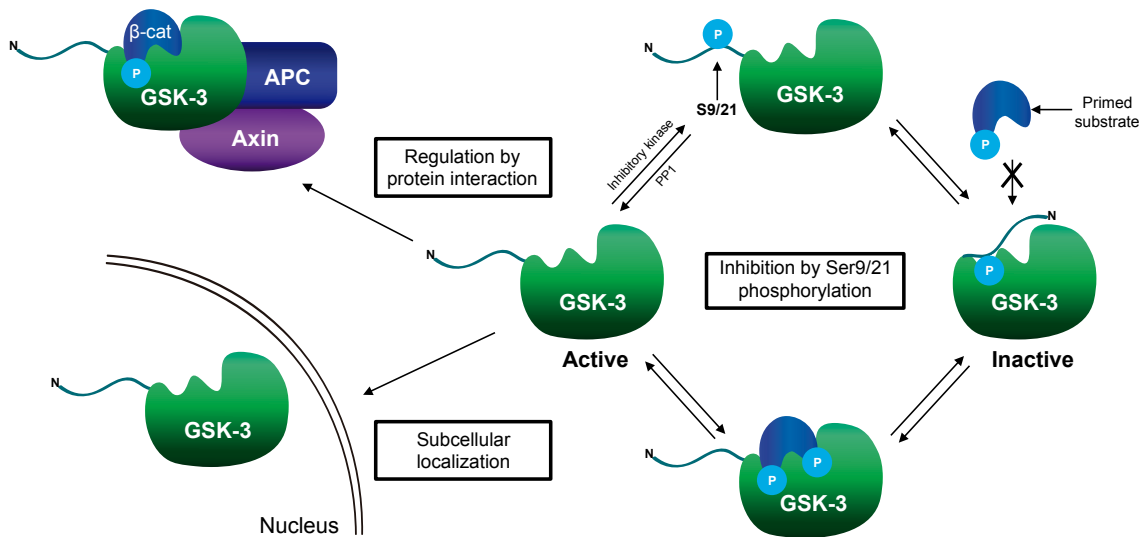


Figure 4 | **Schematic representation of murine GSK-3 α and GSK-3 β .** GSK-3 α and GSK-3 β share a conserved kinase domain. GSK-3 α has a unique glycine rich N-terminal domain. Serine and tyrosine phosphorylation sites are indicated (Woodgett, 1990).

substrates that have been pre-phosphorylated by other kinases (Dajani, et al., 2001). This “primed” residue on GSK-3 substrates is located C-terminal to the site of subsequent GSK-3 phosphorylation (Fiol, Mahrenholz, Wang, Roeske, & Roach, 1987). The overwhelming number of identified substrates GSK-3 α/β phosphorylates leads to the convergence of many regulatory intracellular signaling pathways (Sutherland, 2011).

1.6.3 Properties and Function

Due to the multitude of pathways that involve GSK-3, accurate regulation of this protein is vital to ensure proper control of cellular processes. Three key mechanisms are known to regulate the function of GSK-3, including phosphorylation, subcellular localization, and protein complex formation (Bijur & Jope, 2003; Eldar-Finkelman, et al., 1999; Hoshi et al., 1995; Stambolic & Woodgett, 1994) (Fig. 5). This protein is highly active under resting conditions and is one of the few kinases inhibited by extracellular stimuli (Stambolic & Woodgett, 1994). The activity of GSK-3 is positively regulated by phosphorylation of specific tyrosine residues in the kinase domain of both isoforms, specifically Tyr279 of GSK-3 α and Tyr216 of GSK-3 β . Phosphorylation at positions Ser21 and Ser9 results in inhibition of GSK-3 α and GSK-3 β , respectively (Cross, Alessi, Cohen, Andjelkovich, & Hemmings, 1995; Stambolic & Woodgett, 1994). The negative



Adapted from Beurel and Jope (Prog Neurobiol 2006) (Beurel & Jope, 2006)

Figure 5 | **Regulation of GSK-3 α/β .** Regulation of GSK-3 occurs through several different mechanisms. Phosphorylation of serine 9 in GSK-3 β and ser21 in GSK-3 α results in inhibition of the protein as a result of a pseudosubstrate that blocks the active site of the kinase. Protein phosphatase 1 (PP1) removes the phosphate from GSK-3 leading to reactivation. Unphosphorylated ser9/21 allows for primed substrates to enter the active site of GSK-3 where they are subsequently phosphorylated. GSK-3 is also regulated by subcellular localization. In the WNT signaling pathway, interaction of GSK-3 with the tumor suppressor APC and the scaffolding protein Axin leads to phosphorylation of the transcription factor β -catenin.

regulation by N-terminal serine phosphorylation is achieved through a pseudosubstrate that blocks the active site of GSK-3 to substrate access (Frame & Cohen, 2001). This protein is mainly localized in the cytoplasm, but has been found in other cellular compartments such as the nucleus and mitochondria (Bijur & Jope, 2001). It was recently found that N-terminal cleavage of GSK-3 α results in its accumulation in the nucleus, which suggests that cytoplasmic localization of this protein is regulated through its N-terminal domain (Azoulay-Alfaguter et al., 2011). In the canonical Wnt signaling pathway, GSK-3 acts as a constitutively active antagonist resulting from protein complex formation (Zeng et al., 2005). Absence of Wnt ligands results in GSK-3 binding to the tumor suppressor adenomatous polyposis coli (APC), the scaffolding protein Axin, and

the transcriptional co-activator β -catenin. β -catenin is phosphorylated by GSK-3 and subsequently targeted for proteasome dependent degradation (Wu, Huang, Garcia Abreu, & He, 2009; Yost et al., 1996). The large number of processes regulated by GSK-3 implies that activation of this protein in various cellular pathways is tightly regulated.

The multitude of signal transduction pathways that involve GSK-3 poses a significant challenge in determining the specificity for therapeutic intervention. Over 100 cellular proteins have been identified as substrates for GSK-3 (Sutherland, 2011). Equally challenging is the redundancy the two forms have been shown to play in several molecular pathways, including the canonical Wnt signaling pathway. Despite the structural similarity in the kinase domain of GSK-3 α/β , these two forms are not functionally interchangeable, as GSK-3 β knockout mice are embryonic lethal (Hoeflich et al., 2000; Soutar et al., 2010). GSK-3 β ^{-/-} mice exhibit severe liver degeneration during mid-gestation as a result of increased transcriptional expression of tumor necrosis factor (TNF) (Hoeflich, et al., 2000). On the other hand, GSK-3 α ^{-/-} mice are viable and exhibit improved glucose and insulin sensitivity (MacAulay et al., 2007). These mice also display reduced fat mass, decreased locomotion, and increased sensitivity to environmental cues (Kaidanovich-Beilin & Woodgett, 2011; MacAulay, et al., 2007).

Although most attention has focused on GSK-3 β , advances in the understanding of this kinase have shown that both forms are important in a variety of cellular processes. Small molecule inhibitors, as well as inducible and tissue-specific gene knockout mouse models, have provided new tools for characterizing the two GSK-3 forms in different cellular pathways. Distinguishing the specificity of this protein, as well as the functional

differences between forms, will be critical in understanding its role in cardiovascular disease.

1.7 GLYCOGEN SYNTHASE KINASE-3 AND ATHEROSCLEROSIS

1.7.1 *GSK-3 and Lipid Accumulation*

Fatty acid biosynthesis is a complex process that occurs in both the cytosol and ER and eventually leads to the formation of triglycerides and other complex lipids. Activation of the UPR proteins IRE1, ATF6, and eIF2 α have been shown to promote lipid biosynthesis in hepatocytes (Gaspar et al., 2008; M. Y. Lee, Jung, Lee, & Han, 2008; Oyadomari, Harding, Zhang, Oyadomari, & Ron, 2008; Rutkowski, et al., 2008). In HepG2 cells, ER stress-induced lipid accumulation was significantly reduced upon exposure to the GSK-3 inhibitor valproate (A. J. Kim, et al., 2005). Furthermore, GSK-3 deficient cultured mouse embryonic fibroblasts showed protection against ER stress-induced lipid accumulation (Bowes, Khan, Shi, Robertson, & Werstuck, 2009). In human hepatocarcinoma HuH-7 cells and immortalized mouse liver ML-1 cells that were treated with tunicamycin to induce ER stress, the GSK-3 β inhibitor VIII resulted in a 50% decrease in lipid accumulation (Chang et al., 2011). *In vivo*, both hyperglycemic and hyperhomocysteinemic apolipoprotein E (ApoE)-deficient mice fed a valproate supplemented diet showed a significant decrease in hepatic lipid accumulation (McAlpine, Bowes, Khan, Shi, & Werstuck, 2011). Therefore, inhibition of GSK-3 by various methods seems to negatively regulate lipid biosynthesis in various cell types as well as in mouse liver.

GSK-3 has also been shown to have a significant effect on the expression of proteins involved in lipid biosynthesis. Sterol regulatory element binding proteins (SREBPs) are transcription factors that regulate both cholesterol and lipid biosynthesis. They are made up of three subtypes; SREBP-1a and SREBP-1c are more specific to fatty acid synthesis and glucose/insulin metabolism, whereas SREBP-2 is specific for cholesterol biosynthesis (Pai, Guryev, Brown, & Goldstein, 1998). ER stress has been shown to activate SREBP1/2 (Colgan, Tang, Werstuck, & Austin, 2007; J. N. Lee & Ye, 2004; Werstuck, et al., 2001). Overexpression of the molecular chaperone GRP78 causes resistance to SREBP activation (Werstuck, et al., 2001). In both hepatocytes and adipocytes, GSK-3 was shown to regulate the SREBP-1c protein and to increase transcriptional expression of several downstream targets such as fatty acid synthase (K. H. Kim et al., 2004). In addition, GSK-3 inhibition by valproate supplementation decreased SREBP-2 production as well as free cholesterol biosynthesis (A. J. Kim, et al., 2005). Further research is needed to understand how GSK-3 regulates the SREBP family under conditions of ER stress.

1.7.2 GSK-3 and the Inflammatory Response

During the last decade, GSK-3 has been identified as a key regulator in the immune system and therefore has become a potential target to treat various autoimmune diseases. Inhibitors of GSK-3 have been shown to push the immune response from a pro-inflammatory to an anti-inflammatory cytokine balance (Wang, Brown, & Martin, 2011). Studies have shown that activation of the toll-like receptor (TLR) signaling pathway by LPS-stimulation leads to an increase in the production of inflammatory cytokines

(Medzhitov, Preston-Hurlburt, & Janeway, 1997). TLRs are mainly expressed on cells important in the development of atherosclerotic plaque, such as macrophages and dendritic cells. The link between TLR activation and GSK-3 was first implicated by the ability of activated TLR-2 to increase activation of the transcription factor NF- κ B as a result of PI3K activation (Martin et al., 2003). More specifically, inhibition of PI3K resulted in a reduction of the anti-inflammatory cytokine IL-10 and an increase in IL-12 production (Martin, et al., 2003). Further studies showed that LPS-stimulated TLR-2 resulted in activation of the protein kinase AKT and subsequently increased GSK-3 β phosphorylation at the Ser9 residue, resulting in its inhibition (Martin, Rehani, Jope, & Michalek, 2005). Upon addition of several GSK-3 inhibitors to LPS-stimulated human monocytes, production of IL-10 was increased. Finally, upon siRNA-mediated knockdown of GSK-3 β , levels of pro-inflammatory cytokines such as IL-1 β , IL-6, TNF and IL-12 were reduced (Martin, et al., 2005). These findings suggest a protective role for GSK-3 inhibition on the pro-inflammatory signaling pathway.

Type-1 and type-2 interferons (IFN) have also been implicated in the development of atherosclerosis. IFN- γ is a key regulator of the inflammatory pathway that is highly expressed in atherosclerotic lesions. Studies have shown that incorporation of IFN- γ in LPS-stimulated macrophages results in an increase in GSK-3 α/β activation by suppressing phosphorylation at Ser9/21, which causes a decrease in IL-10 production (Hu et al., 2006). GSK-3 β has also been implicated as a regulator in other signaling cascades, such as the MyD88 and MAPK/ERK1/2 pathways (Rehani, Wang, Garcia, Kinane, & Martin, 2009; Wang et al., 2008). In the MAPK pathway, active GSK-3 β results in a

decrease in ERK1/2 activation, leading to a suppression of the anti-inflammatory cytokine IL-1Ra in LPS-stimulated monocytes (Rehani, et al., 2009). Finally, the effects of GSK-3 inhibition on the immune response have been looked at *in vivo* in different mouse models of inflammation. In a study done by Martin *et al.* (2005), male C57BL/6 mice were injected with *E.coli* K235 LPS to induce an inflammatory response (Martin, et al., 2005). Upon administration of the GSK-3 inhibitor SB216763, survival rates of the mice increased, production of the pro-inflammatory cytokines IL-12p40, IFN- γ , and IL-6 decreased, and IL-10 production increased (Martin, et al., 2005).

Although the effects of GSK-3 inhibition have been studied *in vivo* on multiple disease states such as collagen-induced arthritis (Cuzzocrea et al., 2006), asthma (Bao et al., 2007), and experimentally induced colitis (Whittle et al., 2006), its anti-inflammatory effects in oxLDL stimulated macrophages in the development of atherosclerosis has yet to be determined. However, its important role in the inflammatory response makes it an attractive target in the therapeutic treatment of cardiovascular disease.

1.7.3 GSK-3 and Apoptosis

There is much controversy over the exact role GSK-3 plays in regulating apoptotic signaling pathways. GSK-3 has been described to function as a pro-apoptotic kinase in the mitochondrial intrinsic apoptotic pathway, but as an anti-apoptotic kinase in the extrinsic apoptotic pathway. Studies done in several types of cancer cells, such as pancreatic and colorectal cancer, have shown that inhibition of this protein attenuates cell proliferation and increases apoptosis (Ougolkov, Fernandez-Zapico, Savoy, Urrutia, &

Billadeau, 2005; Shakoori et al., 2007). In leukemic cells, pharmacological inhibition of GSK-3 β , which increased Ser9 phosphorylation, resulted in an increase in apoptosis by dephosphorylating bcl-2 (Mirlashari, 2012). GSK-3 β was also shown to have a role in preventing p53-induced apoptosis, possibly as a protective role in the initial stages of ER stress (Qu et al., 2004). Linking ER stress-induced activation of GSK-3 to programmed cell death will be beneficial in understanding the molecular mechanisms of macrophage apoptosis and necrotic core formation in the development of atherosclerosis.

In the intrinsic apoptotic signaling pathway, which can be stimulated by numerous cell damage pathways such as DNA damage, oxidative stress, and ER stress, GSK-3 activation promotes cell death. Many studies have shown that GSK-3 inhibition can protect cells from ER stress-induced apoptosis, however the exact influence GSK-3 has on the UPR signaling pathway remains unclear (A. J. Kim, et al., 2005; Song, et al., 2002). Under conditions of ER stress, GSK-3 was shown to positively regulate caspase-2 (Raven et al., 2008). In addition, GSK-3 activation in neuronal cells has been shown to promote both caspase-3 and caspase-9 activation, with pharmacological inhibition of GSK-3 attenuating cell death (Brewster et al., 2006; Song, et al., 2002; Takadera, Fujibayashi, Kaniyu, Sakota, & Ohyashiki, 2007). Valproate, a small molecular inhibitor of GSK-3, was shown to protect cells from ER stress-induced apoptosis in HepG2 cells (A. J. Kim, et al., 2005). A recent study by Ibrahim *et al.* (2011) showed that shRNA knockdown of either GSK-3 α or GSK-3 β resulted in protection against hepatocyte lipoapoptosis by preventing upregulation of PUMA, a pro-apoptotic protein that promotes BAX activation (Ibrahim et al., 2011). In terms of the UPR, GSK-3 inhibition has been shown to result in

an upregulation of the molecular chaperone GRP78 as well as the Bcl-2 protein (Hiroi, Wei, Hough, Leeds, & Chuang, 2005). Finally, it was found that the pro-apoptotic transcription factor CHOP/GADD153 is upregulated by GSK-3 in neuronal cells (Meares et al., 2011). ER stress has been shown to activate apoptosis in many other cell types, including endothelial cells and macrophages (Zinszner et al., 1998). Therefore, understanding these cellular mechanisms will be important in the development of GSK-3 inhibitors to treat diseases such as atherosclerosis.

CHAPTER 2: HYPOTHESIS AND OBJECTIVES

2.1 RATIONALES AND HYPOTHESIS

An accumulating amount of evidence suggests that ER stress promotes the activation of several pathways that are involved in the progression of atherosclerosis, including inflammation, lipid accumulation, and apoptosis (Colgan, et al., 2007; A. J. Kim, et al., 2005; Pahl & Baeuerle, 1995; Thorp et al., 2009; Zinszner, et al., 1998). Specifically, our lab and others have shown that several of the common risk factors that accelerate atherosclerosis, including hyperglycemia and dyslipidemia, are associated with elevated levels of ER stress (Bowes, et al., 2009; Khan, et al., 2009; McAlpine, et al., 2011). We believe that cardiovascular risk factors that cause chronic ER stress lead to the induction of pro-atherogenic pathways through activation of the protein GSK-3 α/β (Fig. 6). Valproate, an inhibitor of GSK-3, was shown to attenuate atherosclerosis in an ApoE^{-/-} mouse model of accelerated atherosclerosis (Bowes, et al., 2009). In order to directly test the role of GSK-3 α in atherosclerotic development, GSK-3 α deficient mice were generated and crossed with a LDLR^{-/-} mouse model. We hypothesize that a deficiency of GSK-3 α in LDLR^{-/-} mice will attenuate the initiation and progression of atherosclerosis.

2.2 OBJECTIVES

The overall objective is to characterize the role of GSK-3 α in the development of atherosclerosis using both a novel LDLR/GSK-3 α dKO mouse model as well as bone marrow transplantation strategies. Firstly, the effect of the GSK-3 inhibitor valproate on plaque formation will be analyzed in an LDLR deficient mouse model of accelerated

atherosclerosis. Secondly, we intend to examine the development of atherosclerosis by placing LDLR^{-/-}GSK-3 α ^{+/+}, LDLR^{-/-}GSK-3 α ^{+/-}, and LDLR^{-/-}GSK-3 α ^{-/-} mice on a high fat diet and examining lesion volume in the aortic root. ER stress levels in aortic lesions as well as in the liver will be determined to validate the hypothesis that GSK-3 functions downstream of ER stress. To establish the effect of GSK-3 α deficiency on hepatic lipid accumulation, analysis of total cholesterol and triglycerides as well as expression of lipid biosynthetic proteins will be carried out. Furthermore, the cellular mechanisms by which GSK-3 α activation leads to inflammation and lipid accumulation will be evaluated through examination of peritoneal macrophages. Finally, to assess the effect of GSK-3 α deficient macrophages on lesion development, BMT strategies will be utilized and plaque size in the aortic root will be analyzed.

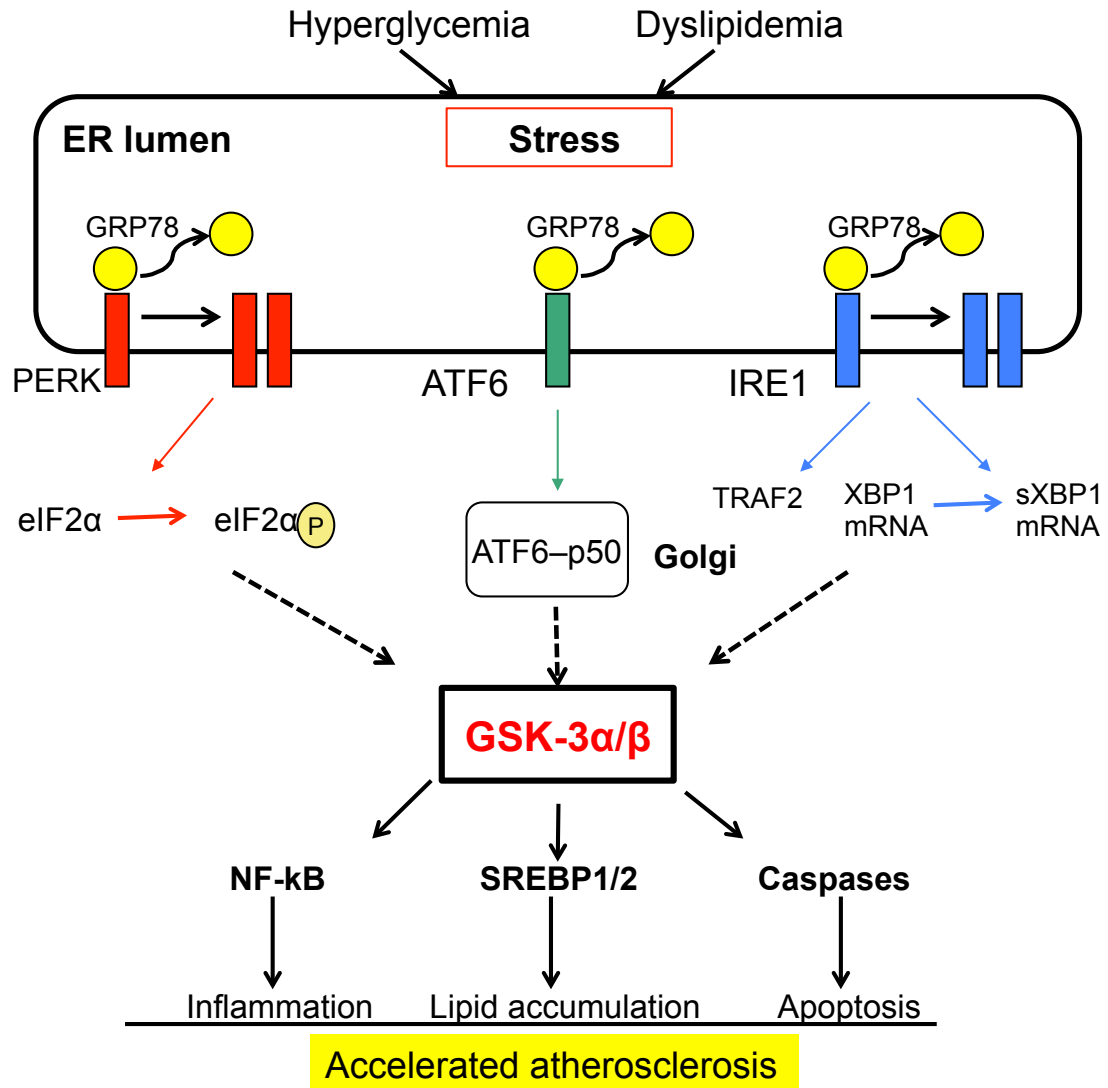


Figure 6 | **Working model of the association between hyperglycemia and dyslipidemia in the induction of ER stress, unfolded protein response activation, and progression of atherosclerosis.** Hyperglycemia and dyslipidemia are characteristics of diabetes. Both of these conditions have been associated with an accumulation of misfolded proteins leading to ER stress. It is well established that conditions of ER stress activate three distinct pathways (PERK, IRE1, and ATF6) that make up the UPR. These pathways act together to alleviate the stress by increasing transcriptional expression of molecular chaperones/foldases and inhibiting further translation of proteins. ER stress is linked to lipid accumulation, apoptosis, and inflammation, all hallmark features of atherosclerosis. There is accumulating evidence that ER stress can also activate the kinase GSK-3α/β, however the mechanism by which this occurs is not yet known.

CHAPTER 3: MATERIALS AND METHODS

3.1 ANIMAL MODEL AND GENOTYPING

Five week old LDLR^{-/-}GSK-3 α ^{+/+}, LDLR^{-/-}GSK-3 α ^{+/-}, and LDLR^{-/-}GSK-3 α ^{-/-} mice were randomly separated into two groups; one group remained on a defined chow diet (Harlan Teklad, TD92078) and the other group was fed a high fat diet containing 21% milk fat and 0.2% cholesterol (Harlan Teklad TD97363) to induce dyslipidemia. A subset of the LDLR^{-/-} mice on both a chow diet and high fat diet were further divided into two groups with a diet supplemented either with or without 625mg/kg sodium valproate (TD02165). All mice were placed on their defined diet for 10 weeks. LDLR^{-/-} mice were purchased from Jackson Labs and GSK-3 α ^{-/-} mice were donated from Dr. Brad Doble (McMaster University). All mice had unlimited access to both food and water during the extent of the study. The McMaster University Animal Research Ethics Board approved all procedures. Mouse ear clippings were punched out and washed with digestion buffer containing 1x PCR buffer, 0.45% NP-40, 0.45% Tween 20, and 10mg/ml Proteinase K for 1 hour at 60°C. Proteinase K was then denatured at 80°C with the Mastercycler gradient thermocycler (Eppendorf). Taq PCR buffer (Invitrogen CAT#18067-017) was supplemented with 2mM MgCl₂ to use with Taq polymerase (Eurofins). PCR was performed with the following settings: 2 minutes at 94°C for 1 cycle, followed by 30 cycles at 94°C (30s), 65°C (50s), and 72°C (1.20s), and finally 1 cycle at 72°C for 10 minutes.

Amplification of the LDLR^{-/-} gene products was carried out using the following primers: Forward- 5`- CCATATGCATCCCCAGTCTT-3` and reverse: 5`AATCCATCTTGTTCAATGGCCGATC-3`. Amplification of the GSK-3 α ^{-/-} gene products was carried out using the following primers: Forward 5`- CCCCCACCAAGTGATTTCACTGCTA-3` and reverse 5`-AACATGAAATCCGGGCTCCA ACTCTAT-3` (Mobix Lab, McMaster University). Primers used for GSK-3 α targeted the lox-P sites that flanked exon 2. A 2% agarose gel was used to visualize the bands.

3.2 PLASMA AND TISSUE ANALYSIS

Plasma was collected from mice fed either a standard chow diet or a high fat diet in all groups. Non-fasted blood glucose levels and fasting blood glucose levels after a 6 hour fast were measured using a DEX glucometer (Bayer). Lipid levels of non-fasted mice were measured using a colorimetric diagnostic kit for both total cholesterol and total triglycerides (Thermal DNA Inc.). Plasma was fractionated using fast performance liquid chromatography with the FRAC-950 FPLC (Amersham Pharmacia Biotech) and total cholesterol concentration was measured from each fraction using the infinity cholesterol reagent (Thermo Scientific).

3.3 TISSUE COLLECTION AND STAINING

Mice were euthanized at 15 weeks of age, flushed through the vasculature with 1x PBS, and perfusion-fixed with 10% neutral buffered formalin. Both the heart and liver were collected and embedded in paraffin for further analysis. Serial sections of the aortic root were collected every 4 μ m. Individual aortic sections were placed on pre-coated glass

slides and stained with hematoxylin and eosin for lesion analysis. Images were collected using a Leitz LABORLUX S microscope connected to a DP71 Olympus camera and analyzed with Image J 1.43M software.

3.4 IMMUNOHISTOCHEMISTRY AND IMMUNOFLUORESCENCE

Immunohistochemical staining was done on aortic and liver sections of LDLR^{-/-} GSK-3 α ^{+/+}, LDLR^{-/-} GSK-3 α ^{+/-}, and LDLR^{-/-} GSK-3 α ^{-/-} 15 week old female mice using the Vectastain ABC system. Sections were stained with primary antibody (KDEL purchased from Assay Designs, CAT#SPA-827, GADD153 purchased from Santa Cruz Biotechnology, CAT#F-168) and visualization was achieved through appropriate biotinylated secondary antibody staining and Nova Red. Immunofluorescent staining was carried out on aortic sections using primary antibodies against α -actin (sc-32251; Santa Cruz Biotechnology) and CD-1076 (CAT#553322; BD Pharmigen). Fluorescent staining of aortic tissue was performed using secondary antibodies tagged with AlexaFluor® 488 and AlexaFluor® 568 and nuclei were counterstained with DAPI. Nonspecific staining was controlled for using a similar section and pre-immune IgG. Images were collected using a Leitz LABORLUX S microscope connected to a DP71 Olympus camera for immunohistochemical stains and a Olympus BX41 microscope connected to a DP72 Olympus camera for immunofluorescent stains. Images were analyzed with Image J 1.43M software.

3.5 IMMUNOBLOT ANALYSIS

Total protein lysates were prepared from mouse liver solubilized in 4x SDS-PAGE sample buffer (0.5M Tris-HCl pH 6.8, glycerol, and 10% SDS) and quantified by Bradford assay. Samples were diluted in SDS-PAGE loading buffer to a protein concentration of 4 μ g/ μ L. Total protein liver lysates (40 μ g) were separated by SDS-PAGE under reducing conditions and transferred to nitrocellulose membranes. Membranes were stained with antibodies against GSK-3 α (CAT# 82361; Thermo Scientific), GSK-3 β (CAT# 610202; BD Transductions), GRP78/94 (CAT# SPA-827; Assay designs) and PDI (CAT# SPA-891; Assay designs). Anti- β -actin (CAT# A3854; Sigma-Aldrich) was used to control for loading variability. Membranes were incubated for 1hr with the appropriate horseradish peroxidase secondary antibody (Life Technologies) and developed using Immobilon Western chemiluminescent horseradish peroxidase substrate (Millipore).

3.6 LIPID STAINING

Neutral lipid accumulation in the liver was determined by Oil Red O staining (Sigma). 8 μ m cryosections of liver were collected on pre-coated glass slides and fixed in 37% formaldehyde for 10 minutes. Sections were stained with a 0.5% w/v stock solution of Oil Red O dissolved in 100% isopropanol and diluted in ddH₂O to a 60% working solution. Nuclei were stained with Mayer's hematoxylin solution (MHS32, Sigma) and slides were mounted in Crystal-mount medium. Lipid staining was quantified using ImageJ 1.43 software and normalized to cross sectional area.

3.7 LIVER LIPID ASSAY

Liver sections were lysed in 500 μ L of a homogenization buffer containing 10mM Hepes (pH 7), 20mM MgCl₂, 10mM 2-Mercaptoethanol, and 0.5% Triton X-100. Samples were extracted 3x with a 3:2 ratio of hexane:isopropanol. The organic phases were pooled together, dried overnight and resuspended in 200 μ L isopropanol. Lipid levels were measured using a colorimetric diagnostic kit total cholesterol (Thermo DNA Inc.). Protein concentrations were measured from each sample using the BCA-Protein Assay Kit – Reducing Agent Compatible (Thermo Scientific).

3.8 ACTIVITY ASSAY

Livers were lysed from LDLR^{-/-}GSK-3 α ^{+/+}, LDLR^{-/-}GSK-3 α ^{+/-}, and LDLR^{-/-}GSK-3 α ^{-/-} mice in a GSK-3 buffer containing 50mM Tris HCl (pH 8), 150mM NaCl, 5mM EDTA, 50mM NaF, 1% Triton X-100, 1mM Benzamidine, 0.1x Roche PhosSTOP, 1mM Na₃VO₄, and 1mM PMSF. GSK-3 α was immunoprecipitated from 900 μ g of total protein using an Ultra Link immobilized Protein A Plus resin (Pierce) and a monoclonal antibody against GSK-3 α (CAT#82361; Thermo Scientific). GSK-3 activity was measured by monitoring the incorporation of ³²P onto phospho-glycogen synthase peptide-2 (pGS-2; Upstate, Billerica, MA). Both total crude liver lysates as well as immunoprecipitated GSK-3 α were incubated for 60 minutes in a mixture containing 20mM MOPS pH 7.4, 25mM Beta glycerol phosphate, 5mM EGTA, and 1mM Na₃VO₄ combined with 1mM MgCl₂, 15 μ M phospho-glycogen synthase peptide-2, 35 μ M ATP, and 0.5 μ Ci/ μ L [γ ³²P]ATP. Following incubation, all samples were placed on ice and 30 μ L was spotted

on Whatman P81 phosphocellulose paper. Each sample washed 3x with 0.75% O-phosphoric Acid, followed by one wash in 10mL acetone. Incorporation of ^{32}P into phospho-glycogen synthase peptide-2 was determined by scintillation counting using the Tri-Carb 2910 TR Liquid Scintillation Counter (PerkinElmer).

3.9 CELL CULTURE AND ISOLATION

At 15 weeks of age, $\text{LDLR}^{-/-}\text{GSK-3}\alpha^{+/+}$, $\text{LDLR}^{-/-}\text{GSK-3}\alpha^{+/-}$, and $\text{LDLR}^{-/-}\text{GSK-3}\alpha^{-/-}$ mice were injected with 1mL 10% thioglycolate (Sigma) to yield stimulated macrophages. Four days after injection, mice were euthanized and macrophages were collected from the peritoneal membrane space, with macrophages from the same genotype pooled together. The cells were cultured in Dulbecco's modified Eagle's medium (Life Technologies) containing 10% fetal bovine serum and 2mM L-glutamine (Sigma-Aldrich). Cells were maintained in a humidified incubator at 37°C with 5% CO_2 .

3.10 FREE CHOLESTEROL STAINING OF PERITONEAL MACROPHAGES

Unesterified cholesterol accumulation in peritoneal macrophages was determined by Filipin staining. Cells were grown on coverslips and treated with either $4\mu\text{g/mL}$ tunicamycin or 5mM glucosamine (Sigma-Aldrich) for 18 hours. Cells were washed three times with medium 1 containing 150mM NaCl, 5mM KCl, 1mM CaCl_2 , 20mM HEPES (pH 7.4), and 2g/L glucose. They were then fixed in 4% paraformaldehyde for 20 minutes at room temperature and washed once with 1x PBS. Cells were then incubated in $50\mu\text{g/mL}$ Filipin (Sigma) in medium 1 for 20 minutes at room temperature, washed three times with medium 1, and coverslips were mounted on glass slides. Filipin stained

unesterified cholesterol complexes were visualized by fluorescence microscopy with excitation at 335 to 385nm (emission at 420nm). The accumulation of unesterified cholesterol in the peritoneal macrophages was analyzed with Image J 1.43 software and quantified using Sigma Plot.

3.11 QUANTITATIVE RT-PCR

Total RNA was extracted from LDLR^{-/-}GSK-3 α ^{+/+}, LDLR^{-/-}GSK-3 α ^{+/-}, and LDLR^{-/-}GSK-3 α ^{-/-} peritoneal macrophages as well as liver samples using the RNeasy Mini Kit (Qiagen, Cat No. 74104). RNA concentration was determined by measuring the absorbance at 260nm. qRT-PCR was performed using 2 μ g of total RNA, which was reverse transcribed using the High Capacity cDNA Reverse Transcription kit (Applied Biosystems) following the manufacturer's guidelines. Amplification of PCR product was carried out using the Mastercycler gradient thermocycler (Eppendorf). qRT-PCR was conducted using a GeneAmp 7300 sequence detection system (Applied Biosystems), and SYBR GreenER qPCR SuperMix (Invitrogen). All PCR reactions were done in biological and technical triplicates to obtain gene expression profiles using selected primers for both inflammatory cytokines and lipid biosynthetic proteins (Table 1). Results from qRT-PCR were analyzed using Data Assist 3.0 software (Applied Biosystems).

Table 1 | qRT-PCR primers and conditions

Gene	Primer Sequence (5' → 3')	Melting temp (°C)	Product size (bp)
IL-1 β	F-CTGCTTCCAACCTTTGACC R-AGCTTCTCCACAGCCACAAT	55	119
IL-10	F-CATGGGTCTTGGGAAGAGAA R-AACTGGCCACAGTTTTTCAGG	55	76
HMG-CoA reductase	F-CTTGTGGAATGCCTTGTGATTG R-AGCCGAAGCAGCACATGAT	55	119
FAS	F-GCTGCGGAAACTTCAGGAAAT R-AGAGACGTGTCACTCCTGGACTT	57	84
SREBP-1c	F-GGAGCCATGGATTGCACATT R-GCTTCCAGAGAGGAGGCCAG	57	170
SREBP-2	F-GCGTTCTGGAGACCATGGA R-ACAAAGTTGCTCTGAAAACAAATCA	55	131
β -actin	F-GGCACCACACCTTCTACAATG R-GGCACCACACCTTCTACAATG	55	132

IL; interleukin, HMG-CoA; 3-hydroxy-3-methylglutaryl-coenzyme A, FAS: fatty acid synthase, and SREBP; sterol regulatory element binding protein

3.12 BONE MARROW EXPERIMENTS

a.) *Bone Marrow Transplantation:*

Five week old LDLR^{-/-}GSK-3 α ^{+/+} and LDLR^{-/-}GSK-3 α ^{-/-} female mice were lethally irradiated with 1200rad split into 2 doses; 800rad for the first dose followed by 400rad 3 hours later (Fig. 7). The ¹³⁷Cs source was generated through the Gammacell 3000 Elan irradiator (Best Theratronics). Under sterile conditions, femurs and tibias were removed from both legs of LDLR^{-/-}GSK-3 α ^{+/+} and LDLR^{-/-}GSK-3 α ^{-/-} male donor mice. Bone marrow was flushed out of the bone using Iscoves medium (Invitrogen) containing 2% heat inactivated FBS and supplemented with 2mM L-glutamine and 50 μ g/mL Pen-Strep. Bone marrow cells were dispersed and injected into recipient mice through tail vein injection (approximately 2x10⁶ cells per mouse). Two weeks after transplantation, mice were placed on a high fat diet containing 21% milk fat and 0.2% cholesterol (Harlan Teklad TD97363) to induce dyslipidemia. Four weeks after transplantation peripheral

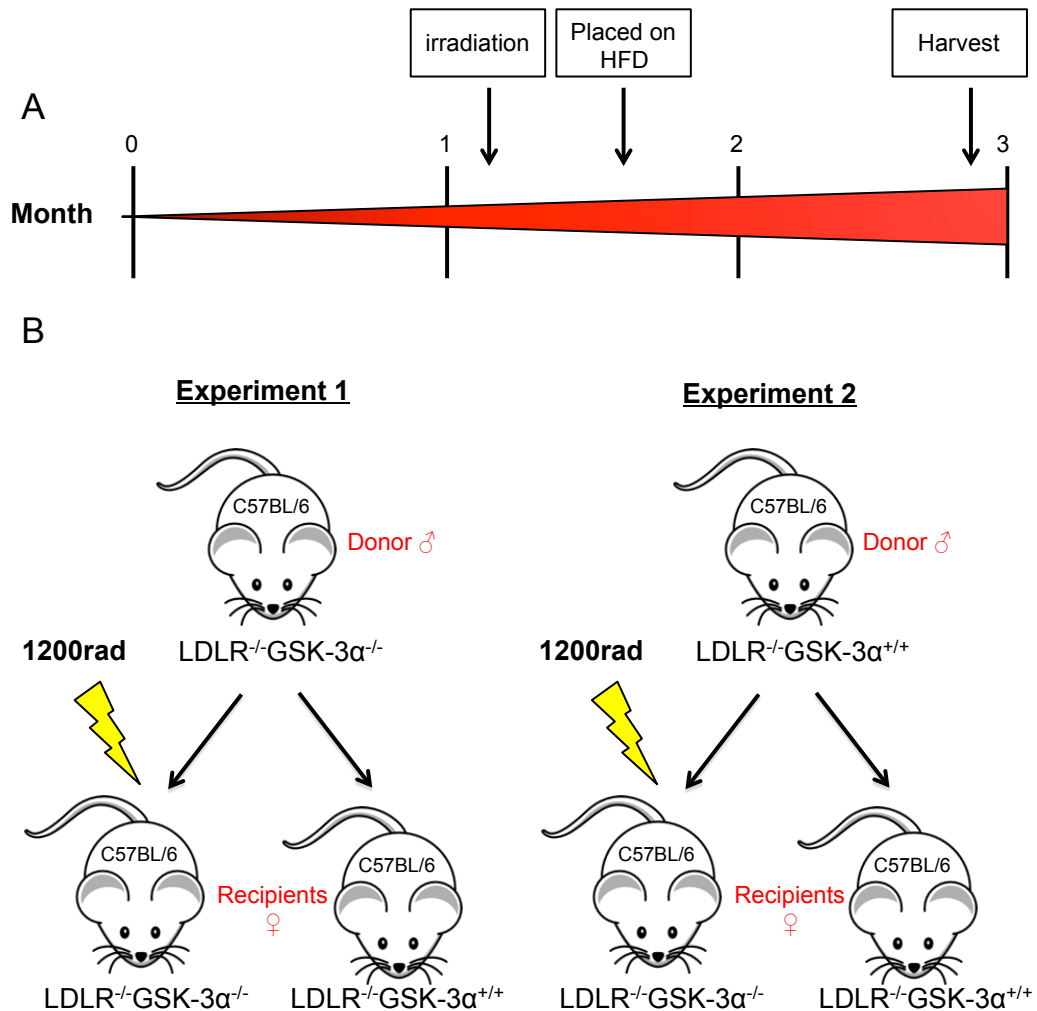


Figure 7 | **Outline of BMT protocol.** A | 5 week old female LDLR^{-/-}GSK-3α^{+/+} and LDLR^{-/-}GSK-3α^{-/-} recipient mice were irradiated and transplanted with bone marrow from male donor mice. All recipient mice were placed on a high fat diet at this time for 10 weeks and harvested at 17 weeks of age. B | Femurs and tibias were removed from both legs of male LDLR^{-/-}GSK-3α^{+/+} and a LDLR^{-/-}GSK-3α^{-/-} donor mice. For experiment 1, 5 week old female recipient LDLR^{-/-}GSK-3α^{+/+} and LDLR^{-/-}GSK-3α^{-/-} mice were irradiated with 1200rad and transplanted with male LDLR^{-/-}GSK-3α^{-/-} donor bone marrow. For experiment 2, 5 week old female recipient LDLR^{-/-}GSK-3α^{+/+} and LDLR^{-/-}GSK-3α^{-/-} mice were irradiated with 1200rad and transplanted with male LDLR^{-/-}GSK-3α^{+/+} donor bone marrow.

blood was collected for PCR analysis to confirm successful reconstitution of bone marrow. Mice were sustained on a high fat diet until 15 weeks of age, at which time recipient mice were euthanized and plasma and tissue were collected for further analyses.

b.) *Genotyping of recipient mice to confirm successful bone marrow transplantation:*

Genomic DNA from peripheral blood was isolated using the blood genomic DNA isolation micro kit (Norgen Biotek, Product# 18200). Taq PCR buffer (Invitrogen CAT#18067-017) was supplemented with 2mM MgCl₂ to use with Taq polymerase (Eurofins). PCR was performed with the following cycle parameters: 2 minutes at 94 for 1 cycle, followed by 30 cycles at 94°C (1min), 65°C (3min), and 72°C (3min), and finally 1 cycle at 72°C for 10 minutes. Amplification of the sex determining region Y (SRY) gene products was carried out using the following primers: Forward: 5'-AGAGATCAGCAA GCAGCTGG-3' and reverse: 5'- TCTTGCCTGTATGTGATGGC-3' (Mobix Lab, McMaster University). GSK-3 α and LDLR KO mice were genotyped as previously stated. A 2% agarose gel was used to visualize individual bands.

c.) *Lesion analysis of BMT mice:*

Mice were euthanized at 15 weeks of age, flushed through the vasculature with 1x PBS, and perfusion-fixed with 10% neutral buffered formalin. The heart was embedded in paraffin and serial sections of the aortic root were collected. Individual aortic sections were placed on pre-coated glass slides and stained with hematoxylin and eosin for lesion analysis. Images were collected using a Leitz LABORLUX S microscope connected to a DP71 Olympus camera and analyzed with Image J 1.43M software.

3.13 STATISTICAL ANALYSES

All data are expressed as mean \pm SEM. Analysis was performed using the unpaired Student's t-test for 2 groups and a one-way analysis of variance (ANOVA) for multiple groups. A value of $P < 0.05$ was considered statistically significant.

CHAPTER 4: RESULTS

4.1 Valproate-supplemented high fat diet fed LDLR^{-/-} mice have decreased atherosclerosis

To determine the effect of sodium valproate on atherosclerotic lesion development in 15 week old female LDLR^{-/-} mice, serial histological sections were collected and plaque and necrotic core volumes were assessed (Fig. 8). Total volume was calculated by measuring the area under the curve (AUC) of the plaque cross-sectional area. There was minimal plaque formation in chow diet-fed LDLR^{-/-} mice (407±144mm³ without VPA and 489±195mm³ with VPA), with no necrotic core formation. LDLR^{-/-} mice placed on a high fat diet had significantly greater lesion and necrotic core volumes compared to chow-fed diet controls. HFD-fed LDLR^{-/-} mice supplemented with VPA had significantly reduced lesion and necrotic core volumes compared with HFD-fed LDLR^{-/-} mice without VPA supplementation (lesion volume: 80±20 x 10³mm³ for HFD without VPA and 33±10 x 10³mm³ for HFD with VPA; necrotic core volume: 29±7 x 10³mm³ for HFD without VPA and 8±2 x 10³mm³ for HFD with VPA).

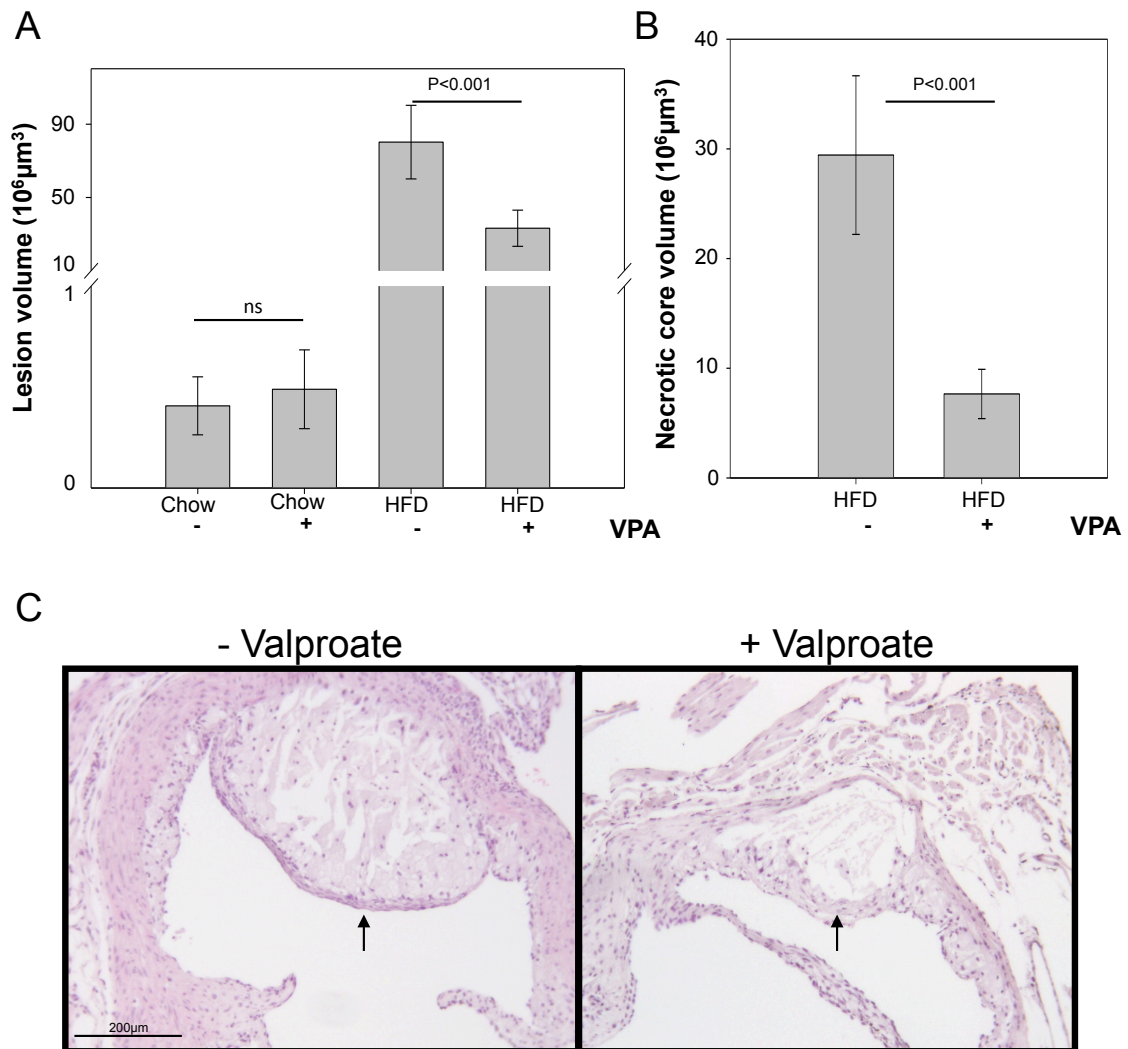


Figure 8 | HFD-fed LDLR^{-/-} mice supplemented with valproate have a significant decrease in aortic lesion and necrotic core volume. A | Quantification of the lesion volume in the ascending aorta of 15 week old female LDLR^{-/-} mice fed either a standard chow diet (n=4) or a high fat diet (HFD; n=9) supplemented with and without valproate (VPA). B | Quantification of the necrotic core volume in the ascending aorta; n=9. C | Representative hematoxylin and eosin stained aortic sinus cross-sections from HFD-fed 15 week old female LDLR^{-/-} mice with and without valproate supplementation. Arrows indicate lesions in the aortic root.

4.2 Characterization of a novel LDLR^{-/-}GSK-3 α ^{-/-} mouse model

4.2.1 Characterization of a novel mouse strain

LDLR^{-/-} mice were crossed with GSK-3 α ^{-/-} mice. F1 generation heterozygous mice (LDLR^{+/-}GSK-3 α ^{+/-}) were crossed to produce double knockout mice in the F2 generation. The results from the genotyping PCR experiments showed successful knockouts of both LDLR and GSK-3 α . PCR analysis showed the LDLR wild-type gene at a band size of 167bp. All three lines contained the LDLR^{-/-} band at 350bp (Fig. 9a). Wild-type GSK-3 α had a band length of 600kb, while the null allele was 250bp in size. Heterozygous GSK-3 α knockouts contained both the 600bp and 250bp bands. In addition, immunoblot analysis of total protein liver lysates was carried out to detect GSK-3 α and GSK-3 β protein from LDLR^{+/+}GSK-3 α ^{+/+}, LDLR^{+/+}GSK-3 α ^{+/-}, and LDLR^{+/+}GSK-3 α ^{-/-} mice (Fig 9b). As expected, GSK-3 β was observed in all three groups, while the GSK-3 α protein was only observed in LDLR^{+/+}GSK-3 α ^{+/+} and LDLR^{+/+}GSK-3 α ^{+/-} mice. Finally, total GSK-3 activity as well as GSK-3 α activity was examined in liver lysates from LDLR^{+/+}GSK-3 α ^{+/+}, LDLR^{+/+}GSK-3 α ^{+/-}, and LDLR^{+/+}GSK-3 α ^{-/-} mice (Fig. 9c & 9d). As expected, no GSK-3 α activity was observed in LDLR^{+/+}GSK-3 α ^{-/-} mice. Furthermore, total GSK-3 activity showed no GSK-3 β compensation in LDLR^{-/-}GSK-3 α ^{-/-} liver lysates. There was approximately a 20% reduction in total GSK-3 activity in liver from GSK-3 α deficient mice.

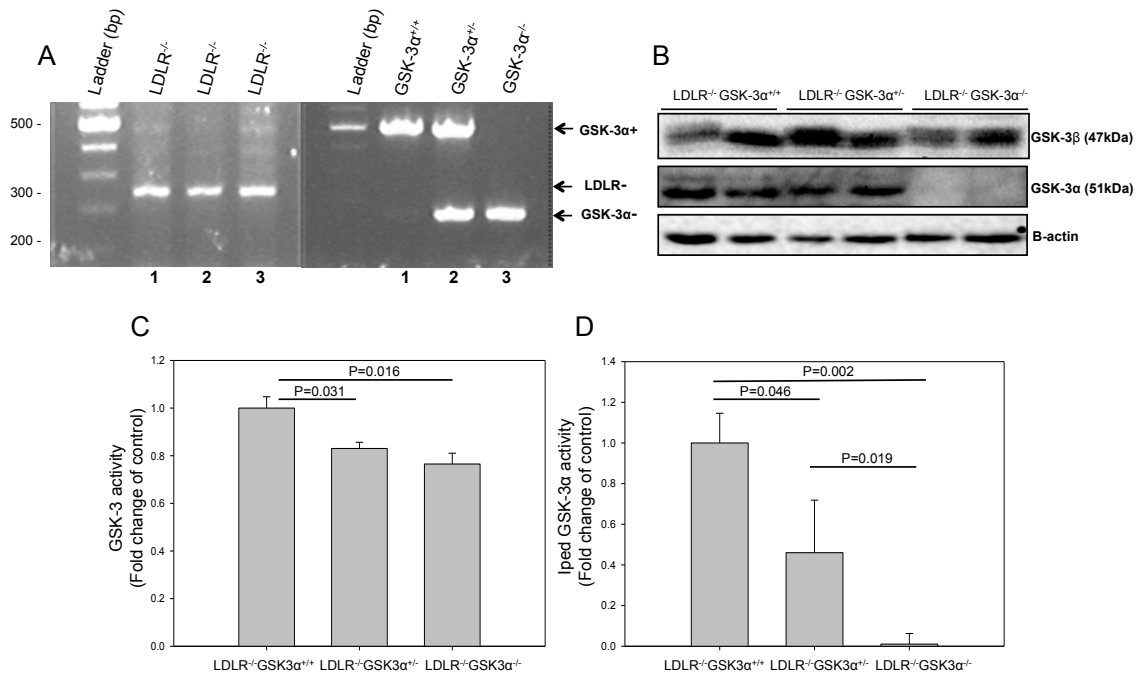


Figure 9 | Characterization of a novel LDLR^{-/-}GSK-3α^{-/-} mouse strain. A | PCR was used to determine genotypes 1.) LDLR^{-/-}GSK-3α^{+/+} mouse; 2.) LDLR^{-/-}GSK-3α^{+/-} mouse; 3.) LDLR^{-/-}GSK-3α^{-/-} mouse. A 2% agarose gel was used to visualize the bands. B | Immunoblot analysis of GSK-3α and GSK-3β protein from liver lysates of LDLR^{-/-}GSK-3α^{+/+}, LDLR^{-/-}GSK-3α^{+/-}, and LDLR^{-/-}GSK-3α^{-/-} mice. Total protein liver lysates were resolved by SDS-PAGE and transferred to nitrocellulose membranes. β-actin was used as the loading control. C | Activity assay of total hepatic GSK-3 from LDLR^{-/-}GSK-3α^{+/+}, LDLR^{-/-}GSK-3α^{+/-}, and LDLR^{-/-}GSK-3α^{-/-} mice (n=3). D | Activity assay of immunoprecipitated hepatic GSK-3α from LDLR^{-/-}GSK-3α^{+/+}, LDLR^{-/-}GSK-3α^{+/-}, and LDLR^{-/-}GSK-3α^{-/-} mice (n=3). GSK-3 activity was measured by monitoring the incorporation of ³²P onto phospho-glycogen synthase peptide-2. Activities are presented as the fold change of the LDLR^{-/-}GSK-3α^{+/+} control.

4.2.2 Metabolic parameters

Body weight, non-fasting- and fasting-blood glucose levels, total plasma cholesterol and triglycerides, as well as liver and adipose weight were analyzed to determine the effect of valproate supplementation or GSK-3α deficiency in 15 week old female LDLR^{-/-} mice. A high fat diet supplemented with 625mg/kg sodium valproate did not result in a significant change in any of these metabolic parameters in LDLR^{-/-} mice (Table 2). There was a significant increase in body weight in HFD-fed LDLR^{-/-}GSK-3α^{+/+},

LDLR^{-/-}GSK-3 α ^{+/-}, and LDLR^{-/-}GSK-3 α ^{-/-} mice compared to chow fed-diet controls (Table 3). There was no significant change in fasting or non-fasting blood glucose levels in either the control or HFD mouse models between the three groups. Mice supplemented with a HFD had a significantly increased level of both total cholesterol and total triglycerides in the plasma compared with age-matched controls. There was no significant difference in either total cholesterol or total triglycerides between LDLR^{-/-}GSK-3 α ^{+/+}, LDLR^{-/-}GSK-3 α ^{+/-}, or LDLR^{-/-}GSK-3 α ^{-/-} mice on either a standard chow diet or HFD. Mice supplemented with a HFD had a significant increase in both liver and adipose weight compared with age-matched chow fed-diet controls. Therefore, GSK-3 α deficiency did not significantly alter any of the metabolic parameters that were assessed.

Table 2 | Metabolic parameters in LDLR^{-/-}GSK-3 α ^{+/+} mice with and without valproate

	-Valproate		+Valproate	
	Chow	HFD	Chow	HFD
Body weight (g)	20.20±1.10	21.40±0.46	21.60±1.30	21.96±0.16
NFBG (mM)	10.00±1.70	7.30±2.20	8.40±1.20	7.90±0.40
Cholesterol (mM)	6.32±0.67	15.87±1.11*	4.42±0.51	17.67±4.47*
Triglycerides (mM)	0.02±0.25	0.58±0.22*	0.01±0.01	0.89±0.28*
Liver weight (g)	0.84±0.10	1.32±0.09*	0.83±0.03	1.10±0.06*
Adipose weight (g)	0.35±0.06	0.52±0.11	0.29±0.03	0.47±0.10

n=5-10 per treatment group; HFD: high fat diet, NFBG; non-fasting blood glucose

*P<0.05 relative to age matched chow fed mice of same treatment

Table 3 | Metabolic parameters in LDLR^{-/-}GSK-3 α ^{+/+}, LDLR^{-/-}GSK-3 α ^{+/-}, and LDLR^{-/-}GSK-3 α ^{-/-} mice

	LDLR ^{-/-} GSK-3 α ^{+/+}		LDLR ^{-/-} GSK-3 α ^{+/-}		LDLR ^{-/-} GSK-3 α ^{-/-}	
	Chow	HFD	Chow	HFD	Chow	HFD
Body weight (g)	21.01±0.60	23.58±0.47*	18.76±0.71	20.90±0.46*	20.21±0.50	23.10±0.61*
NFBG (mM)	8.85±0.37	7.46±0.31	7.43±0.33	8.42±0.34	7.92±0.27	7.06±0.40
FBG (mM)	7.31±0.38	7.29±0.29	8.03±0.87	7.30±0.40	7.35±0.55	8.33±0.61
Cholesterol (mM)	6.66±0.84	20.11±0.15 Ψ	8.31±1.80	17.78±2.74*	6.86±0.31	19.95±0.13 Ψ
Triglycerides (mM)	0.92±0.07	4.78±0.54 Ψ	0.94±0.12	4.68±1.21*	1.06±0.22	3.89±0.31 Ψ
Liver weight (g)	0.84±0.05	1.17±0.03 Ψ	0.83±0.03	1.08±0.07*	0.87±0.03	1.11±0.04 Ψ
Adipose weight (g)	0.14±0.02	0.28±0.05*	0.13±0.02	0.25±0.06*	0.09±0.01	0.21±0.04*

n=5-10 per treatment group; HFD; high fat diet, NFBG; non-fasting blood glucose, FBG; fasting blood glucose

*P<0.05 relative to age matched chow fed mice of the same genotype

Ψ P<0.001 relative to age matched chow fed mice of the same genotype

4.2.3 GSK-3 α deficiency does not significantly change plasma lipid profiles in LDLR^{-/-} mice

To determine the effect of GSK-3 α deficiency on the amount of HDL, LDL, and VLDL levels, plasma was fractionated into 42 samples using FPLC and total cholesterol in each sample was quantified. Fractionated plasma showed no significant change in VLDL, LDL, or HDL levels in both LDLR^{-/-} and LDLR^{+/+} mice on a HFD (Fig. 10).

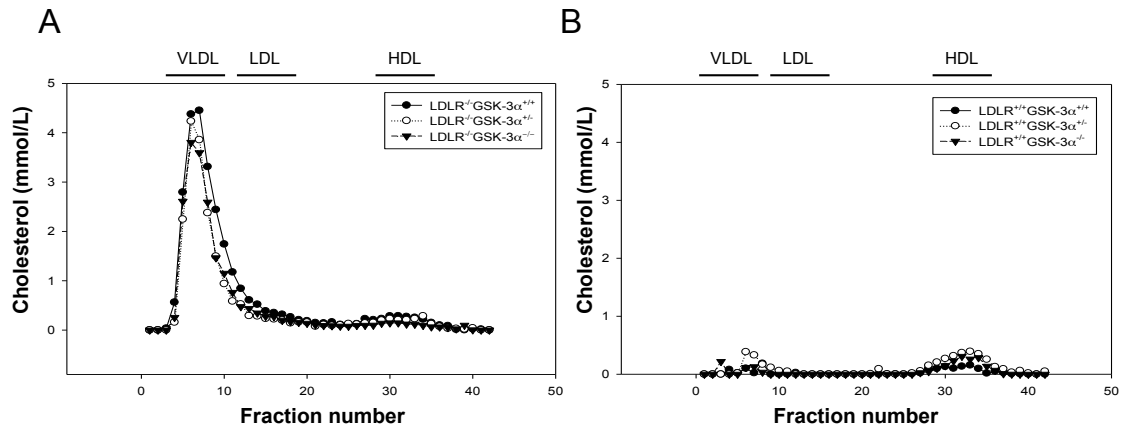


Figure 10 | **Plasma lipid profiles.** The average cholesterol concentration of fractionated plasma from A | LDLR^{-/-} (GSK-3α^{+/+}, GSK-3α^{+/-}, and GSK-3α^{-/-}) and B | LDLR^{+/+} (GSK-3α^{+/+}, GSK-3α^{+/-}, and GSK-3α^{-/-}) HFD-fed female mice. Fractionation of plasma samples was carried out using fast performance liquid chromatography. Lines indicate the position of human VLDL, LDL, and HDL; n=3.

4.3 GSK-3α deficiency has no significant effect on ER stress levels in HFD-fed

LDLR^{-/-} mice

Studies in our lab have shown that the GSK-3 inhibitor valproate has no effect on the ability of ER stress-inducing agents to activate an ER stress response in HepG2 cells (A. J. Kim, et al., 2005). However, downstream effects of ER stress such as lipid accumulation and apoptosis were significantly attenuated when HepG2 cells were pretreated with valproate. Therefore, ER stress levels were examined in all three mouse strains to further verify that GSK-3 functions downstream of ER stress. Serial histological sections of the aortic root and liver were collected and stained with anti-KDEL and anti-GADD153 antibodies. KDEL staining of the aortic sinus, which is specific for the ER stress markers GRP78/94, showed no observable difference in LDLR^{-/-}GSK-3α^{+/+}, LDLR^{-/-}GSK-3α^{+/-}, LDLR^{-/-}GSK-3α^{-/-} mice (Fig. 11a). Similar results were seen when the aortic sinus was stained with GADD153, a protein involved in apoptotic activation during the

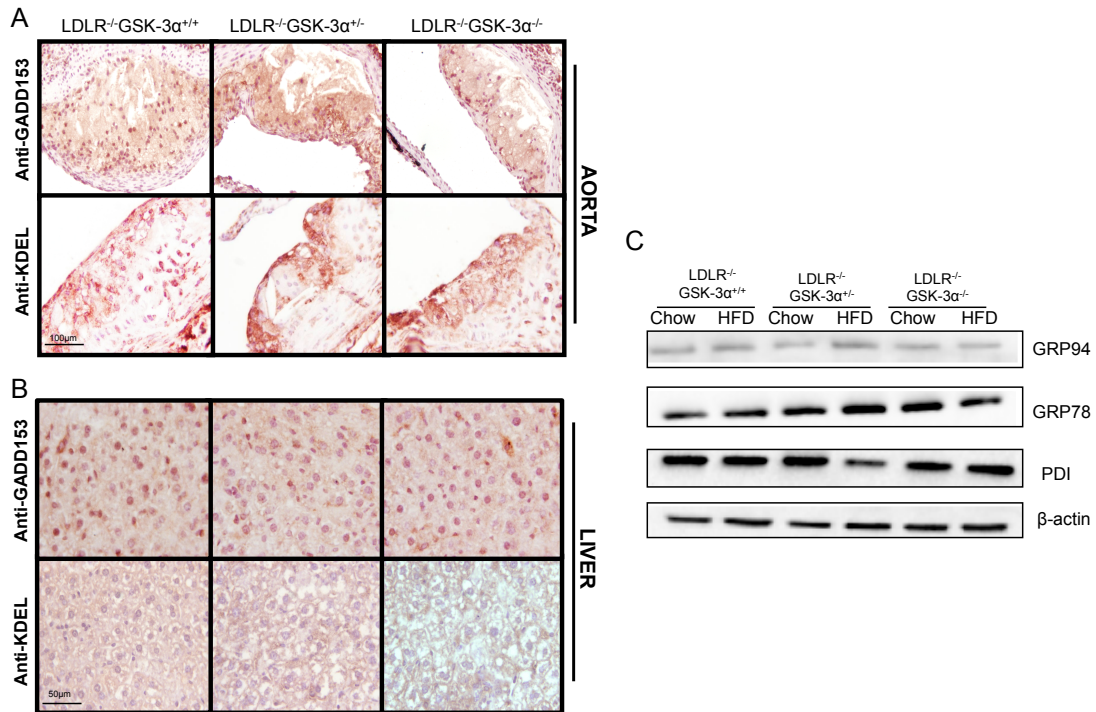


Figure 11 | **GSK-3 α deficiency has no significant effect on ER stress levels in HFD-fed LDLR^{-/-} mice.** A | GADD153 and KDEL primary antibodies were used to stain aortic lesions of 15 week old female LDLR^{-/-} GSK-3 α ^{+/+}, LDLR^{-/-}GSK-3 α ^{+/-}, and LDLR^{-/-}GSK-3 α ^{-/-} mice on a high fat diet. B | GADD153 and KDEL primary antibodies were used to stain liver sections of 15 week old female LDLR^{-/-}GSK-3 α ^{+/+}, LDLR^{-/-}GSK-3 α ^{+/-}, and LDLR^{-/-}GSK-3 α ^{-/-} mice on a high fat diet. C | Immunoblot analysis of liver total protein lysates resolved by SDS-PAGE and transferred to nitrocellulose membranes. Membranes were stained with antibodies against GRP78/94 and PDI as indicated. β -actin was used as the loading control.

unfolded protein response. KDEL and GADD153 staining in the liver also showed no observable differences between any of the three genotypes (Fig. 11b). Furthermore, immunoblot analysis of total protein liver lysates revealed no significant difference in ER stress levels between all three groups (Fig. 11c). This finding is consistent with the notion that GSK-3 α / β functions downstream of ER stress and the UPR.

4.4 Effect of GSK-3 α deficiency on hepatic steatosis

4.4.1 GSK-3 α deficiency significantly reduces hepatic neutral lipid accumulation in LDLR^{-/-} and LDLR^{+/+} mice

We hypothesized that ER stress-induced GSK-3 α/β activation results in an increase in lipid accumulation, possibly through subsequent activation of the sterol regulatory element binding proteins (SREBPs). Results from our lab have shown that valproate supplementation significantly reduced the amount of hepatic lipid content in hyperglycemic ApoE^{-/-} mice (Bowes, et al., 2009). Cryosections of liver from LDLR^{-/-} and LDLR^{+/+} (GSK-3 α ^{+/+}, GSK-3 α ^{+/-}, and GSK-3 α ^{-/-}) were collected on pre-coated glass slides. Neutral lipid content was assessed through Oil Red O staining. Total lipid content was measured as the percent area stained. At 15 weeks of age, LDLR^{-/-} female mice supplemented with a high fat diet had a significantly increased amount of neutral lipid staining in the liver compared to aged-matched chow-fed diet controls (data not shown). LDLR^{-/-}GSK-3 α ^{+/-} and LDLR^{-/-}GSK-3 α ^{-/-} mice had a significantly decreased amount of hepatic lipid accumulation compared with LDLR^{-/-}GSK-3 α ^{+/+} controls on a HFD (21.84 \pm 0.28% for LDLR^{-/-}GSK-3 α ^{+/+} mice, 12.58 \pm 0.26% for LDLR^{-/-}GSK-3 α ^{+/-} mice, and 9.49 \pm 0.15% for LDLR^{-/-}GSK-3 α ^{-/-} mice) (Figs. 12a & 12c). Similar results were seen in LDLR^{+/+}GSK-3 α ^{+/-} and LDLR^{+/+}GSK-3 α ^{-/-} mice compared with LDLR^{+/+}GSK-3 α ^{+/+} age-matched controls (16.31 \pm 0.23% for LDLR^{+/+}GSK-3 α ^{+/+} mice, 13.25 \pm 0.24% for LDLR^{+/+}GSK-3 α ^{+/-} mice, and 8.16 \pm 0.15% for LDLR^{+/+}GSK-3 α ^{-/-} mice) (Figs. 12b and 12c). Therefore, whole body GSK-3 α deficiency resulted in protection from diet-induced hepatic steatosis in both LDLR^{+/+} and LDLR^{-/-} female mice at 15 weeks of age.

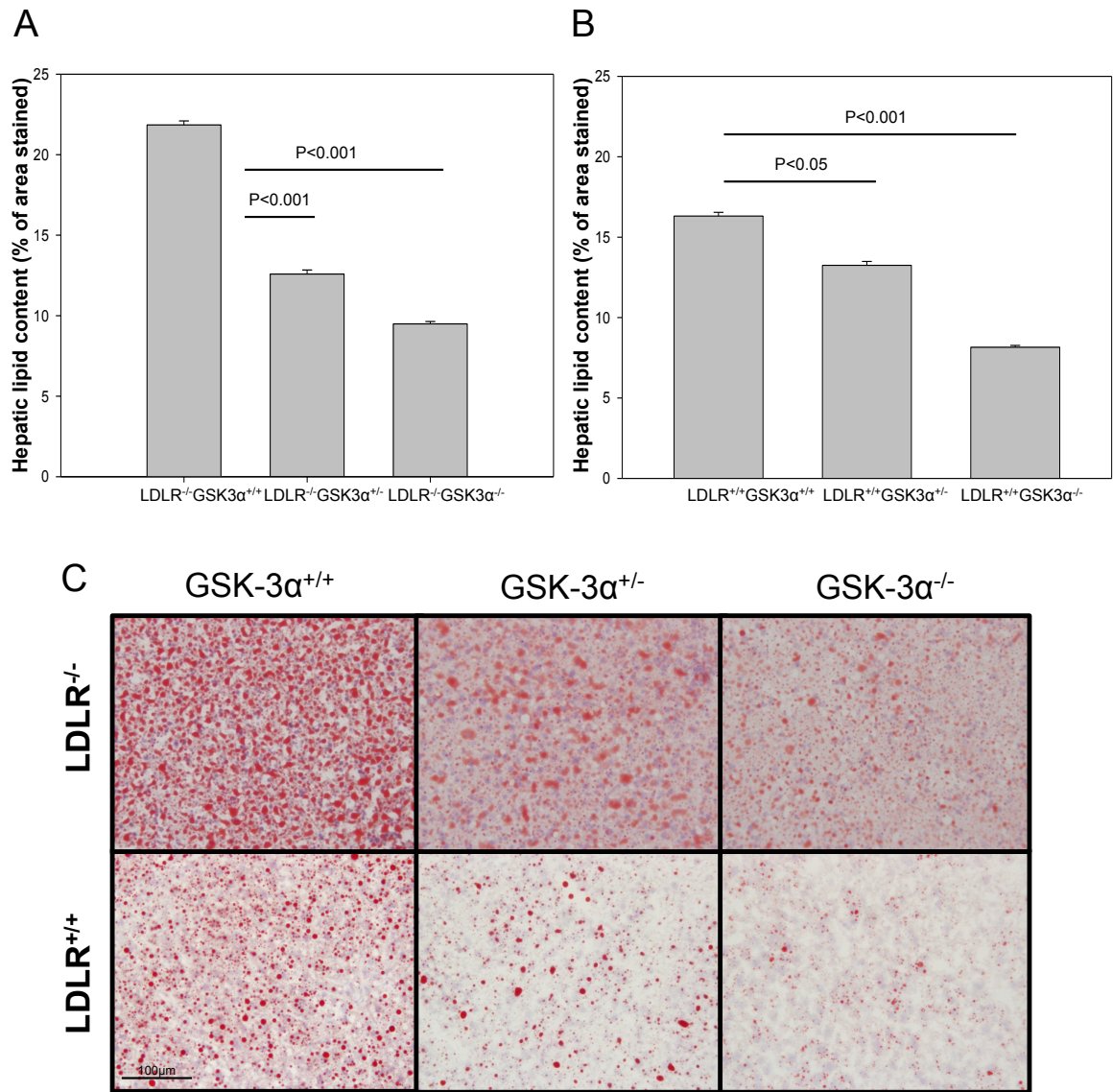


Figure 12 | **GSK-3α deficiency significantly reduces hepatic lipid accumulation in HFD-fed LDLR^{-/-} and LDLR^{+/+} mice.** Hepatic lipid content was analyzed using Oil red O staining. A | Quantification of hepatic lipid content in 15 week old LDLR^{-/-}GSK-3α^{+/+}, LDLR^{-/-}GSK-3α^{+/-}, and LDLR^{-/-}GSK-3α^{-/-} mice fed a high fat diet (n=5). B | Quantification of hepatic lipid content in 15 week old LDLR^{+/+}GSK-3α^{+/+}, LDLR^{+/+}GSK-3α^{+/-}, and LDLR^{+/+}GSK-3α^{-/-} mice fed a high fat diet (n=3). C | Representative images of liver cryo-cross-sections stained with Oil Red O.

4.4.2 Effect of GSK-3 α deficiency on total hepatic cholesterol and lipid biosynthesis protein levels.

To assess the effect of GSK-3 α deficiency on the total amount of cholesterol in the liver, sections of total liver were collected from LDLR^{+/+}GSK-3 α ^{+/+}, LDLR^{+/+}GSK-3 α ^{+/-}, and LDLR^{+/+}GSK-3 α ^{-/-} mice, lysed, and separated into organic and aqueous phases using a hexane:isopropanol solvent. Total cholesterol was significantly decreased in HFD-fed LDLR^{+/+}GSK-3 α ^{-/-} mice compared with both LDLR^{+/+}GSK-3 α ^{+/+}, and LDLR^{+/+}GSK-3 α ^{+/-} mice (1.49±0.42mg/mg protein for LDLR^{+/+} GSK-3 α ^{+/+} mice, 1.62±0.0442mg/mg protein for LDLR^{+/+}GSK-3 α ^{+/-} mice, and 1.01±0.16mg/mg protein for LDLR^{+/+}GSK-3 α ^{-/-} mice) (Fig. 13a). There was no significant change in total cholesterol in the liver on mice supplemented with a standard chow diet.

To determine the effect of GSK-3 α deficiency in decreasing both cholesterol and triglycerides in the liver, expression of several proteins involved in lipid biosynthesis were analyzed using qRT-PCR. Livers from LDLR^{-/-}GSK-3 α ^{+/+}, LDLR^{-/-}GSK-3 α ^{+/-}, and LDLR^{-/-}GSK-3 α ^{-/-} mice were isolated and total RNA was extracted and analyzed by qRT-PCR. No significant differences in transcript levels were seen, however, there was a trend toward increasing mRNA levels of the transcription factors SREBP-1c and SREBP-2, as well as the enzymes HMG-CoA reductase, and FAS in GSK-3 α deficient mice (Fig. 13c).

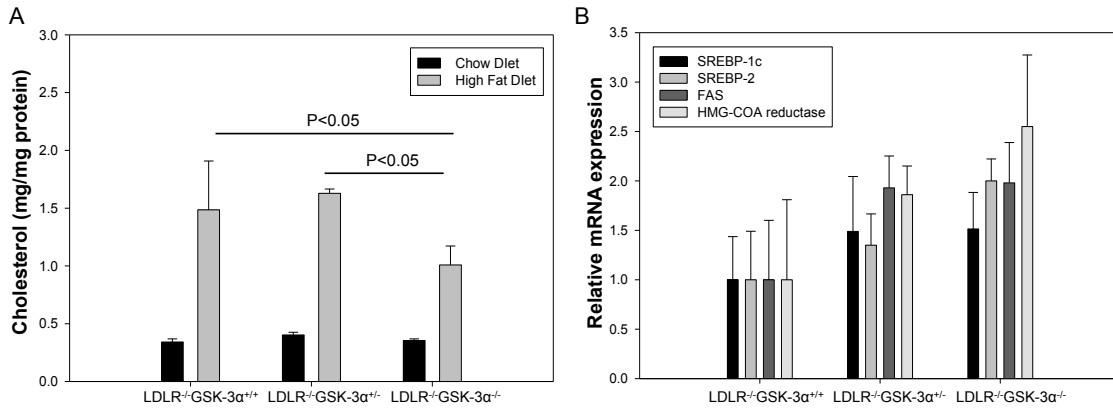


Figure 13 | **Effect of GSK-3 α deficiency on total hepatic cholesterol and lipid biosynthesis protein levels in LDLR^{-/-} mice.** Quantification of total cholesterol and lipid biosynthetic protein mRNA levels from liver lysates of LDLR^{-/-}GSK-3 α ^{+/+}, LDLR^{-/-}GSK-3 α ^{+/-}, and LDLR^{-/-}GSK-3 α ^{-/-} mice. A | Total cholesterol in the liver of LDLR^{-/-}GSK-3 α ^{+/+}, LDLR^{-/-}GSK-3 α ^{+/-}, and LDLR^{-/-}GSK-3 α ^{-/-} mice on either a chow diet or HFD. B | mRNA levels of SREBP-1c, SREBP-2, HMG-CoA reductase, and FAS from indicated groups. *P<0.05 relative to LDLR^{-/-}GSK-3 α ^{+/+} of the same treatment group. n=3

4.4.3 GSK-3 α deficiency does not detectably alter the aortic sinus in LDLR^{+/+} mice

The aortic root was analyzed in 15 week old LDLR^{+/+}GSK-3 α ^{+/+}, LDLR^{+/+}GSK-3 α ^{+/-}, and LDLR^{+/+}GSK-3 α ^{-/-} female mice to determine if GSK-3 α deficiency resulted in any changes in lesion formation. Serial histological sections of the aortic root were collected every 4 μ m and stained with hematoxylin and eosin to visualize the aortic valves (Fig. 14). No lesions were observed in the aortic root from any of the three groups.

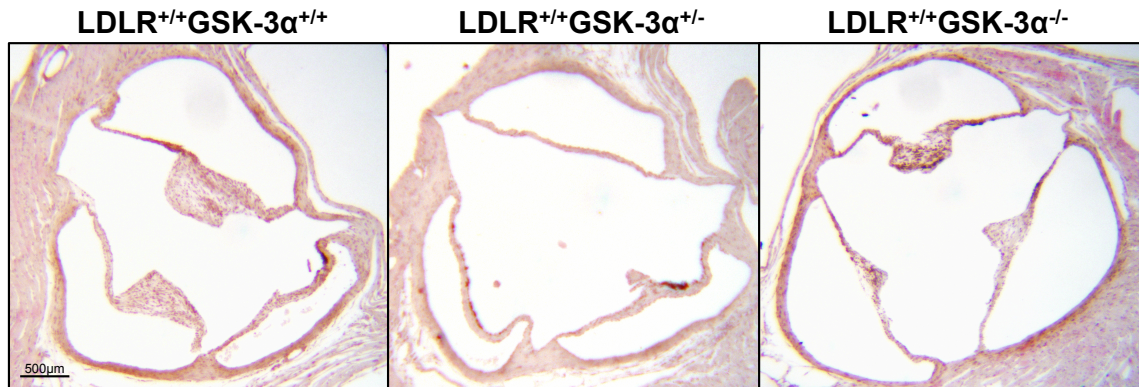


Figure 14 | **GSK-3 α deficiency does not result in lesion development in the aorta of HFD-fed LDLR^{+/+} mice.** Representative hematoxylin and eosin stained aortic sinus cross-sections from 15 week old female LDLR^{+/+}GSK-3 α ^{+/+}, LDLR^{+/+}GSK-3 α ^{+/-}, and LDLR^{+/+}GSK-3 α ^{-/-} mice.

4.5 Effect of GSK-3 α deficiency on atherosclerosis

4.5.1 GSK-3 α deficiency significantly attenuates atherosclerosis in HFD-fed

LDLR^{-/-} mice

To determine the effect of GSK-3 α deficiency on atherosclerotic development in LDLR^{-/-} mice, serial histological sections were collected from LDLR^{-/-}GSK-3 α ^{+/+}, LDLR^{-/-}GSK-3 α ^{+/-}, and LDLR^{-/-}GSK-3 α ^{-/-} mice and plaque cross-sectional area as well as plaque and necrotic core volume were assessed. No lesion formation was observed in the aortas of 15 week old LDLR^{-/-}GSK-3 α ^{+/+}, LDLR^{-/-}GSK-3 α ^{+/-}, or LDLR^{-/-}GSK-3 α ^{-/-} mice fed a standard chow diet (data not shown). Lesion development was observed with supplementation of a high fat diet. Both heterozygous and homozygous GSK-3 α KO mice had significantly smaller plaque cross sectional areas in the aortic root relative to LDLR^{-/-} controls (Figs. 15a & 15c). In addition, both lesion and necrotic core volumes were significantly reduced in LDLR^{-/-}GSK-3 α ^{+/-} and LDLR^{-/-}GSK-3 α ^{-/-} mice on a high fat diet compared with age-matched LDLR^{-/-} controls (lesion volume: $80 \pm 20 \times 10^3 \text{mm}^3$

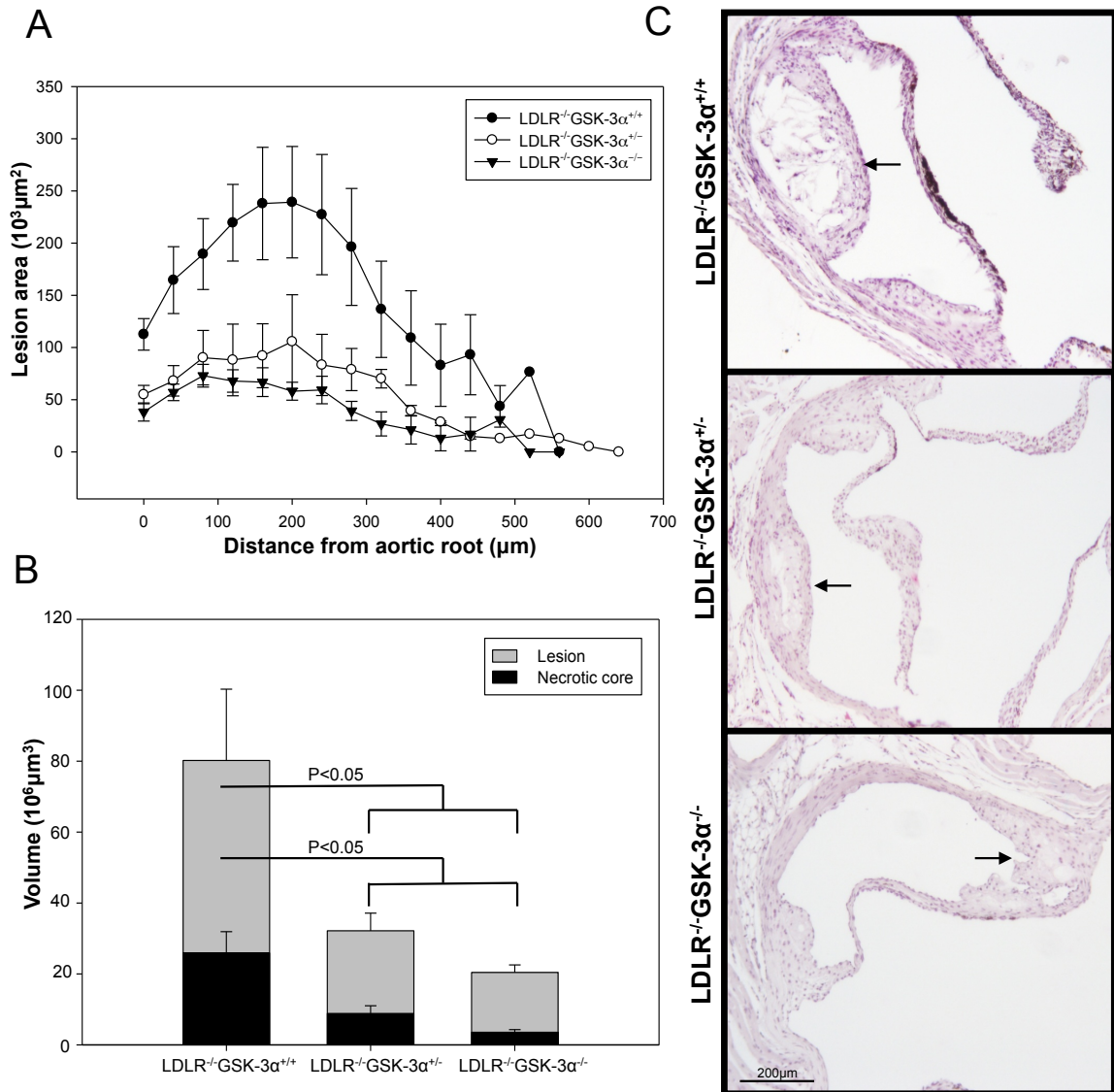


Figure 15 | **GSK-3 α deficiency significantly attenuates atherosclerosis in HFD-fed LDLR^{-/-} mice.** A | Quantification of the lesion area in the ascending aorta of 15 week old LDLR^{-/-}GSK-3 α ^{+/+}, LDLR^{-/-}GSK-3 α ^{+/-}, and LDLR^{-/-}GSK-3 α ^{-/-} mice fed a high fat diet (n=8-9). B | Quantification of the lesion and necrotic core volume in the ascending aorta (n=8-9). C | Representative hematoxylin and eosin stained aortic sinus cross sections from 15 week old female LDLR^{-/-}GSK-3 α ^{+/+}, LDLR^{-/-}GSK-3 α ^{+/-}, and LDLR^{-/-}GSK-3 α ^{-/-} mice. Arrows indicate lesions in the aortic root.

for LDLR^{-/-}GSK-3 α ^{+/+} mice, $32 \pm 5 \times 10^3 \text{mm}^3$ for LDLR^{-/-}GSK-3 α ^{+/-} mice, and $20 \pm 2 \times 10^3 \text{mm}^3$ for LDLR^{-/-}GSK-3 α ^{-/-} mice; necrotic core volume: $26 \pm 6 \times 10^3 \text{mm}^3$ for LDLR^{-/-}

GSK-3 α ^{+/+} mice, $9 \pm 2 \times 10^3 \text{mm}^3$ for LDLR^{-/-}GSK-3 α ^{+/-} mice, and $3 \pm 0.7 \times 10^3 \text{mm}^3$ for LDLR^{-/-}GSK-3 α ^{-/-} mice) (Fig. 15b).

4.5.2 Effect of GSK-3 α deficiency on macrophages and smooth muscle cells

Accumulation of macrophages and migration of smooth muscle cells (SMCs) into the intima of the arteries leads to atherosclerotic plaque formation. Therefore, the presence of macrophages and SMCs was assessed in the aortic root of LDLR^{-/-}GSK-3 α ^{+/+}, LDLR^{-/-}GSK-3 α ^{+/-}, and LDLR^{-/-}GSK-3 α ^{-/-} mice on a HFD. Serial histological sections were collected and stained with primary antibodies against α -actin and Mac-3. In addition to decreased lesion and necrotic core volume, mice that were deficient in GSK-3 α had a reduction in both macrophages and SMCs in atherosclerotic lesions (Fig. 16). LDLR^{-/-}GSK-3 α ^{+/+} mice had more macrophages and SMCs in the lesion, whereas LDLR^{-/-}GSK-3 α ^{-/-} mice had predominantly macrophages with few SMCs.

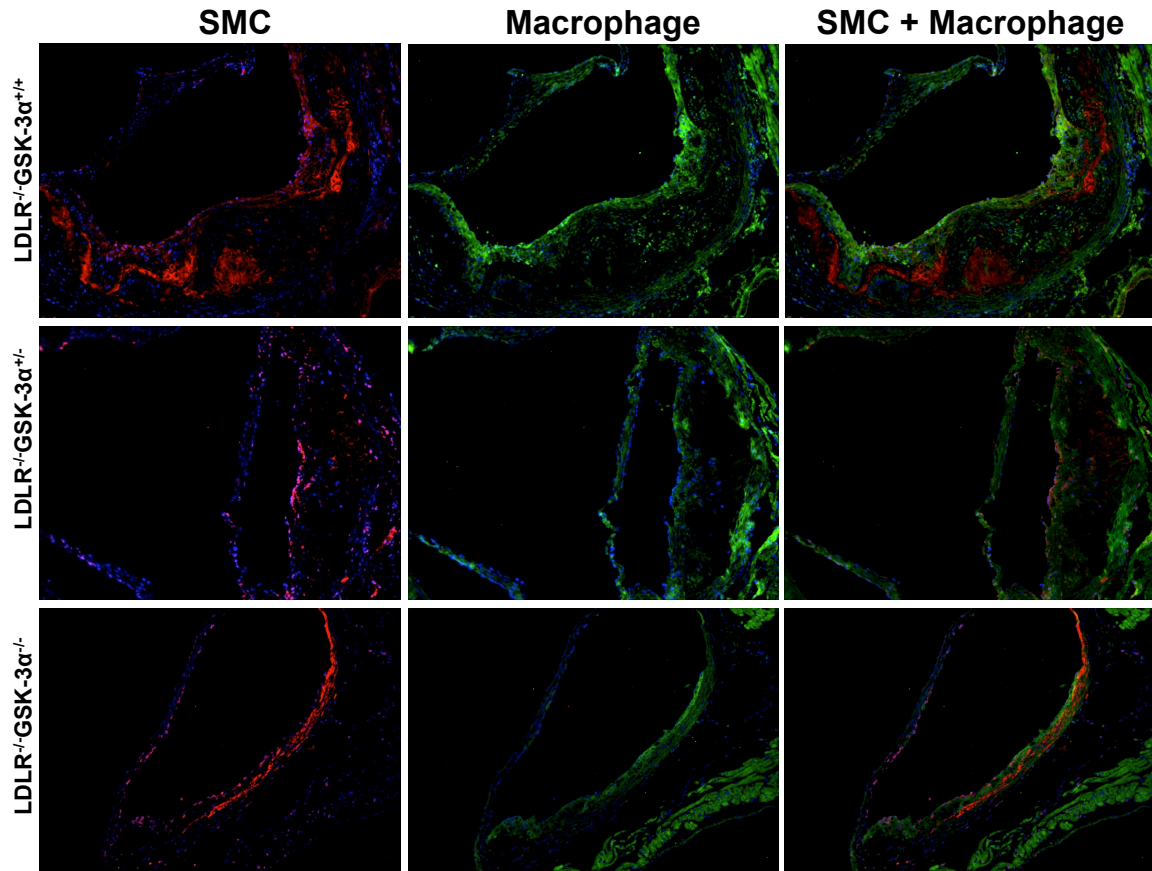


Figure 16 | **Effect of GSK-3 α deficiency on macrophages and smooth muscle cells in HFD-fed LDLR^{-/-} mice.** Representative immunochemical stained cross-sections of the aortic root from 15 week old HFD-fed LDLR^{-/-}GSK-3 α ^{+/+}, LDLR^{-/-}GSK-3 α ^{+/-}, and LDLR^{-/-}GSK-3 α ^{-/-} mice. Sections were stained for α -actin for SMCs (red), CD-1076 for Mac-3 (green), and then images were combined.

4.6 ER stress-induced free cholesterol accumulation was significantly reduced in GSK-3 α deficient peritoneal macrophages

We have shown that whole body deletion of GSK-3 α is sufficient to attenuate atherosclerosis, as well as to reduce hepatic lipid accumulation, in an LDLR-deficient mouse model. While the molecular mechanisms that underlie this effect are unknown, we hypothesized that the activation of GSK-3 α results in lipid accumulation, apoptosis, and inflammation, all hallmark features of atherosclerosis. Since our data shows that GSK-3 α

deficiency can protect against accelerated atherosclerosis, we next wanted to characterize changes to several of these pathways that accelerate atherogenesis. LDLR^{-/-}GSK-3 α ^{+/+}, LDLR^{-/-}GSK-3 α ^{+/-}, and LDLR^{-/-}GSK-3 α ^{-/-} peritoneal macrophages were isolated and treated with glucosamine and tunicamycin to induce ER stress. Peritoneal macrophages were grown on coverslips and stained with the unesterified cholesterol-binding chemical Filipin (Fig. 17a). The percent area stained divided by the total cell area was used to quantify Filipin staining. Unesterified cholesterol accumulation was significantly decreased in ER stress-induced GSK-3 α deficient peritoneal macrophages compared with LDLR^{-/-}GSK-3 α ^{+/+} controls (Fig. 17b). In addition, a significant increase in unesterified cholesterol upon induction of ER stress could only be seen in LDLR^{-/-}GSK-3 α ^{+/+} peritoneal macrophages, further suggesting that deletion of the GSK-3 α gene protects these cells from ER stress-induced cholesterol accumulation.

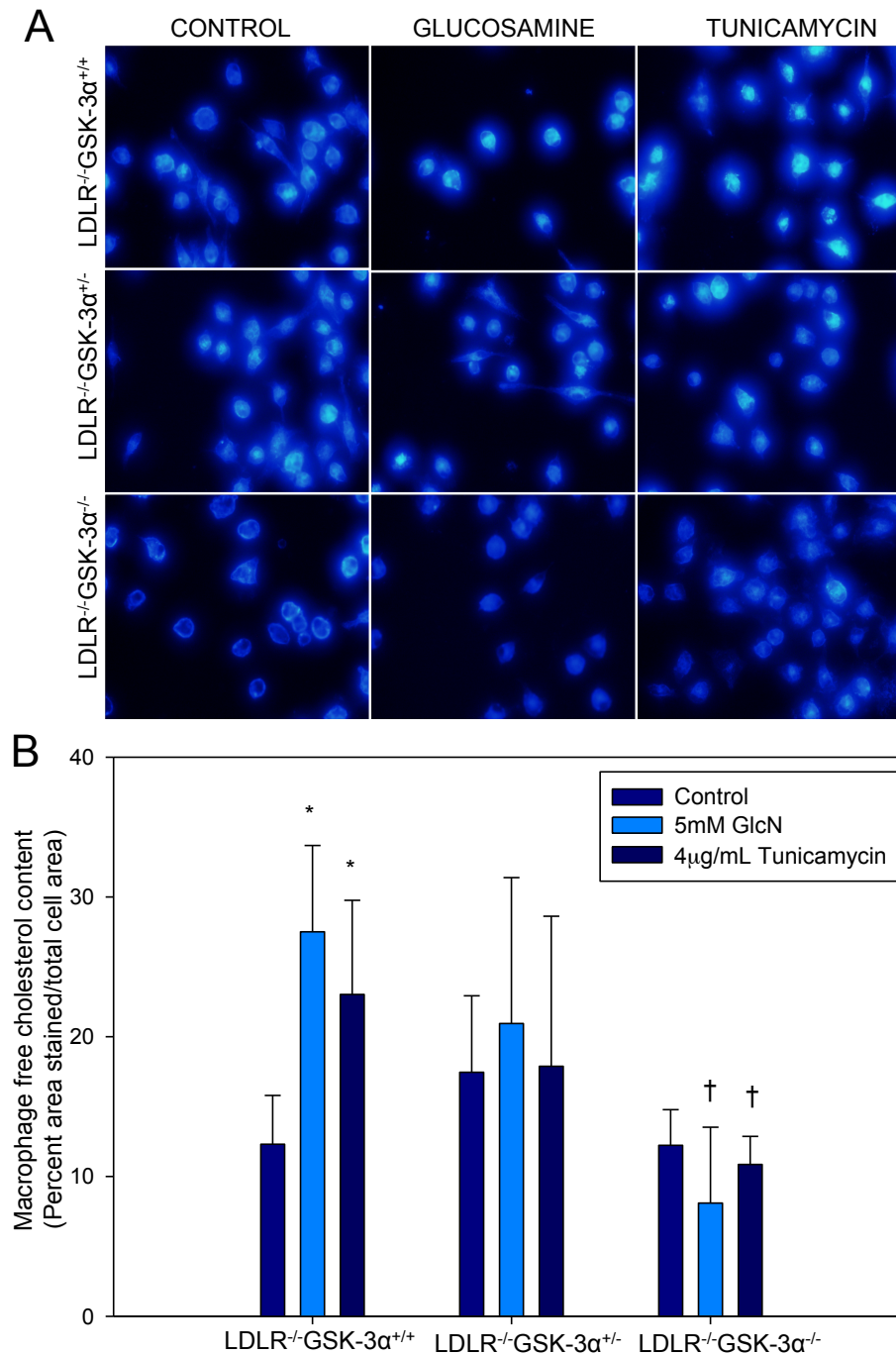


Figure 17 | ER stress-induced free cholesterol accumulation is significantly reduced in GSK-3 α deficient peritoneal macrophages. A | Representative images of Filipin stained peritoneal macrophages from high fat diet fed 15 week old female LDLR^{-/-}GSK-3 α ^{+/+}, LDLR^{-/-}GSK-3 α ^{+/-}, and LDLR^{-/-}GSK-3 α ^{-/-} mice treated with either 5mM glucosamine or 4µg/mL tunicamycin for 18 hours as indicated. Filipin stained free cholesterol was visualized by fluorescence microscopy. B | Quantification of Filipin stained peritoneal macrophages treated as described in A. *P<0.05 relative to control mice of same genotype. #P<0.05 relative to LDLR^{-/-}GSK-3 α ^{+/+} mice of same treatment group. n=3 per treatment group.

4.7 Effect of ER stress-induced GSK-3 α deficient peritoneal macrophages on inflammatory cytokine production

To determine the effect of GSK-3 α deficiency on the inflammatory response, several pro- and anti- inflammatory markers were analyzed using qRT-PCR. LDLR^{-/-} GSK-3 α ^{+/+}, LDLR^{-/-}GSK-3 α ^{+/-}, and LDLR^{-/-}GSK-3 α ^{-/-} peritoneal macrophages were isolated and treated with glucosamine and tunicamycin to induce ER stress. Total RNA was extracted from the peritoneal macrophages and reverse transcribed into cDNA. mRNA levels of the anti-inflammatory cytokine IL-10 were significantly increased in ER stress-induced GSK-3 α deficient peritoneal macrophages, with no significant effect on the mRNA level of the pro-inflammatory cytokine IL-1 β (Fig. 18).

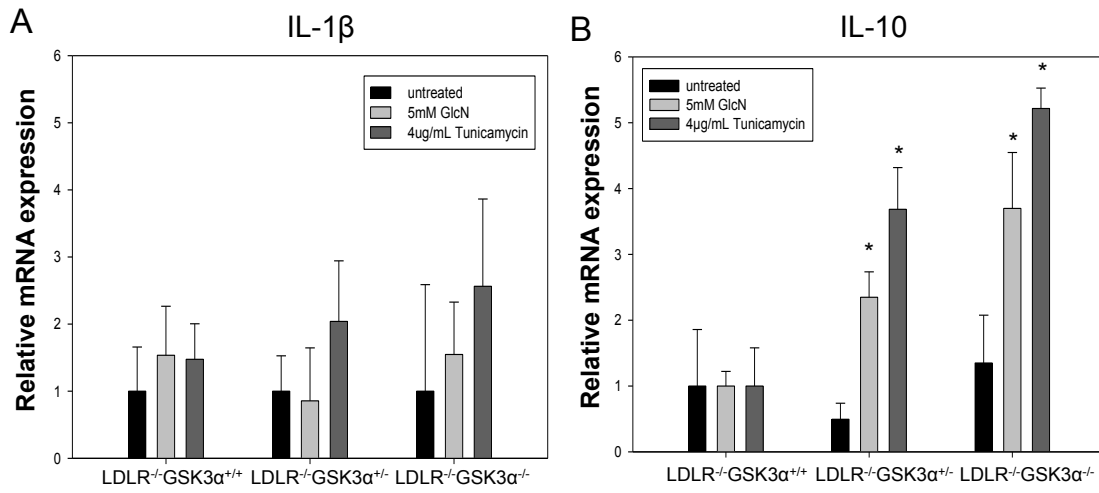


Figure 18 | **Effect of ER stress-induced GSK-3 α deficient peritoneal macrophages on IL-10 and IL-1 β mRNA levels.** Quantification of mRNA levels using RT-PCR in peritoneal macrophages from LDLR^{-/-}GSK-3 α ^{+/+}, LDLR^{-/-}GSK-3 α ^{+/-}, and LDLR^{-/-}GSK-3 α ^{-/-} mice. A | mRNA levels of IL-1 β from indicated groups. B | mRNA levels of IL-10 from indicated groups. *P<0.05 relative to LDLR^{-/-}GSK-3 α ^{+/+} of the same treatment group. n=3 per treatment group.

4.8 Effect of GSK-3 α ^{+/+} and GSK-3 α ^{-/-} bone marrow derived macrophages on atherosclerosis in LDLR^{-/-} mice

Bone marrow transplantation procedures were used to further investigate the role of GSK-3 α in atherosclerosis development. Macrophages play an important role in the initiation and progression of atherosclerosis. Bone marrow transplantation procedures provide a fast and effective way to generate tissue-specific knockout genotypes in a mouse model.

4.8.1 Genotyping of BMT mice

A 245bp band indicative of the SRY gene was visualized in peripheral blood 4 weeks after transplantation, indicating successful reconstitution of bone marrow (Fig. 19). All recipient mice contained the LDLR^{-/-} band at 350bp. Wild-type GSK-3 α was seen in

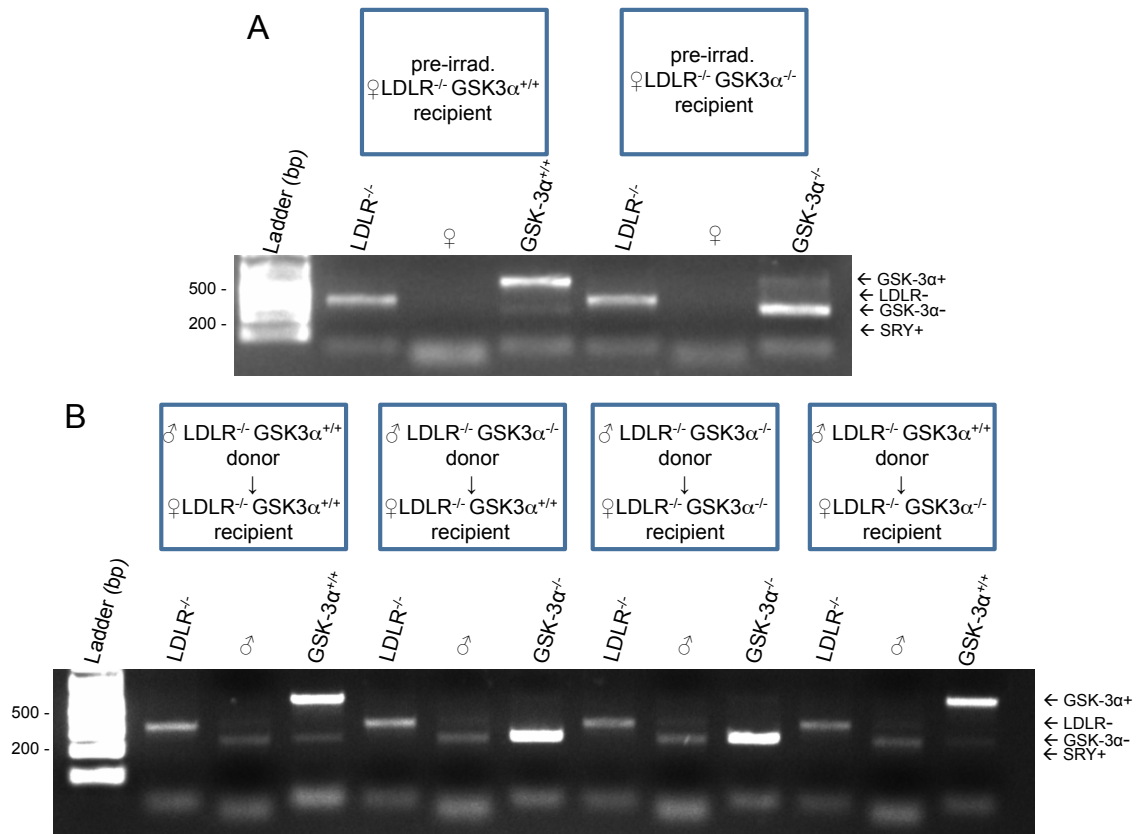


Figure 19 | **Genotype analysis of BMT recipient mice.** PCR techniques were used to identify the genetic characteristics from BMT mice either before irradiation or 4 weeks after bone marrow transplantation from male (SRY+) LDLR^{-/-}GSK-3α^{+/+}(L) or LDLR^{-/-}GSK-3α^{-/-}(LG) bone marrow. A | Genomic ear clippings from female LDLR^{-/-}GSK-3α^{+/+} and LDLR^{-/-}GSK-3α^{-/-} recipient mice. B | Peripheral blood from L→L, L→LG, LG→LG, and LG→L mice. A 2% agarose gel was used to visualize the bands.

recipient mice that were transplanted with LDLR^{-/-}GSK-3α^{+/+} bone marrow, as indicated by the band at 600bp. A 250bp band indicative of the null GSK-3α allele was seen in both LDLR^{-/-}GSK-3α^{+/+} and LDLR^{-/-}GSK-3α^{-/-} recipient mice transplanted with LDLR^{-/-}GSK-3α^{-/-} bone marrow. No wild-type GSK-3α was visualized in these mice.

4.8.2 Metabolic parameters

Body weight, fasting blood glucose levels, total plasma cholesterol and triglycerides, as well as liver and adipose weight were measured to evaluate the effect of bone marrow transplantation on the various experimental groups (Table 4). There was no significant difference in body weight, liver weight, or fasting blood glucose levels between $LDLR^{-/-}GSK-3\alpha^{+/+} \rightarrow LDLR^{-/-}GSK-3\alpha^{+/+}$ (L→L), $LDLR^{-/-}GSK-3\alpha^{+/+} \rightarrow LDLR^{-/-}GSK-3\alpha^{-/-}$ (L→LG), $LDLR^{-/-}GSK-3\alpha^{-/-} \rightarrow LDLR^{-/-}GSK-3\alpha^{-/-}$ (LG→LG) and $LDLR^{-/-}GSK-3\alpha^{-/-} \rightarrow LDLR^{-/-}GSK-3\alpha^{+/+}$ (LG→L) mice. Furthermore, plasma collected from the various experimental groups showed no significant difference in either total cholesterol or total triglycerides. The LG→L experimental group had a significant decrease in adipose weight compared with L→LG mice, suggesting that incorporation of GSK-3 α deficient macrophages in $LDLR^{-/-}$ mice has an effect on adipose tissue.

Table 4 | **Metabolic parameters in BMT mice**

	L(D)L(R)	LG(D)L(R)	LG(D)LG(R)	L(D)LG(R)
Body weight (g)	19.41±0.68	18.48±0.51	21.10±0.78	20.94±0.80
FBG (mM)	9.61±0.37	9.95±1.23	8.47±0.84	8.53±0.41
Cholesterol (mM)	30.46±0.62	29.72±4.26	32.24±2.44	25.32±2.51
Triglycerides (mM)	3.45±0.13	3.21±0.43	4.01±0.72	2.36±0.59
Liver weight (g)	1.04±0.03	0.90±0.03	0.99±0.03	0.88±0.05
Adipose weight (g)	0.21±0.05	0.10±0.02*	0.24±0.03	0.25±0.05

n=3-9 per treatment group; FBG; fasting blood glucose, L; LDLR^{-/-}, LG; LDLR^{-/-}GSK-3α^{-/-}, D; donor, R; recipient
*P<0.05 relative to age matched LG mice substituted with LDLR^{-/-}GSK-3α^{+/+} bone marrow

4.8.3 Lesion analysis in BMT mice

To determine the effect of GSK-3α deficient macrophages on atherosclerotic development in HFD-fed LDLR^{-/-} mice, serial histological sections were collected and plaque volume as well as plaque area in the aortic sinus were assessed. Plaque formation was seen in all BMT groups when placed on a high fat diet. There was no significant difference in lesion volume between L→L, L→LG, LG→LG and LG→L mice (lesion volume: 38±3 x 10³mm³ for L→L mice, 42±9 x 10³mm³ for LG→L mice, 70±26 x 10³mm³ for L→LG mice, and 18±9 x 10³mm³ for LG→LG mice) (Fig. 20b). LG→L and LG→LG transplanted mice had a significant decrease in lesion area in the aortic sinus compared with the L→LG group (lesion area 0.20±0.03mm² for L→L mice, 0.25±0.03mm² for L→LG mice, 0.13±0.007mm² for LG→L mice, and 0.08±0.02mm² for LG→LG mice) (Fig. 20a & 20c).

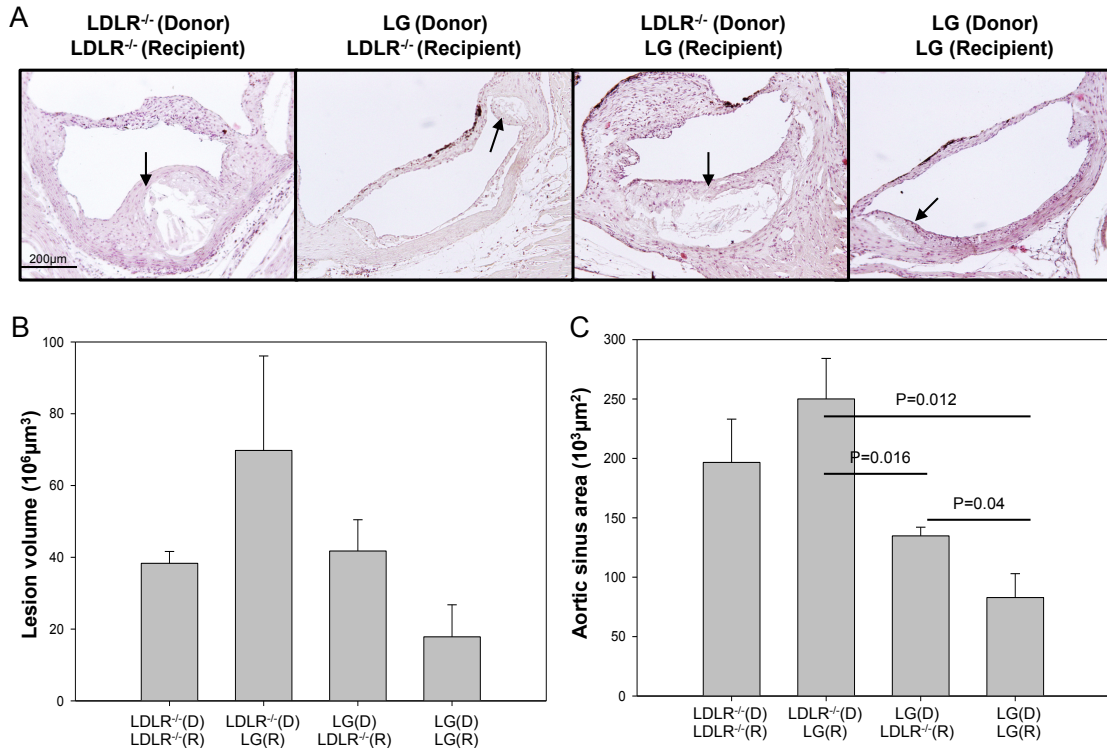


Figure 20 | Effect of GSK-3 α deficient bone marrow derived macrophages on atherogenesis in HFD-fed LDLR^{-/-} mice. High fat diet fed 15 week old female LDLR^{-/-}GSK-3 α ^{+/+} and LDLR^{-/-}GSK-3 α ^{-/-} recipient mice transplanted with bone marrow from male LDLR^{-/-}GSK-3 α ^{+/+} and LDLR^{-/-}GSK-3 α ^{-/-} (LG) donor mice. **A** | Representative hematoxylin and eosin stained aortic sinus cross sections. **B** | Quantification of the lesion volume in the ascending aorta (n=3-5). **C** | Quantification of the cross-sectional area of the aortic sinus (n=3-5).

CHAPTER 5: DISCUSSION

Cardiovascular disease is the number one killer in the developing world, and extensive research has gone into determining molecular mechanisms that contribute to this disease. Multiple studies have suggested that ER stress and the unfolded protein response play important roles in the initiation and progression of atherosclerosis – a major underlying cause of CVD (Bowes, et al., 2009; Erbay, et al., 2009; Zhou, et al., 2004). Our knowledge of the metabolic pathways that link ER stress to atherogenesis is incomplete. Emerging evidence has supported a role for the molecular enzyme glycogen synthase kinase (GSK)-3 in activating several of the hallmark processes involved in atherosclerosis, such as lipid accumulation, inflammation and apoptosis. GSK-3 α/β is a constitutively active serine/threonine kinase implicated in a multitude of signal transduction pathways (Doble & Woodgett, 2003; Frame & Cohen, 2001; Grimes & Jope, 2001). This kinase has been linked to a variety of pathophysiological conditions, including bipolar disorder, Alzheimer's disease, diabetes, and cancer (Gao, Holscher, Liu, & Li, 2012; Nishiguchi, Breen, Russ, St Clair, & Collier, 2006; Patel & Woodgett, 2008). In the present study we investigated the potential role of GSK-3 α in the development of atherosclerosis by creating and characterizing lesion formation in a novel LDLR/GSK-3 α double knockout mouse model.

Strong evidence supports a role for ER stress-induced cellular mechanisms in the induction of pro-atherogenic pathways that accelerate the development of atherosclerosis (Khan, et al., 2009; Robertson, Kim, & Werstuck, 2006). Several cardiovascular risk factors, such as diabetes, dyslipidemia, obesity, and smoking, have been shown to induce

vascular ER stress (McAlpine, et al., 2011; Sage et al., 2011). Chronic ER stress and subsequent UPR induction results in the activation of metabolic pathways that are involved in pro-atherogenic lesion development, such as lipid accumulation, inflammation and apoptosis (Colgan, et al., 2007; A. J. Kim, et al., 2005; Thorp, et al., 2009; Zinszner, et al., 1998). Furthermore, UPR activation in atherosclerosis-prone regions has been detected prior to lesion development (Civelek, Manduchi, Riley, Stoeckert, & Davies, 2009; Khan, et al., 2009). Evidence from our lab has shown that GSK-3 α/β inhibitors can attenuate ER stress-induced lipid accumulation and apoptosis without significantly affecting the level of ER stress, as measured by UPR induction (A. J. Kim, et al., 2005). This suggests that GSK-3 functions downstream of ER stress. The present study further supports this hypothesis by showing that GSK-3 α deficiency in LDLR^{-/-} mice, fed a standard chow diet or high fat diet, does not significantly affect vascular or hepatic ER stress levels. Specifically, the expression of UPR proteins including GRP78/94 and PDI, were not significantly different in mice lacking GSK-3 α compared with age-matched controls.

Mood stabilizing agents such as lithium and valproate have been shown to selectively inhibit GSK-3 α/β (Chen, Huang, Jiang, & Manji, 1999; Kaladchibachi, Doble, Anthopoulos, Woodgett, & Manoukian, 2007; Kirshenboim, Plotkin, Shlomo, Kaidanovich-Beilin, & Eldar-Finkelman, 2004). Valproate is a small branched-chain fatty acid that is widely used in the treatment of several neurological disorders, including epilepsy and bipolar disorder (Rosenberg, 2007). In addition to GSK-3 inhibition, valproate has also been shown to promote inositol depletion, to potentiate the function of

the neurotransmitter GABA, and to inhibit the enzyme histone deacetylase (HDAC) (Johannessen, 2000; O'Donnell et al., 2000; Phiel et al., 2001). A recent study has shown that epileptic patients taking valproate have a significantly decreased risk of myocardial infarction (Olesen et al., 2011). The effect appears to be specific for valproate and is not seen with other anti-convulsants (Olesen, et al., 2011). Evidence from our lab has shown that HepG2 cells pretreated with valproate were protected from ER stress-induced lipid accumulation and apoptosis. Hyperglycemic ApoE-deficient mice supplemented with a diet containing valproate had decreased hepatic GSK-3 β activity as well as reduced lipid accumulation in the liver (Bowes, et al., 2009). Furthermore, these mice exhibited a reduction in lesion volume in the aortic root compared with age-matched controls (Bowes, et al., 2009). In the present study, we show that HFD-fed LDLR^{-/-} mice supplemented with valproate had a significant decrease in lesion and necrotic core volume. LDLR^{-/-} mice fed a standard chow diet had minimal to no plaque and necrotic core formation. Valproate supplementation did not alter body, liver, or adipose weight in these mice. In addition, plasma parameters such as non-fasting blood glucose as well as total cholesterol and triglycerides were not significantly changed with valproate supplementation. The fact that lipid levels in the plasma were not altered suggests that the effects of valproate on decreased lesion development could be localized to the vascular wall. Cholesterol and triglyceride levels in the liver of LDLR^{-/-} mice will need to be assessed to determine the effect of valproate on hepatic lipid metabolism.

There are several limitations to using valproate in the study of GSK-3 and atherosclerosis. Among these are its multiple side effects in humans, such as weight gain,

fatigue, dizziness, drowsiness, headache, and nausea, as well as its ability to inhibit other enzymes, including the HDACs (Dreifuss & Langer, 1988; Phiel, et al., 2001). Secondly, all known inhibitors of GSK-3 lack the ability to differentiate between the α and β forms. This makes it difficult to determine the specific roles of each form of this protein. At the present time, the only available way to examine the specific roles of GSK-3 α and GSK-3 β *in vivo* is genetic deletion. As GSK-3 β mice are not viable, we crossed GSK-3 α deficient mice into the atherosclerosis prone LDLR^{-/-} knockout mouse model. Evidence from this *in vivo* model shows that a deficiency of GSK-3 α confers protection against diet-induced accelerated atherosclerosis. LDLR^{-/-} mice that lacked GSK-3 α had a significant reduction in necrotic core volume, a characteristic indicative of the stage of plaque development. Macrophage apoptosis plays an important role in the development of the necrotic core, suggesting that apoptosis is attenuated in GSK-3 α deficient macrophages. Furthermore, a reduced number of macrophages as well as vascular smooth muscle cells were observed in lesions of GSK-3 α deficient mice. Despite the changes in lesion formation, GSK-3 α ^{-/-} mice exhibited no significant differences in fasting and non-fasting blood glucose, body mass, liver or adipose weight, and plasma cholesterol and triglyceride levels were comparable to LDLR^{-/-} controls. ER stress-induced peritoneal macrophages isolated from GSK-3 α deficient mice showed a reduction in unesterified cholesterol accumulation. Unesterified cholesterol has been linked to the induction of ER stress in various cell types and results in increased apoptosis (Feng, et al., 2003). Therefore, GSK-3 α activity in macrophages could result in the induction of apoptosis as a result of increased unesterified cholesterol.

The majority of cholesterol and triglyceride synthesis occurs in the liver. Cells obtain cholesterol from the circulation in the form of LDL via the LDLR, which are further modified to give rise to free cholesterol in lysosomes. An abnormal lipid level in the plasma, resulting in hypercholesterolemia and hypertriglyceridemia, is one of the major risk factors for CVD. Furthermore, non-alcoholic fatty liver disease (NAFLD) is associated with the development of atherosclerosis (Targher & Arcaro, 2007). To determine the effect of GSK-3 α deficiency on lipid metabolism, hepatic lipid levels were examined. In our HFD-fed LDLR^{-/-} mice, GSK-3 α deficiency resulted in an attenuation of hepatic steatosis. GSK-3 α deficient mice as well as mice heterozygous for the GSK-3 α gene had a decrease in hepatic neutral lipid accumulation. Furthermore, a significant decrease in total hepatic cholesterol was observed in mice lacking GSK-3 α . Hepatic lipid accumulation was not detected in mice fed a standard chow diet, and there were no evident differences between LDLR^{-/-}GSK-3 α ^{+/+}, LDLR^{-/-}GSK-3 α ^{+/-}, and LDLR^{-/-}GSK-3 α ^{-/-} mice. In addition, GSK-3 α deficiency was associated with a decrease in hepatic lipid accumulation in HFD-fed LDLR^{+/+} mice. Together, these results suggest that GSK-3 α plays a role in hepatic cholesterol and triglyceride metabolism. These results are consistent with previous findings in ApoE-deficient mice showing a decrease in lipid accumulation in the liver with valproate supplementation (Bowes, et al., 2009). However, we did observe an interesting variation in these different systems.

Regulation of cholesterol and triglyceride biosynthesis is controlled by the sterol regulatory element binding proteins (SREBP)-1 and 2. SREBPs are an important class of transcription factors that respond to changes in the amount of cholesterol and triglycerides

within cells. When lipid concentration is low, SREBPs are activated and promote the increased transcriptional expression of lipid biosynthetic proteins such as HMG-CoA reductase and fatty acid synthase (Pai, et al., 1998). Previous results from our lab have shown that hyperglycemic ApoE^{-/-} mice supplemented with a diet containing valproate had a reduction in transcripts encoding SREBP-1c and SPREBP-2 as well as HMG-CoA reductase and FAS in the liver. In the present study, whole body deletion of GSK-3 α resulted in an increase in the hepatic expression of SREBP-1c/2, HMG-CoA reductase, and FAS. There are several differences in these two experimental models that may explain this apparent discrepancy. First, in GSK-3 α knockout mice, GSK-3 α/β activity was reduced by 20%, suggesting that 80% of activity in the liver of these mice is a result of GSK-3 β . The specific effect of valproate supplementation on hepatic GSK-3 α/β is not known, however it is expected that both forms were inhibited to some degree. Differences in total GSK-3 α/β activity may have different consequences on the expression of genes involved in lipid metabolism. Alternatively, GSK-3 β could play a specific role in the regulation of expression of these genes, while GSK-3 α is required for protein activation. Finally, monitoring mRNA transcript levels does not provide any information regarding post-translational modifications as well as protein activation. Further experiments will need to be performed to examine the activities of SREBP-1c, SREBP-2, HMG-CoA reductase, and FAS. Overall, these results support a role for ER stress-induced activation of GSK-3 α in the induction of cholesterol and triglyceride accumulation.

In addition to lipid regulation, GSK-3 plays a pivotal role in regulating the inflammatory response. Evidence supports a role for GSK-3 inhibition in the upregulation

of IL-10 (Martin, et al., 2005). Consistent with previous findings, we show that GSK-3 α deficient macrophages exposed to ER stress-inducing agents have significantly increased levels of IL-10 expression. IL-10 is a potent anti-inflammatory cytokine produced by a variety of immune cells, including; TH2 cells, macrophages, and CD8⁺ cells (Saraiva & O'Garra, 2010). Studies have shown that IL-10-deficient mice have increased lesion formation, while reduction in atherosclerotic plaque is seen in their transgenic counterparts that overexpress IL-10 (Caligiuri et al., 2003; Mallat et al., 1999; Pinderski Oslund et al., 1999). The observed increase in IL-10 production in ER stress-induced GSK-3 α deficient macrophages could suggest a possible mechanism for attenuating lesion and necrotic core development in LDLR^{-/-}GSK-3 α ^{-/-} mice. IL-10 has been shown to be a potent inhibitor of several pro-inflammatory cytokines, including; IL-1 β , TNF- α , IL-6 and IL-12 (Moore, de Waal Malefyt, Coffman, & O'Garra, 2001). Furthermore, GSK-3 inhibition, as well as siRNA knockdown, results in a decrease in the production of pro-inflammatory cytokines such as IL-1 β , IL-6, TNF- α and IL-12 (Martin, et al., 2005). Here we show that GSK-3 α deficiency had no significant effect on IL-1 β mRNA levels in ER stress-induced peritoneal macrophages. Previous results have shown that IL-1 β ^{-/-}ApoE^{-/-} mice have a 30% significant decrease in atherosclerosis with no change in plasma lipid profiles (Kirii et al., 2003). Furthermore, studies looking at GSK-3 inhibition have shown an IL-10-mediated suppression of IL-1 β expression (Antoniv & Ivashkiv, 2011). The fact that IL-1 β was not significantly altered with GSK-3 α deficiency could suggest a specific role for GSK-3 β in regulating this pro-inflammatory cytokine. Further examination of inflammatory cytokine expression from macrophages isolated from GSK-3 α knockout

mice will need to be carried out in order to elucidate a specific role for GSK-3 α in inflammation and atherosclerotic development.

As whole body deletion of GSK-3 α resulted in attenuated atherosclerosis, our next step of experimentation was to more specifically examine the effect of GSK-3 α deficient bone marrow derived macrophages on lesion development. Macrophages are important in intracellular lipid accumulation and are the predominant cell type in the initiation and progression of atherosclerosis. The experiment presented in this study involved the ablation of bone marrow hematopoietic stem cells in LDLR^{-/-} or LDLR^{-/-}GSK-3 α ^{-/-} mice followed by injection of donor LDLR^{-/-}GSK-3 α ^{+/+} or LDLR^{-/-}GSK-3 α ^{-/-} bone marrow. Plaque volume in the aortic root was not significantly different between any of the BMT groups. However, GSK-3 α deficient LDLR^{-/-} mice transplanted with autologous bone marrow had a significant reduction in lesion area in the aortic sinus compared with GSK-3 α deficient mice transplanted with GSK-3 α ^{+/+} bone marrow. GSK-3 α ^{+/+} recipient mice reconstituted with GSK-3 α deficient bone marrow had a decrease in aortic sinus lesion formation compared with control mice of the same recipient group. These findings provide further evidence that macrophage-specific GSK-3 α deficiency results in the attenuation of accelerated atherosclerosis.

Together, these findings support a role for GSK-3 α activity in the initiation and progression of atherosclerosis. These findings are also consistent with our hypothesis that GSK-3 functions downstream of ER stress. This is the first time a whole body deletion of GSK-3 α has been examined in a mouse model of accelerated atherosclerosis. These results are an important step towards understanding the molecular mechanisms by which

GSK-3 α/β activity leads to the induction of pro-atherogenic pathways. Understanding how GSK-3 signals through ER stress pathways in the development of atherosclerosis is fundamental in identifying future points of intervention and therapeutic strategies.

CHAPTER 6: CONCLUSION AND FUTURE DIRECTIONS

Here we report that the GSK-3 inhibitor valproate as well as a whole body knockout of GSK-3 α in HFD-fed LDLR knockout mice reduced the development of atherosclerosis. On a standard chow diet, LDLR^{-/-}GSK-3 α ^{-/-} mice were phenotypically indistinguishable from LDLR^{-/-} mice. On a high fat diet, LDLR^{-/-} mice developed an extensive amount of plaque in the aortic root. Lesion development was significantly reduced in mice deficient for GSK-3 α . LDLR^{-/-}GSK-3 α ^{-/-} mice had fewer macrophages and SMCs in the atherosclerotic lesion compared with LDLR^{-/-}GSK-3 α ^{+/+} mice. GSK-3 α deficient mice also had a reduction in lipid accumulation in the liver. Oil red O staining of liver sections showed a significant decrease in the amount of neutral lipids in LDLR^{-/-}GSK-3 α ^{-/-} mice compared with controls. Furthermore, total hepatic cholesterol was significantly reduced with GSK-3 α deficiency. qRT-PCR analysis of liver lysates showed an increasing trend in expression levels of lipid biosynthetic proteins in GSK-3 α deficient mice compared with controls. Total hepatic GSK-3 activity was 20% lower in LDLR^{-/-}GSK-3 α ^{-/-} mice relative to LDLR^{-/-}GSK-3 α ^{+/+} mice, suggesting that 80% of hepatic activity in these mice is due to GSK-3 β . Isolation of ER stress-induced peritoneal macrophages from GSK-3 α deficient mice showed a significant decrease in unesterified cholesterol as well as a significant increase in the anti-inflammatory cytokine IL-10. Finally, LDLR^{-/-}GSK-3 α ^{+/+} mice transplanted with LDLR^{-/-}GSK-3 α ^{-/-} bone marrow had a significant reduction in lesion formation in the aortic sinus compared with LDLR^{-/-}GSK-3 α ^{-/-} mice transplanted with LDLR^{-/-}GSK-3 α ^{+/+} bone marrow.

Possible future studies include examination of additional pro-inflammatory cytokine expression in both the liver as well as ER stress-induced GSK-3 α deficient peritoneal macrophages, and analysis of lipid biosynthetic protein activity in the liver of GSK-3 α deficient mice. These studies would give further insight into the role of GSK-3 α activity in regulating both pro- and anti-inflammatory pathways as well as its role in activating several proteins involved in lipid regulation. Furthermore, due to the limiting number of macrophages isolated, analysis of IL-10 expression in GSK-3 α deficient mice should be repeated to verify our results. Finally, the effects of valproate supplementation on hepatic lipid metabolism in LDLR^{-/-} mice should be examined to determine if this GSK-3 inhibitor has similar effects in regulating lipid accumulation as in GSK-3 α deficient mice. Ultimately, to fully discern the roles of GSK-3 α and GSK-3 β in atherogenesis, tissue-specific deletion models of both forms will need to be generated to specifically measure the effects of kinase differences in relevant cell types, including; hepatocytes, monocytes, endothelial cells, and vascular SMCs.

CHAPTER 7: REFERENCES

- Antoniv, T. T., & Ivashkiv, L. B. (2011). Interleukin-10-induced gene expression and suppressive function are selectively modulated by the PI3K-Akt-GSK3 pathway. *Immunology*, *132*(4), 567-577.
- Azoulay-Alfaguter, I., Yaffe, Y., Licht-Murava, A., Urbanska, M., Jaworski, J., Pietrokovski, S., . . . Eldar-Finkelman, H. (2011). Distinct molecular regulation of glycogen synthase kinase-3alpha isozyme controlled by its N-terminal region: functional role in calcium/calpain signaling. *J Biol Chem*, *286*(15), 13470-13480.
- Bao, Z., Lim, S., Liao, W., Lin, Y., Thiemermann, C., Leung, B. P., & Wong, W. S. (2007). Glycogen synthase kinase-3beta inhibition attenuates asthma in mice. *Am J Respir Crit Care Med*, *176*(5), 431-438.
- Barrett-Connor, E. L., Cohn, B. A., Wingard, D. L., & Edelstein, S. L. (1991). Why is diabetes mellitus a stronger risk factor for fatal ischemic heart disease in women than in men? The Rancho Bernardo Study. *JAMA*, *265*(5), 627-631.
- Bax, B., Carter, P. S., Lewis, C., Guy, A. R., Bridges, A., Tanner, R., . . . Reith, A. D. (2001). The structure of phosphorylated GSK-3beta complexed with a peptide, FRATtide, that inhibits beta-catenin phosphorylation. *Structure*, *9*(12), 1143-1152.
- Bence, N. F., Sampat, R. M., & Kopito, R. R. (2001). Impairment of the ubiquitin-proteasome system by protein aggregation. *Science*, *292*(5521), 1552-1555.
- Beriault, D. R., Sharma, S., Shi, Y., Khan, M. I., & Werstuck, G. H. (2011). Glucosamine-supplementation promotes endoplasmic reticulum stress, hepatic steatosis and accelerated atherogenesis in apoE^{-/-} mice. *Atherosclerosis*, *219*(1), 134-140.
- Beurel, E., & Jope, R. S. (2006). The paradoxical pro- and anti-apoptotic actions of GSK3 in the intrinsic and extrinsic apoptosis signaling pathways. *Prog Neurobiol*, *79*(4), 173-189.
- Bijur, G. N., & Jope, R. S. (2001). Proapoptotic stimuli induce nuclear accumulation of glycogen synthase kinase-3 beta. *J Biol Chem*, *276*(40), 37436-37442.
- Bijur, G. N., & Jope, R. S. (2003). Glycogen synthase kinase-3 beta is highly activated in nuclei and mitochondria. *Neuroreport*, *14*(18), 2415-2419.
- Borradaile, N. M., Han, X., Harp, J. D., Gale, S. E., Ory, D. S., & Schaffer, J. E. (2006). Disruption of endoplasmic reticulum structure and integrity in lipotoxic cell death. *Journal of lipid research*, *47*(12), 2726-2737.

- Bowes, A. J., Khan, M. I., Shi, Y., Robertson, L., & Werstuck, G. H. (2009). Valproate attenuates accelerated atherosclerosis in hyperglycemic apoE-deficient mice: evidence in support of a role for endoplasmic reticulum stress and glycogen synthase kinase-3 in lesion development and hepatic steatosis. *Am J Pathol*, *174*(1), 330-342.
- Brewster, J. L., Linseman, D. A., Bouchard, R. J., Loucks, F. A., Precht, T. A., Esch, E. A., & Heidenreich, K. A. (2006). Endoplasmic reticulum stress and trophic factor withdrawal activate distinct signaling cascades that induce glycogen synthase kinase-3 beta and a caspase-9-dependent apoptosis in cerebellar granule neurons. *Mol Cell Neurosci*, *32*(3), 242-253.
- Brown, M.S., & Goldstein, J.L. (1986). A receptor-mediated pathway for cholesterol homeostasis. *Science*, *232*(4746), 34-47.
- Brownlee, M. (2001). Biochemistry and molecular cell biology of diabetic complications. *Nature*, *414*(6865), 813-820.
- Caligiuri, G., Rudling, M., Ollivier, V., Jacob, M. P., Michel, J. B., Hansson, G. K., & Nicoletti, A. (2003). Interleukin-10 deficiency increases atherosclerosis, thrombosis, and low-density lipoproteins in apolipoprotein E knockout mice. *Mol Med*, *9*(1-2), 10-17.
- Chang, Y. S., Tsai, C. T., Huangfu, C. A., Huang, W. Y., Lei, H. Y., Lin, C. F., . . . Lai, M. D. (2011). ACSL3 and GSK-3beta are essential for lipid upregulation induced by endoplasmic reticulum stress in liver cells. *J Cell Biochem*, *112*(3), 881-893.
- Chen, G., Huang, L. D., Jiang, Y. M., & Manji, H. K. (1999). The mood-stabilizing agent valproate inhibits the activity of glycogen synthase kinase-3. *J Neurochem*, *72*(3), 1327-1330.
- Civelek, M., Manduchi, E., Riley, R. J., Stoeckert, C. J., Jr., & Davies, P. F. (2009). Chronic endoplasmic reticulum stress activates unfolded protein response in arterial endothelium in regions of susceptibility to atherosclerosis. *Circ Res*, *105*(5), 453-461.
- Colgan, S. M., Tang, D., Werstuck, G. H., & Austin, R. C. (2007). Endoplasmic reticulum stress causes the activation of sterol regulatory element binding protein-2. *The international journal of biochemistry & cell biology*, *39*(10), 1843-1851.
- Cross, D. A., Alessi, D. R., Cohen, P., Andjelkovich, M., & Hemmings, B. A. (1995). Inhibition of glycogen synthase kinase-3 by insulin mediated by protein kinase B. *Nature*, *378*(6559), 785-789.
- Cuzzocrea, S., Mazzon, E., Di Paola, R., Muia, C., Crisafulli, C., Dugo, L., . . . Thiemermann, C. (2006). Glycogen synthase kinase-3beta inhibition attenuates

- the degree of arthritis caused by type II collagen in the mouse. *Clin Immunol*, *120*(1), 57-67.
- Cybulsky, M. I., & Gimbrone, M. A., Jr. (1991). Endothelial expression of a mononuclear leukocyte adhesion molecule during atherogenesis. *Science*, *251*(4995), 788-791.
- Dajani, R., Fraser, E., Roe, S. M., Young, N., Good, V., Dale, T. C., & Pearl, L. H. (2001). Crystal structure of glycogen synthase kinase 3 beta: structural basis for phosphate-primed substrate specificity and autoinhibition. *Cell*, *105*(6), 721-732.
- Doble, B. W., & Woodgett, J. R. (2003). GSK-3: tricks of the trade for a multi-tasking kinase. *Journal of cell science*, *116*(Pt 7), 1175-1186.
- Dreifuss, F. E., & Langer, D. H. (1988). Side effects of valproate. *Am J Med*, *84*(1A), 34-41.
- Eldar-Finkelman, H., Schreyer, S. A., Shinohara, M. M., LeBoeuf, R. C., & Krebs, E. G. (1999). Increased glycogen synthase kinase-3 activity in diabetes- and obesity-prone C57BL/6J mice. *Diabetes*, *48*(8), 1662-1666.
- Erbay, E., Babaev, V. R., Mayers, J. R., Makowski, L., Charles, K. N., Snitow, M. E., . . . Hotamisligil, G. S. (2009). Reducing endoplasmic reticulum stress through a macrophage lipid chaperone alleviates atherosclerosis. *Nat Med*, *15*(12), 1383-1391.
- Faideau, B., Larger, E., Lepault, F., Carel, J. C., & Boitard, C. (2005). Role of beta-cells in type 1 diabetes pathogenesis. *Diabetes*, *54 Suppl 2*, S87-96.
- Feng, B., Yao, P. M., Li, Y., Devlin, C. M., Zhang, D., Harding, H. P., . . . Tabas, I. (2003). The endoplasmic reticulum is the site of cholesterol-induced cytotoxicity in macrophages. *Nat Cell Biol*, *5*(9), 781-792.
- Fiol, C. J., Mahrenholz, A. M., Wang, Y., Roeske, R. W., & Roach, P. J. (1987). Formation of protein kinase recognition sites by covalent modification of the substrate. Molecular mechanism for the synergistic action of casein kinase II and glycogen synthase kinase 3. *J Biol Chem*, *262*(29), 14042-14048.
- Frame, S., & Cohen, P. (2001). GSK3 takes centre stage more than 20 years after its discovery. *The Biochemical journal*, *359*(Pt 1), 1-16.
- Gao, C., Holscher, C., Liu, Y., & Li, L. (2012). GSK3: a key target for the development of novel treatments for type 2 diabetes mellitus and Alzheimer disease. *Rev Neurosci*, *23*(1), 1-11.
- Gaspar, M. L., Jesch, S. A., Viswanatha, R., Antosh, A. L., Brown, W. J., Kohlwein, S. D., & Henry, S. A. (2008). A block in endoplasmic reticulum-to-Golgi trafficking

- inhibits phospholipid synthesis and induces neutral lipid accumulation. *J Biol Chem*, 283(37), 25735-25751.
- Giacco, F., & Brownlee, M. (2010). Oxidative stress and diabetic complications. *Circ Res*, 107(9), 1058-1070.
- Gotoh, T., Oyadomari, S., Mori, K., & Mori, M. (2002). Nitric oxide-induced apoptosis in RAW 264.7 macrophages is mediated by endoplasmic reticulum stress pathway involving ATF6 and CHOP. *J Biol Chem*, 277(14), 12343-12350.
- Grimes, C. A., & Jope, R. S. (2001). The multifaceted roles of glycogen synthase kinase 3beta in cellular signaling. *Prog Neurobiol*, 65(4), 391-426.
- Guariguata, L., Whiting, D., Weil, C., & Unwin, N. (2011). The International Diabetes Federation diabetes atlas methodology for estimating global and national prevalence of diabetes in adults. *Diabetes Res Clin Pract*, 94(3), 322-332.
- Gwiazda, K. S., Yang, T. L., Lin, Y., & Johnson, J. D. (2009). Effects of palmitate on ER and cytosolic Ca²⁺ homeostasis in beta-cells. *American journal of physiology. Endocrinology and metabolism*, 296(4), E690-701.
- Haffner, S. M. (1998). The importance of hyperglycemia in the nonfasting state to the development of cardiovascular disease. *Endocr Rev*, 19(5), 583-592.
- Hetz, C. (2012). The unfolded protein response: controlling cell fate decisions under ER stress and beyond. *Nat Rev Mol Cell Biol*, 13(2), 89-102.
- Hiroi, T., Wei, H., Hough, C., Leeds, P., & Chuang, D. M. (2005). Protracted lithium treatment protects against the ER stress elicited by thapsigargin in rat PC12 cells: roles of intracellular calcium, GRP78 and Bcl-2. *Pharmacogenomics J*, 5(2), 102-111.
- Hoeflich, K. P., Luo, J., Rubie, E. A., Tsao, M. S., Jin, O., & Woodgett, J. R. (2000). Requirement for glycogen synthase kinase-3beta in cell survival and NF-kappaB activation. *Nature*, 406(6791), 86-90.
- Hoshi, M., Sato, M., Kondo, S., Takashima, A., Noguchi, K., Takahashi, M., . . . Imahori, K. (1995). Different localization of tau protein kinase I/glycogen synthase kinase-3 beta from glycogen synthase kinase-3 alpha in cerebellum mitochondria. *J Biochem*, 118(4), 683-685.
- Hu, X., Paik, P. K., Chen, J., Yarilina, A., Kockeritz, L., Lu, T. T., . . . Ivashkiv, L. B. (2006). IFN-gamma suppresses IL-10 production and synergizes with TLR2 by regulating GSK3 and CREB/AP-1 proteins. *Immunity*, 24(5), 563-574.

- Ibrahim, S. H., Akazawa, Y., Cazanave, S. C., Bronk, S. F., Elmi, N. A., Werneburg, N. W., . . . Gores, G. J. (2011). Glycogen synthase kinase-3 (GSK-3) inhibition attenuates hepatocyte lipoapoptosis. *J Hepatol*, *54*(4), 765-772.
- Ishiguro, K., Shiratsuchi, A., Sato, S., Omori, A., Arioka, M., Kobayashi, S., . . . Imahori, K. (1993). Glycogen synthase kinase 3 beta is identical to tau protein kinase I generating several epitopes of paired helical filaments. *FEBS Lett*, *325*(3), 167-172.
- Ishibashi, S., Brown, M. S., Goldstein, J.L., Gerard, R.D., Hammer, R.E., & Herz Joachrim. (1993). Hypercholesterolemia in low density lipoprotein receptor knockout mice and its reversal by adenovirus-mediated gene delievery. *J Clin Invest*, *92*(2), 883-893.
- Ishibashi, S., Goldstein, J.L., Brown, M. S., Herz Joachrim & Burns, D.K. (1994). Massive Xanthomatosis and atherosclerosis in cholesterol-fed low density lipoprotein receptor-negative mice. *J Clin Invest*, *93*(5), 1885-1893.
- Johannessen, C. U. (2000). Mechanisms of action of valproate: a commentary. *Neurochem Int*, *37*(2-3), 103-110.
- Jousse, C., Bruhat, A., Harding, H. P., Ferrara, M., Ron, D., & Fafournoux, P. (1999). Amino acid limitation regulates CHOP expression through a specific pathway independent of the unfolded protein response. *FEBS Lett*, *448*(2-3), 211-216.
- Kaidanovich-Beilin, O., & Woodgett, J. R. (2011). GSK-3: Functional Insights from Cell Biology and Animal Models. *Front Mol Neurosci*, *4*, 40.
- Kaladchibachi, S. A., Doble, B., Anthopoulos, N., Woodgett, J. R., & Manoukian, A. S. (2007). Glycogen synthase kinase 3, circadian rhythms, and bipolar disorder: a molecular link in the therapeutic action of lithium. *J Circadian Rhythms*, *5*, 3.
- Khan, M. I., Pichna, B. A., Shi, Y., Bowes, A. J., & Werstuck, G. H. (2009). Evidence supporting a role for endoplasmic reticulum stress in the development of atherosclerosis in a hyperglycaemic mouse model. *Antioxidants & redox signaling*, *11*(9), 2289-2298.
- Kim, A. J., Shi, Y., Austin, R. C., & Werstuck, G. H. (2005). Valproate protects cells from ER stress-induced lipid accumulation and apoptosis by inhibiting glycogen synthase kinase-3. *Journal of cell science*, *118*(Pt 1), 89-99.
- Kim, K. H., Song, M. J., Yoo, E. J., Choe, S. S., Park, S. D., & Kim, J. B. (2004). Regulatory role of glycogen synthase kinase 3 for transcriptional activity of ADD1/SREBP1c. *J Biol Chem*, *279*(50), 51999-52006.
- Kirii, H., Niwa, T., Yamada, Y., Wada, H., Saito, K., Iwakura, Y., . . . Seishima, M. (2003). Lack of interleukin-1beta decreases the severity of atherosclerosis in

- ApoE-deficient mice. *Arteriosclerosis, thrombosis, and vascular biology*, 23(4), 656-660.
- Kirshenboim, N., Plotkin, B., Shlomo, S. B., Kaidanovich-Beilin, O., & Eldar-Finkelman, H. (2004). Lithium-mediated phosphorylation of glycogen synthase kinase-3beta involves PI3 kinase-dependent activation of protein kinase C-alpha. *J Mol Neurosci*, 24(2), 237-245.
- Korshunov, S. S., Skulachev, V. P., & Starkov, A. A. (1997). High protonic potential actuates a mechanism of production of reactive oxygen species in mitochondria. *FEBS Lett*, 416(1), 15-18.
- Laviola, L., Belsanti, G., Davalli, A. M., Napoli, R., Perrini, S., Weir, G. C., . . . Giorgino, F. (2001). Effects of streptozocin diabetes and diabetes treatment by islet transplantation on in vivo insulin signaling in rat heart. *Diabetes*, 50(12), 2709-2720.
- Laybutt, D. R., Preston, A. M., Akerfeldt, M. C., Kench, J. G., Busch, A. K., Biankin, A. V., & Biden, T. J. (2007). Endoplasmic reticulum stress contributes to beta cell apoptosis in type 2 diabetes. *Diabetologia*, 50(4), 752-763.
- Lee, J. N., & Ye, J. (2004). Proteolytic activation of sterol regulatory element-binding protein induced by cellular stress through depletion of Insig-1. *J Biol Chem*, 279(43), 45257-45265.
- Lee, M. Y., Jung, S. C., Lee, J. H., & Han, H. J. (2008). Estradiol-17beta protects against hypoxia-induced hepatocyte injury through ER-mediated upregulation of Bcl-2 as well as ER-independent antioxidant effects. *Cell Res*, 18(4), 491-499.
- Lee, W. L., Cheung, A. M., Cape, D., & Zinman, B. (2000). Impact of diabetes on coronary artery disease in women and men: a meta-analysis of prospective studies. *Diabetes care*, 23(7), 962-968.
- Lee, Y. W., Kim, P. H., Lee, W. H., & Hirani, A. A. (2010). Interleukin-4, Oxidative Stress, Vascular Inflammation and Atherosclerosis. *Biomol Ther (Seoul)*, 18(2), 135-144.
- Li, J., & Holbrook, N. J. (2004). Elevated gadd153/chop expression and enhanced c-Jun N-terminal protein kinase activation sensitizes aged cells to ER stress. *Exp Gerontol*, 39(5), 735-744.
- Li, Y., Schwabe, R. F., DeVries-Seimon, T., Yao, P. M., Gerbod-Giannone, M. C., Tall, A. R., . . . Tabas, I. (2005). Free cholesterol-loaded macrophages are an abundant source of tumor necrosis factor-alpha and interleukin-6: model of NF-kappaB- and map kinase-dependent inflammation in advanced atherosclerosis. *J Biol Chem*, 280(23), 21763-21772.

- Lin, Y., Berg, A. H., Iyengar, P., Lam, T. K., Giacca, A., Combs, T. P., . . . Scherer, P. E. (2005). The hyperglycemia-induced inflammatory response in adipocytes: the role of reactive oxygen species. *J Biol Chem*, 280(6), 4617-4626.
- Lloyd-Jones, D. M., Larson, M. G., Beiser, A., & Levy, D. (1999). Lifetime risk of developing coronary heart disease. *Lancet*, 353(9147), 89-92.
- Lonn, E., Yusuf, S., Hoogwerf, B., Pogue, J., Yi, Q., Zinman, B., . . . Gerstein, H. C. (2002). Effects of vitamin E on cardiovascular and microvascular outcomes in high-risk patients with diabetes: results of the HOPE study and MICRO-HOPE substudy. *Diabetes care*, 25(11), 1919-1927.
- MacAulay, K., Doble, B. W., Patel, S., Hansotia, T., Sinclair, E. M., Drucker, D. J., . . . Woodgett, J. R. (2007). Glycogen synthase kinase 3alpha-specific regulation of murine hepatic glycogen metabolism. *Cell Metab*, 6(4), 329-337.
- Mallat, Z., Besnard, S., Duriez, M., Deleuze, V., Emmanuel, F., Bureau, M. F., . . . Tedgui, A. (1999). Protective role of interleukin-10 in atherosclerosis. *Circ Res*, 85(8), e17-24.
- Martin, M., Rehani, K., Jope, R. S., & Michalek, S. M. (2005). Toll-like receptor-mediated cytokine production is differentially regulated by glycogen synthase kinase 3. *Nat Immunol*, 6(8), 777-784.
- Martin, M., Schifferle, R. E., Cuesta, N., Vogel, S. N., Katz, J., & Michalek, S. M. (2003). Role of the phosphatidylinositol 3 kinase-Akt pathway in the regulation of IL-10 and IL-12 by *Porphyromonas gingivalis* lipopolysaccharide. *J Immunol*, 171(2), 717-725.
- McAlpine, C. S., Bowes, A. J., Khan, M. I., Shi, Y., & Werstuck, G. H. (2011). Endoplasmic Reticulum Stress and Glycogen Synthase Kinase-3beta Activation in Apolipoprotein E-Deficient Mouse Models of Accelerated Atherosclerosis. *Arteriosclerosis, thrombosis, and vascular biology*, 32(1), 82-U204.
- Meares, G. P., Mines, M. A., Beurel, E., Eom, T. Y., Song, L., Zmijewska, A. A., & Jope, R. S. (2011). Glycogen synthase kinase-3 regulates endoplasmic reticulum (ER) stress-induced CHOP expression in neuronal cells. *Exp Cell Res*, 317(11), 1621-1628.
- Medzhitov, R., Preston-Hurlburt, P., & Janeway, C. A., Jr. (1997). A human homologue of the *Drosophila* Toll protein signals activation of adaptive immunity. *Nature*, 388(6640), 394-397.
- Mirlashari. (2012). Glycogen synthase kinase-3 (GSK-3) inhibition induces apoptosis in leukemic cells through mitochondria-dependent pathway. *Leukemia Research*, 36(4), 499-508.

- Mohler, M. L., He, Y., Wu, Z., Hwang, D. J., & Miller, D. D. (2009). Recent and emerging anti-diabetes targets. *Med Res Rev*, 29(1), 125-195.
- Moore, K. W., de Waal Malefyt, R., Coffman, R. L., & O'Garra, A. (2001). Interleukin-10 and the interleukin-10 receptor. [Review]. *Annual review of immunology*, 19, 683-765.
- Mukai, F., Ishiguro, K., Sano, Y., & Fujita, S. C. (2002). Alternative splicing isoform of tau protein kinase I/glycogen synthase kinase 3beta. *J Neurochem*, 81(5), 1073-1083.
- Navab, M., Berliner, J. A., Watson, A. D., Hama, S. Y., Territo, M. C., Lusis, A. J., . . . Fogelman, A. M. (1996). The Yin and Yang of oxidation in the development of the fatty streak. A review based on the 1994 George Lyman Duff Memorial Lecture. *Arteriosclerosis, thrombosis, and vascular biology*, 16(7), 831-842.
- Nicholls, S. J., Tuzcu, E. M., Sipahi, I., Grasso, A. W., Schoenhagen, P., Hu, T., . . . Nissen, S. E. (2007). Statins, high-density lipoprotein cholesterol, and regression of coronary atherosclerosis. *JAMA*, 297(5), 499-508.
- Nishiguchi, N., Breen, G., Russ, C., St Clair, D., & Collier, D. (2006). Association analysis of the glycogen synthase kinase-3beta gene in bipolar disorder. *Neurosci Lett*, 394(3), 243-245.
- Norris, S. L., Nichols, P. J., Caspersen, C. J., Glasgow, R. E., Engelgau, M. M., Jack, L., . . . McCulloch, D. (2002). The effectiveness of disease and case management for people with diabetes. A systematic review. *Am J Prev Med*, 22(4 Suppl), 15-38.
- O'Donnell, T., Rotzinger, S., Nakashima, T. T., Hanstock, C. C., Ulrich, M., & Silverstone, P. H. (2000). Chronic lithium and sodium valproate both decrease the concentration of myo-inositol and increase the concentration of inositol monophosphates in rat brain. *Brain Res*, 880(1-2), 84-91.
- Olesen, J. B., Hansen, P. R., Abildstrom, S. Z., Andersson, C., Weeke, P., Schmiegelow, M., . . . Gislason, G. H. (2011). Valproate attenuates the risk of myocardial infarction in patients with epilepsy: a nationwide cohort study. *Pharmacoepidemiol Drug Saf*, 20(2), 146-153.
- Ougolkov, A. V., Fernandez-Zapico, M. E., Savoy, D. N., Urrutia, R. A., & Billadeau, D. D. (2005). Glycogen synthase kinase-3beta participates in nuclear factor kappaB-mediated gene transcription and cell survival in pancreatic cancer cells. *Cancer Res*, 65(6), 2076-2081.

- Oyadomari, S., Harding, H. P., Zhang, Y., Oyadomari, M., & Ron, D. (2008). Dephosphorylation of translation initiation factor 2 α enhances glucose tolerance and attenuates hepatosteatosis in mice. *Cell Metab*, 7(6), 520-532.
- Oyadomari, S., & Mori, M. (2004). Roles of CHOP/GADD153 in endoplasmic reticulum stress. *Cell death and differentiation*, 11(4), 381-389.
- Ozcan, L., & Tabas, I. (2012). Role of endoplasmic reticulum stress in metabolic disease and other disorders. *Annu Rev Med*, 63, 317-328.
- Ozcan, U., Cao, Q., Yilmaz, E., Lee, A. H., Iwakoshi, N. N., Ozdelen, E., . . . Hotamisligil, G. S. (2004). Endoplasmic reticulum stress links obesity, insulin action, and type 2 diabetes. *Science*, 306(5695), 457-461.
- Pahl, H. L., & Baeuerle, P. A. (1995). A novel signal transduction pathway from the endoplasmic reticulum to the nucleus is mediated by transcription factor NF-kappa B. *The EMBO journal*, 14(11), 2580-2588.
- Pai, J. T., Guryev, O., Brown, M. S., & Goldstein, J. L. (1998). Differential stimulation of cholesterol and unsaturated fatty acid biosynthesis in cells expressing individual nuclear sterol regulatory element-binding proteins. *J Biol Chem*, 273(40), 26138-26148.
- Pasterkamp, G., de Kleijn, D. P., & Borst, C. (2000). Arterial remodeling in atherosclerosis, restenosis and after alteration of blood flow: potential mechanisms and clinical implications. *Cardiovasc Res*, 45(4), 843-852.
- Patel, S., Doble, B., & Woodgett, J. R. (2004). Glycogen synthase kinase-3 in insulin and Wnt signalling: a double-edged sword? *Biochem Soc Trans*, 32(Pt 5), 803-808.
- Patel, S., & Woodgett, J. (2008). Glycogen synthase kinase-3 and cancer: good cop, bad cop? *Cancer Cell*, 14(5), 351-353.
- Phiel, C. J., Wilson, C. A., Lee, V. M., & Klein, P. S. (2003). GSK-3 α regulates production of Alzheimer's disease amyloid-beta peptides. *Nature*, 423(6938), 435-439.
- Phiel, C. J., Zhang, F., Huang, E. Y., Guenther, M. G., Lazar, M. A., & Klein, P. S. (2001). Histone deacetylase is a direct target of valproic acid, a potent anticonvulsant, mood stabilizer, and teratogen. *J Biol Chem*, 276(39), 36734-36741.
- Pinderski Oslund, L. J., Hedrick, C. C., Olvera, T., Hagenbaugh, A., Territo, M., Berliner, J. A., & Fyfe, A. I. (1999). Interleukin-10 blocks atherosclerotic events in vitro and in vivo. *Arteriosclerosis, thrombosis, and vascular biology*, 19(12), 2847-2853.

- Pyram, R., Kansara, A., Banerji, M. A., & Loney-Hutchinson, L. (2012). Chronic kidney disease and diabetes. *Maturitas*, *71*(2), 94-103.
- Qiu, W., Avramoglu, R. K., Rutledge, A. C., Tsai, J., & Adeli, K. (2006). Mechanisms of glucosamine-induced suppression of the hepatic assembly and secretion of apolipoprotein B-100-containing lipoproteins. *Journal of lipid research*, *47*(8), 1749-1761.
- Qu, L., Huang, S., Baltzis, D., Rivas-Estilla, A. M., Pluquet, O., Hatzoglou, M., . . . Koromilas, A. E. (2004). Endoplasmic reticulum stress induces p53 cytoplasmic localization and prevents p53-dependent apoptosis by a pathway involving glycogen synthase kinase-3beta. *Genes & development*, *18*(3), 261-277.
- Raven, J. F., Baltzis, D., Wang, S., Mounir, Z., Papadakis, A. I., Gao, H. Q., & Koromilas, A. E. (2008). PKR and PKR-like endoplasmic reticulum kinase induce the proteasome-dependent degradation of cyclin D1 via a mechanism requiring eukaryotic initiation factor 2alpha phosphorylation. *J Biol Chem*, *283*(6), 3097-3108.
- Rehani, K., Wang, H., Garcia, C. A., Kinane, D. F., & Martin, M. (2009). Toll-like receptor-mediated production of IL-1Ra is negatively regulated by GSK3 via the MAPK ERK1/2. *J Immunol*, *182*(1), 547-553.
- Rizzuto, R., Pinton, P., Ferrari, D., Chami, M., Szabadkai, G., Magalhaes, P. J., . . . Pozzan, T. (2003). Calcium and apoptosis: facts and hypotheses. *Oncogene*, *22*(53), 8619-8627.
- Robertson, L. A., Kim, A. J., & Werstuck, G. H. (2006). Mechanisms linking diabetes mellitus to the development of atherosclerosis: a role for endoplasmic reticulum stress and glycogen synthase kinase-3. *Canadian journal of physiology and pharmacology*, *84*(1), 39-48.
- Rosenberg, G. (2007). The mechanisms of action of valproate in neuropsychiatric disorders: can we see the forest for the trees? *Cell Mol Life Sci*, *64*(16), 2090-2103.
- Ross, R. (1999). Atherosclerosis is an inflammatory disease. [Review]. *American heart journal*, *138*(5 Pt 2), S419-420.
- Ross, R., & Glomset, J. A. (1973). Atherosclerosis and the arterial smooth muscle cell: Proliferation of smooth muscle is a key event in the genesis of the lesions of atherosclerosis. *Science*, *180*(4093), 1332-1339.
- Rubinfeld, B., Albert, I., Porfiri, E., Fiol, C., Munemitsu, S., & Polakis, P. (1996). Binding of GSK3beta to the APC-beta-catenin complex and regulation of complex assembly. *Science*, *272*(5264), 1023-1026.

- Rutkowski, D. T., Wu, J., Back, S. H., Callaghan, M. U., Ferris, S. P., Iqbal, J., . . . Kaufman, R. J. (2008). UPR pathways combine to prevent hepatic steatosis caused by ER stress-mediated suppression of transcriptional master regulators. *Dev Cell*, *15*(6), 829-840.
- Rylatt, D. B., Aitken, A., Bilham, T., Condon, G. D., Embi, N., & Cohen, P. (1980). Glycogen synthase from rabbit skeletal muscle. Amino acid sequence at the sites phosphorylated by glycogen synthase kinase-3, and extension of the N-terminal sequence containing the site phosphorylated by phosphorylase kinase. *Eur J Biochem*, *107*(2), 529-537.
- Sage, A. T., Holtby-Ottenhof, S., Shi, Y., Damjanovic, S., Sharma, A. M., & Werstuck, G. H. (2011). Metabolic Syndrome and Acute Hyperglycemia Are Associated With Endoplasmic Reticulum Stress in Human Mononuclear Cells. *Obesity*, *20*(4), 748-755.
- Saraiva, M., & O'Garra, A. (2010). The regulation of IL-10 production by immune cells. *Nat Rev Immunol*, *10*(3), 170-181.
- Shakoori, A., Mai, W., Miyashita, K., Yasumoto, K., Takahashi, Y., Ooi, A., . . . Minamoto, T. (2007). Inhibition of GSK-3 beta activity attenuates proliferation of human colon cancer cells in rodents. *Cancer Sci*, *98*(9), 1388-1393.
- Shaw, P. C., Davies, A. F., Lau, K. F., Garcia-Barcelo, M., Waye, M. M., Lovestone, S., . . . Anderton, B. H. (1998). Isolation and chromosomal mapping of human glycogen synthase kinase-3 alpha and -3 beta encoding genes. *Genome*, *41*(5), 720-727.
- Smith, J. D., & Breslow, J. L. (1997). The emergence of mouse models of atherosclerosis and their relevance to clinical research. *Journal of internal medicine*, *242*(2), 99-109.
- Song, L., De Sarno, P., & Jope, R. S. (2002). Central role of glycogen synthase kinase-3beta in endoplasmic reticulum stress-induced caspase-3 activation. *J Biol Chem*, *277*(47), 44701-44708.
- Soutar, M. P., Kim, W. Y., Williamson, R., Pegg, M., Hastie, C. J., McLauchlan, H., . . . Sutherland, C. (2010). Evidence that glycogen synthase kinase-3 isoforms have distinct substrate preference in the brain. *J Neurochem*, *115*(4), 974-983.
- Stambolic, V., & Woodgett, J. R. (1994). Mitogen inactivation of glycogen synthase kinase-3 beta in intact cells via serine 9 phosphorylation. *The Biochemical journal*, *303* (Pt 3), 701-704.

- Steinberg, D., Carew, T. E., Fielding, C., Fogelman, A. M., Mahley, R. W., Sniderman, A. D., & Zilversmit, D. B. (1989). Lipoproteins and the pathogenesis of atherosclerosis. *Circulation*, *80*(3), 719-723.
- Sutherland, C. (2011). What Are the bona fide GSK3 Substrates? *Int J Alzheimers Dis*, *2011*, 505607.
- Suzuki, T., Lu, J., Zahed, M., Kita, K., & Suzuki, N. (2007). Reduction of GRP78 expression with siRNA activates unfolded protein response leading to apoptosis in HeLa cells. [Research Support, Non-U.S. Gov't]. *Archives of biochemistry and biophysics*, *468*(1), 1-14.
- Takadera, T., Fujibayashi, M., Kaniyu, H., Sakota, N., & Ohyashiki, T. (2007). Caspase-dependent apoptosis induced by thapsigargin was prevented by glycogen synthase kinase-3 inhibitors in cultured rat cortical neurons. *Neurochem Res*, *32*(8), 1336-1342.
- Tani, S., Matsumoto, M., Nakamura, Y., Nagao, K., & Hirayama, A. (2012). Association of the low-density lipoprotein cholesterol/high-density lipoprotein cholesterol ratio and body mass index with coronary plaque regression. *Am J Cardiovasc Drugs*, *12*(4), 279-286.
- Targher, G., & Arcaro, G. (2007). Non-alcoholic fatty liver disease and increased risk of cardiovascular disease. *Atherosclerosis*, *191*(2), 235-240.
- Thorp, E., Li, G., Seimon, T. A., Kuriakose, G., Ron, D., & Tabas, I. (2009). Reduced apoptosis and plaque necrosis in advanced atherosclerotic lesions of Apoe^{-/-} and Ldlr^{-/-} mice lacking CHOP. *Cell Metab*, *9*(5), 474-481.
- Travers, K. J., Patil, C. K., Wodicka, L., Lockhart, D. J., Weissman, J. S., & Walter, P. (2000). Functional and genomic analyses reveal an essential coordination between the unfolded protein response and ER-associated degradation. *Cell*, *101*(3), 249-258.
- Wang, H., Brown, J., & Martin, M. (2011). Glycogen synthase kinase 3: a point of convergence for the host inflammatory response. *Cytokine*, *53*(2), 130-140.
- Wang, H., Garcia, C. A., Rehani, K., Cekic, C., Alard, P., Kinane, D. F., . . . Martin, M. (2008). IFN-beta production by TLR4-stimulated innate immune cells is negatively regulated by GSK3-beta. *J Immunol*, *181*(10), 6797-6802.
- Wei, P., Bai, L., Song, W., & Hao, G. (2009). Characterization of two soil metagenome-derived lipases with high specificity for p-nitrophenyl palmitate. *Arch Microbiol*, *191*(3), 233-240.
- Werstuck, G. H., Khan, M. I., Femia, G., Kim, A. J., Tedesco, V., Trigatti, B., & Shi, Y. (2006). Glucosamine-induced endoplasmic reticulum dysfunction is associated

- with accelerated atherosclerosis in a hyperglycemic mouse model. *Diabetes*, 55(1), 93-101.
- Werstuck, G. H., Lentz, S. R., Dayal, S., Hossain, G. S., Sood, S. K., Shi, Y. Y., . . . Austin, R. C. (2001). Homocysteine-induced endoplasmic reticulum stress causes dysregulation of the cholesterol and triglyceride biosynthetic pathways. *The Journal of clinical investigation*, 107(10), 1263-1273.
- Whittle, B. J., Varga, C., Posa, A., Molnar, A., Collin, M., & Thiemermann, C. (2006). Reduction of experimental colitis in the rat by inhibitors of glycogen synthase kinase-3beta. *Br J Pharmacol*, 147(5), 575-582.
- Woodgett, J. R. (1990). Molecular cloning and expression of glycogen synthase kinase-3/factor A. *The EMBO journal*, 9(8), 2431-2438.
- Woodgett, J. R., & Cohen, P. (1984). Multisite phosphorylation of glycogen synthase. Molecular basis for the substrate specificity of glycogen synthase kinase-3 and casein kinase-II (glycogen synthase kinase-5). *Biochim Biophys Acta*, 788(3), 339-347.
- World Health Organization. Cardiovascular diseases. Fact Sheet No. 317. <http://www.who.int/mediacentre/factsheets/fs317/en/index.html>. Updated September 2011.
- Wu, G., Huang, H., Garcia Abreu, J., & He, X. (2009). Inhibition of GSK3 phosphorylation of beta-catenin via phosphorylated PPPSPXS motifs of Wnt coreceptor LRP6. *PLoS One*, 4(3), e4926.
- Xu, C., Kim, N. G., & Gumbiner, B. M. (2009). Regulation of protein stability by GSK3 mediated phosphorylation. *Cell Cycle*, 8(24), 4032-403.
- Yost, C., Torres, M., Miller, J. R., Huang, E., Kimelman, D., & Moon, R. T. (1996). The axis-inducing activity, stability, and subcellular distribution of beta-catenin is regulated in *Xenopus* embryos by glycogen synthase kinase 3. *Genes & development*, 10(12), 1443-1454.
- Yusuf, S., Dagenais, G., Pogue, J., Bosch, J., & Sleight, P. (2000). Vitamin E supplementation and cardiovascular events in high-risk patients. The Heart Outcomes Prevention Evaluation Study Investigators. *The New England journal of medicine*, 342(3), 154-160.
- Yusuf, S., Hawken, S., Ounpuu, S., Dans, T., Avezum, A., Lanas, F., . . . Lisheng, L. (2004). Effect of potentially modifiable risk factors associated with myocardial infarction in 52 countries (the INTERHEART study): case-control study. *Lancet*, 364(9438), 937-952.

- Zeng, X., Tamai, K., Doble, B., Li, S., Huang, H., Habas, R., . . . He, X. (2005). A dual-kinase mechanism for Wnt co-receptor phosphorylation and activation. *Nature*, *438*(7069), 873-877.
- Zhou, J., Werstuck, G. H., Lhotak, S., de Koning, A. B., Sood, S. K., Hossain, G. S., . . . Austin, R. C. (2004). Association of multiple cellular stress pathways with accelerated atherosclerosis in hyperhomocysteinemic apolipoprotein E-deficient mice. *Circulation*, *110*(2), 207-213.
- Zimmet, P., Alberti, K. G., & Shaw, J. (2001). Global and societal implications of the diabetes epidemic. *Nature*, *414*(6865), 782-787.
- Zinszner, H., Kuroda, M., Wang, X., Batchvarova, N., Lightfoot, R. T., Remotti, H., . . . Ron, D. (1998). CHOP is implicated in programmed cell death in response to impaired function of the endoplasmic reticulum. [Research Support, Non-U.S. Gov't; Research Support, U.S. Gov't, P.H.S.]. *Genes & development*, *12*(7), 982-995.